Regulation of EGF receptor trafficking by the lysine deacetylase HDAC6

Dissertation

zur Erlangung des Doktorgrades

der Naturwissenschaften

vorgelegt beim Fachbereich 14

Biochemie, Chemie und Pharmazie

der Johann Wolfgang Goethe-Universität

in Frankfurt am Main

von

Yonathan Lissanu Deribe

aus Addis Ababa, Äthiopien

Frankfurt am Main 2009

D30

Table of contents

Table of contents

Table of contents

Abstract

Epidermal growth factor (EGF) receptor belongs to the broad family of enzymatic receptors called receptor tyrosine kinases (RTKs). Generally, the binding of a ligand to these receptors leads to activation of their intracellular kinase activity that sets in motion a cascade of signaling events. In order to ensure appropriate responses to physiological stimuli, the cell is endowed with the ability to regulate signal transduction via numerous mechanisms such as dephosphorylation of the RTK and its substrates as well as downregulation of the RTK.

Activation of EGFR is a potent mitogenic (proliferative) and motogenic (cell motility) signal that plays crucial roles during embryonic development and maintenance of adult tissue. EGFR signaling is primarily regulated by ligand-induced receptor internalization with subsequent degradation in lysosomes. While the complex of proteins that are recruited to EGFR after its activation is well understood, proteins that interact with the receptor in the absence of ligand binding are still not systematically studied.

With the goal of identifying novel binding partners of non-activated EGFR, a membrane based yeast-two hybrid screen (MYTH) was conducted. MYTH is based on the principle of in vivo reconstitution of the N-terminus (Nub) and C-terminus (Cub) halves of ubiquitin once brought into close proximity. A chimeric protein consisting of EGFR fused to Cub and a transcription factor was used as a bait to screen Nub-tagged cDNA library. Analysis of resultant yeast transformants revealed a total of 87 proteins to interact with EGFR. Of these only 11 were previously shown to bind to EGFR. A majority of the other proteins were shown to interact with the receptor by yeast retransformation. Fifteen were confirmed to bind to EGFR by co-immunoprecipitation assays in mammalian cells.

One of the novel EGFR interactors identified in the screen was histone deacetylase 6 (HDAC6). This deacetylase is localized in the cytoplasm and known to deacetylate α-tubulin, HSP90 and cortactin. The juxtamembrane region of EGFR binds to the C-terminus of HDAC6. Functionally, overexpression of wild type HDAC6 stabilized ligand-induced degradation of the receptor. On the other hand, deacetylase deficient or EGFR binding compromised mutants of HDAC6 were able to stabilize EGFR only partially. Downmodulation of HDAC6 expression by RNAi markedly accelerated

degradation of the receptor. Taken together, HDAC6 is a negative regulator of EGFR downregulation that is dependent on its deacetylase activity and ability to bind to the receptor.

Imaging studies revealed that HDAC6 does not affect internalization of EGFR from the plasma membrane but rather influences the post-endocytic trafficking of the receptor-ligand complex to lysosomes. Pulse-chase experiments using fluorophore-tagged EGF showed that EGFR is transported faster towards the peri-nuclear region and delivered to late endosomes rapidly in HDAC6 depleted cells.

HDAC6 is demonstrated to act, at least partly, by regulating the acetylation of α-tubulin. Upon EGFR activation, acetylation of α-tubulin on lysine 40 is progressively increased as shown by mass spectrometry and immunoblotting. Forced expression of a dominant negative mutant of α-tubulin, but not wild type α-tubulin, led to reduced speed and processive movement of early endosomes in GFP-Rab5 expressing cells. In a surprising twist, EGFR is able to phosphorylate HDAC6 on Tyr570. Phosphorylation of Tyr570 and Ser568 leads to inactivation of the deacetylase function of HDAC6 as shown by in vivo and in vitro assays. In summary, HDAC6 diminishes EGFR downregulation by slowing the transport of intracellular vesicles. The inhibitory effect is removed once HDAC6 is phosphorylated on key residues.

In line with these findings, two recent reports have shown that hyper-acetylation of α-tubulin induced by inhibition of HDAC6 increases the transport of brain derived neurotrophic factor and JNK interacting protein-1 in different cell systems. Acetylated microtubules are more efficient in recruiting motor proteins like kinesin-1 and dynein. These findings indicate that HDAC6 plays an important regulatory role in intracellular trafficking pathways. However, several outstanding issues still remain unresolved. How does acetylation of microtubules influence vesicular trafficking? In this regard, the temporal and spatial dynamics of α-tubulin acetylation following EGFR activation should be studied. Furthermore, whether HDAC6 affects the trafficking of other endocytic cargos and additional organelles is an interesting question to address.

Zusammenfassung

Einleitung

Der epidermale Wachstumsfaktor-Rezeptor (EGFR) gehört zu der umfassenden Familie enzymatisch aktiver Rezeptoren, die als Rezeptortyrosinkinasen (RTKs) bezeichnet werden. RTKs stellen eine große Gruppe der Zelloberflächenrezeptoren dar, die eine intrinsische Tyrosinkinaseaktivität aufweisen. Sie katalysieren infolge extrazellulärer Stimuli den Transfer der gamma-Phosphatgruppe eines ATP-Moleküls auf Hydroxylgruppen von Tyrosinresten[3]. Die allgemeine Struktur von RTKs lässt sich in eine extrazelluläre Ligandenbindedomäne, eine einzige Transmembrandomäne und eine zytoplasmatische, katalytisch aktive Region gliedern, auf die der für die Regulation der Signalweiterleitung verantwortliche C-Terminus folgt.

Die Bindung eines Liganden an diese Rezeptoren führt im allgemeinen zur Aktivierung ihrer intrazellulären Kinaseaktivität, die eine Kaskade von Signalvorgängen in Gang setzt. Im Fall des EGFR bindet der Ligand (EGF) als Monomer an den Rezeptor in einem Verhältnis von 2:2 und induziert Konformationsänderungen, die zur Dimerisierung des Rezeptors führen. Daraufhin werden Signalwege innerhalb der Zelle eingeleitet, indem Proteine, die eine Phosphotyrosinbindedomäne aufweisen, an phosporylierte Tyrosinreste im C-terminalen Bereich des Rezeptors binden. Die Aktivität des EGFR sowie anderer RTKs ist streng reguliert, um eine angemessene und physiologische Antwort auf einen Stimulus zu generieren.

Mehrere Mechanismen wie die Dephosphorylierung des Rezeptors und weiterer Komponenten des Signalweges stellen sicher, dass die Signalweiterleitung entsprechend beendet wird. Der wichtigste Mechanismus, um die Weiterleitung des Signals herunterzuregulieren, besteht jedoch in der schnellen Endozytose und dem anschließendem Abbau sowohl des Rezeptors als auch des Liganden. Die Aktivierung infolge der Bindung eines Liganden führt zur Anhäufung des Rezeptors in von Clathrin überzogenen Einstülpungen (CCPs) auf der Plasmamembran, die sich anschließend durch Bildung von „Clathrin bedeckten Vesikeln" (CCVs) abschnüren. Der EGFR wird über CCVs, frühe Endosomen und multivesikuläre Körper schließlich zum Abbau ins Lysosom gebracht. Das Schicksal der Fracht entscheidet sich auf der Ebene des frühen Endosoms: entweder kommt es zur Rückführung an die Plasmamembran oder zum Abbau im Lysosom. Welcher Weg eingeschlagen wird,

hängt von der Ubiquitinierung der Fracht ab, die von einem Proteinkomplex (*endosomal-sorting complex required for transport* (ESCRT)) erkannt wird. Mikrotubuli und die an diese assoziierten Motorproteine wie Dynein sind für den Transport früher Endosomen zu späten Endosomen essentiell und somit auch für den Abbau der Fracht.

In der vorliegenden Doktorarbeit wurde ein modifizierter *membrane yeast two-hybrid screen* (MYTH) durchgeführt, um neue Interaktionspartner des Liganden-unbesetzten, inaktiven EGFR zu identifizieren. Das Prinzip des MYTH besteht auf dem *split-ubiquitin* System, wobei ein "quasi natives Ubiquitinmolekül" rekonstituiert wird, wenn die N-terminale und C-terminale Hälfte des Ubiquitinmoleküls (Nub bzw. Cub) in einer Zelle separat exprimiert werden. Ein Transmembranprotein, an das Cub fusioniert ist, kann dabei als Köder benutzt werden, um eine cDNA *library*, die an Nub gekoppelt vorliegt, auf neue Bindungspartner hin zu untersuchen. Einer der in dem Screen neu identifizierten EGFR-Bindungspartner ist die Histondeacetylase 6 (HDAC6). HDAC6 ist eine einzigartige Deacetylase, die aus zwei katalytischen Domänen und einer Ubiquitin-bindenden Zinkfingerdomäne besteht und fast ausschließlich im Zytoplasma lokalisiert ist. Dadurch, dass sie -Tubulin deacetyliert, spielt HDAC6 u. a. eine wichtige Rolle bei der chemotaktisch induzierten Zellmotilität, der Fusion des HIV-1 Viruspartikels mit der Zellmembran sowie der Bildung von Immunsynapsen. HDAC6 sorgt auch für die Aufrechterhaltung des richtigen Acetylierungsgrades von HSP90, der für die Interaktion mit seinen Ko-Chaperonen und weiteren Assoziationspartnern benötigt wird. Unabhängig von ihrer Deacetylaseaktivität dient HDAC6 durch Bindung an polyubiquitinierte Proteine einerseits und Dynein andererseits als Adaptorprotein. Diese Rolle von HDAC6 ist für die Beseitigung falsch gefalteter Proteine und Aggresomen von Bedeutung.

Das Hauptziel dieser Doktorarbeit ist die Identifizierung neuer EGFR Bindungspartner, die an den inaktiven Rezeptor gebunden sind, sowie die funktionelle Charakterisierung putativer Interaktionspartner.

Ergebnisse und Diskussion

Zunächst wurde ein geeigneter EGFR-Köder für die Verwendung im MYTH generiert, indem das Signalpeptid des menschlichen EGFR (bestehend aus den Aminosäuren 1-24) durch die ersten 85 Aminosäuren des α-Mating Faktors (MFα),

die Cub und einem Transkriptionsfaktor (MFα-EGFR-C-T) ersetzt wurde. Fraktionierung der zellulären Komponenten und Immunblots, hefegenetische und bildgebende Methoden wurden angewandt, um die Transformation, Expression und Lokalisation des Köderproteins in der Plasmamembran der Hefe sicherzustellen. Zur Identifizierung von EGFR-Interaktionspartnern wurde das MFα-EGFR-C-T-Konstrukt als Köderprotein für einen im großen Maßstab durchgeführten MYTH Screen eingesetzt; die verwendete Nub-gekoppelte cDNA *library* entstammte fötalem Hirngewebe. Der Screen offenbarte insgeamt 87 Proteine, die mit EGFR interagieren. Die Proteine, die das EGFR-MYTH Interaktom ausmachen, gliedern sich nach GeneOntology in mehrere funktionelle Gruppen, die unter anderem eine Rolle bei der zellulären Organisation, dem Stoffwechsel und dem Abbau von Proteinen spielen. Vierzehn der identifizierten EGFR-Bindungspartner stellen entweder ausgewiesene integrale oder membranassoziierte Proteine dar; dies unterstreicht, dass zur Identifizierung von Membranproteinen der MYTH geeignet ist. Nur von 11 der 87 gefundenen Proteine war die Interaktion mit EGFR durch Proteomanalysen oder biochemischen Methoden schon gezeigt worden. Erwartungsgemäß wurden phosphotyrosinabhängige Interaktionen, die den Großteil der Bindungspartner des aktiven EGFR ausmachen, nicht beobachtet. Die Interaktion einiger vermeintlicher Bindungspartner mit dem EGFR in Säugerzellem wurde mittels Ko-Immunpräzipitation endogener sowie überexprimierter Proteine bestätigt. Darüber hinaus deuteten weitere bioinformatische Analysen auf die hohe Qualität des Screens hin. Zusammengefasst zeigt die erfolgreiche Anwendung dieses Screens, dass mit einem geeigneten Köderkonstrukt der MYTH eine sehr gute Methode darstellt, um Membranproteine zu analysieren.

Einer der in dem Screen neu identifizierten EGFR-Bindungspartner war die Histondeacetylase 6 (HDAC6). Diese Deacetylase befindet sich im Zytoplasma und entfernt Acetylgruppen von α-Tubulin, HSP90 und Cortactin. Zunächst wurde gezeigt, dass HDAC6 den endogenen EGFR ligandenunabhängig koimmunpräzipitieren kann. Durch Versuche in Säuger- und Hefezellen wurden die Bindedomänen identifiziert, wodurch festgestellt wurde, dass die intrazelluläre, der Transmembrandomäne folgende Region des EGFR den C-Terminus von HDAC6 bindet. Des Weiteren zeigten fluoreszensmikroskopische Methoden, dass HDAC6 und EGFR sowohl im Bereich der Plasmamembran als auch an intrazellulären Vesikeln

nach der Internalisierung des Rezeptors kolokalisieren. Kürzlich konnte gezeigt werden, dass die intrazelluläre, der Transmembrandomäne folgende Region des EGFR für die Aktivierung der Kinasedomäne essentiell ist; vor diesem Hintergrund wäre es interessant zu untersuchen, ob die Interaktion mit HDAC6 irgendeinen Einfluss auf die Kinaseaktvität hat. Darüber hinaus würde eine dreidimensionale Struktur von HDAC6 im Komplex mit EGFR wertvolle Informationen über die Konformation und die Beziehung der Kinase- und der Deacetylasedomäne liefern.

Überexpression von Wildtyp HDAC6 führt zur Stabilisierung des Liganden-induzierten Abbaus des Rezeptors, während eine enzymatisch inaktive oder eine EGFR nicht-bindende Variante von HDAC6 den Rezeptor nur teilweise stabilisieren konnten. Die Herunterregulierung der Expression von HDAC6 mittels RNAi beschleunigte den Abbau des Rezeptors deutlich. Es ist von Bedeutung anzumerken, dass die Überexpression von HDAC6 einen viel geringeren Effekt zeigt als die Depletion mittels RNAi von endogenem HDAC6. Dies liegt wahrscheinlich an der hohen Expression von HDAC6, wobei die Depletion eine größere Wirkung zeigen kann als die Überexpression, da die zelluläre Maschine, deren Bestandteil HDAC6 ist, schon gesättigt sein könnte.

Um die zeitliche und räumliche Kinetik von Endosomen, die EGFR tragen, zu untersuchen, wurden „pulse-chase" Experimente durchgeführt für welche EGF-Moleküle verwendet wurden, die durch Fluorophore markiert worden waren. Die Analyse erfolgte indem die Vesikel zunächst identifiziert und die Bewegungungen anschließend mit, für Untersuchungen an Vesikeln spezifischen Algorithmen berechnet wurden. Dabei wurde festgestellt, dass HDAC6 nicht die Internaliesierung des EGFR von der Plasma beeinflusst, sondern eine Rolle beim postendozytotischen Transport des Rezeptor-Liganden-Komplexes zu den Lysosomen spielt. In Zellen die kein oder kaum HDAC6 exprimieren wird der EGFR sehr schnell zu den späten Endosomen transportiert und wird auch schneller zur perinukleären Region gebracht.

Die Kombination aus verbesserter Mikroskopie, der Markierung von Intrazellulären Komponenten und speziellen Algorithmen hat wichtige Auswirkungen auf unser Verständnis der hochdynamischen Vorgänge in Zellen. Die Anwendung dieser Methoden in der vorliegenden Studie ermöglichte eine quantitative Beschreibung der Prozesse die Ablaufen, nachdem der EGFR internalisiert wurde. Die bei HDAC6 beobachteten Effekte erinnern an die Effekte von KIF16B, einem Mitglied der

Kinesinfamilie, bei der es sich um Motorproteine handelt. KIF16B ist ein Motorprotein das zum Plusende der Mikrotubuli, also richtung Plasmamebran, wandert und das bei Überexpression dazu führt, dass frühe Endosomen zum Zellkortex gebracht werden. Wichtig hierbei ist, dass dies den ligandenabhängigen Abbau des EGFR inhibiert. Im Gegensatz dazu führt das Ausschalten von KIF16B durch siRNA zum schnelleren Transport von frühen Endosomen zum perinukleären Bereich und beschleunigt dessen Abbau.

Es ist bekannt, dass HDAC6 zumindest teilweise den Acetylierungsstatus von α-Tubulin reguliert. Eine umfassende Suche nach anderen Zielproteinen von HDAC6, die eine Rolle beim Vorgang der Endozytose spielen, offenbarte keine weiteren Substrate, wobei solche nicht definitiv ausgeschlossen werden können. Nach Aktivierung des EGFR nimmt der Acetylierungsgrad des Lysinrestes 40 von α-Tubulin stark zu; dies wurde sowohl mittels massenspektrometrischer Proteinsequenzierung als auch Immunblots gezeigt. Die Auswirkung dieses Anstiegs der Acetylierung von α-Tubulin auf den Vesikeltransport wurde mit Hilfe von „Live Cell Imaging" untersucht, wobei die Dynamik der Lokalisation GFP-Rab5 markierter früher Endosomen unter Zuhilfenahme computergestützer Auswertungsverfahren analysiert wurde. Dazu wurde α-Tubulin (Wildtyp) oder einer dominant-negativen Mutante (K40A), die nicht acetyliert, aber nichtsdestotrotz in Mikrotubuli (MT) eingebaut werden kann, überexprimiert. Der Einbau der K40A Mutante von α-Tubulin führte zur einer Verringerung der Geschwindigkeit sowie der prozessiven Bewegungen früher Endosomen; dies weist auf die Bedeutung von Acetylierungsvorgängen bei der effizienten Fortbewegung von Endosomen hin.

Interessanterweise führt die Inhibierung der enzymatischen Aktivität von HDAC6 in Neuronen in Abhängigkeit des Acteylierungsgrades der MT zu einer beschleunigten Sekretion des *brain derived neurotrophic factor* (BDNF). Ein denkbarer Mechanismus stellt die gesteigerte Rekrutierung von Motorproteinen wie z.B. Kinesin-1 an hyperacetylierte MT dar. Zusammenfassend lässt sich sagen, dass die Acteylierung von α-Tubulin einen wichtigen Mechanismus darstellt, um die Kinetik intrazellulärer Transportvorgänge zu regulieren.

Interessanterweise ist bekannt, dass der EGFR Tyrosinreste von HDAC6 *in vitro* phosphoryliert. In Zellen führt die Stimulierung mit EGF zu vermehrter Phosporylierung von HDAC6 an Tyrosinresten. Mit Hilfe der Massenspektrometrie

wurden folgende Phosporylierungstellen identifiziert: Tyr570 und Ser568. Um deren funktionelle Bedeutung hinsichtlich der Deacetylaseaktivität von HDAC6 genauer zu untersuchen, wurden Punktmutanten generiert, die an diesen Stellen entweder einen Glutamat- oder einen Phenylalanin- bzw. Alaninrest aufweisen; erstgenannte Mutation imitiert phosphorylierte Tyrosin- bzw. Serinreste, wohingegen letztgenannte nicht-phosphorylierbare Varianten von HDAC6 darstellen. Die Phosphorylierung von Tyr570 und Ser658 führte zur Inaktivierung der Deacetylasefunktion von HDAC6. Des Weiteren wies HDAC6, das *in vitro* mit Phosphatase behandelt wurde, eine höhere Deacetylaseaktivität auf; demnach beeinflußt die Phosphorylierung die enzymatische Aktivität von HDAC6 negativ. Andere HDACs werden ebenfalls durch Phosphorylierungen reguliert; so inaktiviert z. B. die Phosporylierung des Serinrests 39 von HDAC8 durch die Proteinkinase A (PKA) dessen Aktivität beinahe vollständig. Die Auswirkung hinsichtlich HDAC6 kann auch an EGFR-Signalwegen beobachtet werden. In Zellen, deren HDAC6 Proteinlevel verringert war, zeigte sich eine leicht verminderte Aktivierung von ERK1/2 sowie eine erhöhte Akt Aktivität. Zellen, in denen HDAC6 mittels RNAi herunterreguliert ist, reagieren weniger stark auf EGFR; dies zeigte sich u. a. daran, dass sich A549 Zellen nach Stimulation mit EGF nicht abrundeten und eine geringere Proliferationsrate aufwiesen.

Zusammenfassend lässt sich sagen, dass HDAC6 die Herunterregulierung des EGFR dadurch verringert, dass der Transport intrazellulärer Vesikel zum Lysosom verlangsamt abläuft und dieser inhibitorische Effekt aufgehoben ist, sobald HDAC6 an spezifischen Aminosäureresten phosphoryliert wird.

Ausblick

Während diese Ergebnisse interessant sind, geben sie aber auch Anlass zu einer Anzahl von Fragen, die beantwortet werden müssen. Die Funktion der Bindung von HDAC6 an den ligandenunbesetzten Rezeptor bleibt weiterhin unklar. Es ist möglich, dass HDAC6 Einfluss auf die Aktivierung des Rezeptors nimmt. Darüber hinaus wäre es von Interesse zu untersuchen, ob HDAC6 bei der Regulation weiterer RTKs und dem Transport anderer intrazellulärer Organellen eine Rolle spielt. Des Weiteren ist es nötig, ein besseres Verständnis des molekularen Mechanismus zu erhalten, welcher der Regulation intrazellulärer Transportvorgänge durch Acetylierung von MTs *in vivo* zu Grunde liegt. Zum Beispiel würde eine Komplementationsexperiment, wobei

endogenes Tubulin depletiert und durch Wildtyp oder entsprechende Mutanten (eine nicht-acetylierbare K40A, eine ladungs-erhaltende K40R sowie eine acetylgruppe-imitierende K40Q Mutante) ersetzt ist, wichtige Informationen über die Bedeutung der Acetylierung von α-Tubulin *in vivo* liefern. Ein idealer Modellorganismus in dieser Hinsicht ist das Wimperntierchen *Tetrahymena thermophila,* da in dessen Genom α-Tubulin nur in einfacher Kopie vorliegt. Die Substitution von Wildtyp α-Tubulin mit Mutationsvarianten ist in diesem Organismus bereits mit Erfolg gelungen und kann verwendet werden, um die Rolle von Acetylierungsvorgängen beim Vesikeltransport zu untersuchen. Schließlich sollten vergleichende Struktur-untersuchungen von acetylierten versus nicht-acetylierten MTs Einblicke in die biophysikalische Basis des Einflusses der Acetylierung auf den durch Motorproteine vermittelten Transport geben.

1. INTRODUCTION

1.1 Epidermal growth factor receptor (EGFR)

1.1.1 Growth factors and their cognate receptors

The first cellular growth factors were discovered through a combination of serendipity and keen observation. Stanley Cohen, working with Rita-Montalcini in 1959, used crude extracts from mouse salivary glands to stimulate growth of nerve fibers in mice and stumbled upon not only nerve growth factor (NGF) but also epidermal growth factor (EGF)[1]. Subsequently, a 170KDa protein was identified to be the receptor for EGF in an affinity chromatography experiment[2]. Currently, EGFR is known to be a member of the ErbB receptor family that in turn is part of the super family of receptor tyrosine kinases (RTKs) in mammalian cells.

RTKs are a large group of cell surface receptors possessing an intrinsic tyrosine kinase activity. They catalyze the transfer of gamma phosphate of ATP to hydroxyl groups of tyrosine residues in response to external stimuli[3]. The general protein architecture consists of a ligand binding extracellular domain, a single-pass transmembrane stretch, a cytoplasmic catalytic domain followed by a regulatory/signaling C-terminal tail[4].

Based on mode of activation, RTKs can be broadly classified into three classes. Class I RTKs exist as inactive monomers at the plasma membrane that form active dimers upon the simultaneous binding of a bi-valent monomeric ligand to two receptor monomers. Typical members of this class include growth hormone receptor (GHR) and erythropoietin receptor (EPOR). Class II receptors (e.g. insulin receptor) exist as disulfide-bridged inactive dimers, which are activated by undergoing conformational change upon ligand binding. A broad group falls under Class III, in which the binding of a homodimer ligand to inactive monomers induces the formation of dimers and receptor activation[4, 5]. Vascular endothelial growth factor receptor (VEGFR) and platelet derived growth factor receptor (PDGFR) are typical representatives of this group. Activation of the intrinsic tyrosine kinase activity of RTKs usually leads to auto- and trans-phosphorylation on C- terminal tyrosine residues, which triggers a cascade of signal transduction in the cell.

1.1.2 ErbB family receptors

EGFR belongs to the ErbB family of receptors. The name ErbB was coined as a result of homology of these proteins to avian erythroblastoma viral gene product *v-erbB*. The ErbB family consists of four receptors: EGFR (or ErbB1) as the founding member, ErbB2/Her2/Neu, ErbB3/HER3 and ErbB4/HER4. The receptors form homo- as well as hetero-dimers for signaling[6, 7]. These dimers bind to 13 polypeptide ligands, except for the ErbB2 homodimer, that currently has no known ligand. Based on ligand-receptor affinity measurements, EGFR binds to TGF-α, EGF, β-cellulin and amphiregulin whereas EGFR-ErbB4 heterodimer binds epiregulin and HB-EGF. Neuregulin 1 acts as ErbB3-ErbB4 heterodimer ligand whereas neuregulins 2, 3 and 4 bind to ErbB4 homodimer. It is interesting to note that the ErbB2-ErbB4 heterodimer binds all ligands with moderate to high affinity[8]. All of these ligands are synthesized as transmembrane proteins containing the EGF module. This module comprises of 40 amino acids and contains six cysteine residues in conserved spacing which interacts with the ligand binding domain of their respective receptors[9].

1.1.3 Mechanism of activation of EGFR

EGFR is an 1186 amino acids glycosylated protein comprising of an extracellular domain, a transmembrane segment, a juxtamembrane part, a kinase domain and a C-terminal tail. In broad terms, a monomeric ligand like EGF binds to the extracellular ligand binding EGF module that results in activation of the tyrosine kinase activity. Following full activation, several tyrosine residues are phosphorylated in the C-terminal tail of EGFR acting as docking points for phospho-tyrosine binding domains. As a prototypical RTK, EGFR has been extensively studied for close to three decades. However, the precise molecular mechanism of how ligand binding induces receptor activation is still debated. The main obstacle for the lack of complete understanding is the absence of a high-resolution X-ray structure of the full-length receptor bound to its ligand. Recently, there has been some success in determining structures of isolated domains and particularly of the extracellular ligand-binding domain in complex with its ligand[10].

Compared to other models of monomeric ligand-RTK binding that occurs in a 1:2 ratio, EGFR follows a unique mechanism. The monomeric ligand (EGF) binds to

EGFR in a 2:2 ratio[11]. Structural studies show that the extracellular domain of the inactive receptor exists in an auto-inhibited conformation. Binding of a ligand to each EGFR monomer triggers conformational changes abolishing the auto-inhibition which results in a strictly receptor-only mediated dimerization (i.e. no "cross-linker" ligand)[10-12] (Fig. 1A).

The cytoplasmic EGFR kinase domain adopts a unique structure. The kinase domain is intrinsically auto-inhibited and an intermolecular interaction facilitates its activation. Actually, the structure of active EGFR kinase domains resembles that of cyclin dependent kinases (CDKs) and not other RTKs. Activation results from formation of an asymmetric dimer in which the C-terminal lobe of one kinase (the donor) acts like cyclins on CDKs in allosterically activating the other kinase (the acceptor)[12-14]. This EGFR structure also explains why the activation loop of EGFR kinase domain does not need to be phosphorylated, unlike other RTK kinase domains. In a remarkable structure-function interplay, an activating mutation of EGFR identified in lung cancer patients (V665M) can now be explained as being disruptive of this auto-inhibition and thus leading to constitutively active kinase[14].

1.1.4 Signaling through EGFR

1.1.4.1 Principles of signal transduction downstream of RTKs

Signal propagation through EGFR and other RTKs can be seen as a product of the kinase activity and the scaffolding/docking platform function of the receptor. Work form the late 70`s and early 80`s with transforming viruses (e.g. Rous sarcoma virus) has facilitated the understanding of the mechanism of downstream signaling that leads to changes in cellular phenotype[15]. The demonstration of the tyrosine kinase activity of the oncogenic *v-Src* gene product, and the subsequent identification of the cellular homolog c-Src and the presence of similar domains in RTKs were influential in the early study of signaling[16, 17]. Three principles for activation of effector proteins downstream of RTK signaling have been proposed. The first effect is the direct phosphorylation of target proteins by the kinase domains of RTKs. The second is recruitment of phosphorylated tyrosine binding proteins to the receptor. The third

principle is the change in cellular localization of effectors by translocation to the membrane[5, 6, 17].
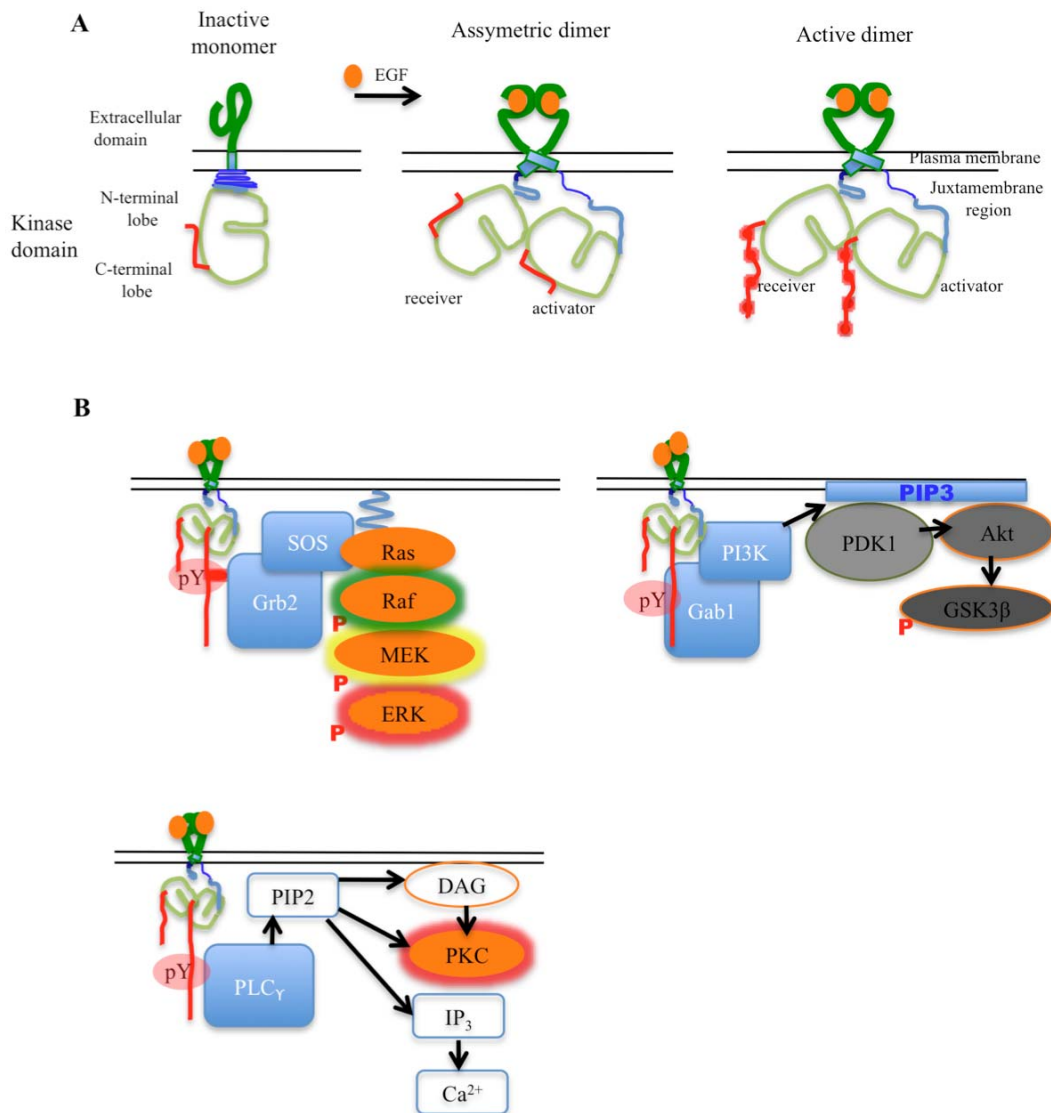
Figure 1. Activation and signaling by EGFR (A) Proposed mechanism of activation of EGFR. Based on recent crystal structures the mode of activation of EGFR appears to be unique compared to other RTKs. In the absence of ligand binding, the extracellular domains of EGFR exist in a compact conformation. Ligand binding induces the formation of an extended conformation. This removes the inhibition on the intrinsic ability of the transmembrane and cytoplasmic domains to dimerize. Rather than phosphorylation, the formation of an "asymmetric dimer" and allosteric activation of the "receiver" kinase by the "activator" is the major driving force for full activation of the receptor. This leads to phosphorylation of tyrosines in the C-terminal tail. **(B)** Major signaling pathways activated by EGFR. A common theme in RTK signaling is the recruitment of target or adaptor proteins to phosphorylated tyrosines. Grb2/Sos recruitment activates Ras which inturn activates the first kinase in the MAP kinase cascade (upper left). The activation of the lipid kinase PI3K leads to formation of PIP3 that acts as platform for recruitment of PH domain containing proteins like Akt, which get activated by phophorylation on key serine and threonine residues (upper right).The cleavage of PIP2 by PLC$_\gamma$ gives rise to two classical second messengers, DAG and IP3. These activate PKC and facilitate release of Ca^{2+} from intracellular stores respectively.

Modular protein domains play central roles in these processes. The phosphotyrosine-binding domain (PTB) and Src homology domain (SH2) that interact with phosphorylated tyrosines are found in many of the signaling proteins[18, 19]. Other domains commonly found in signaling molecules include the SH3 domain that binds peptides containing proline in the motif PXXP[20] and the plekstrin homology (PH) domain that interacts with membrane bound phosphorylated phosphatidyl inositol molecules[21].

1.1.4.2 Signaling pathways activated by EGFR

The RAS/MAP kinase signaling cascade

Active EGFR stimulates the exchange of GTP for GDP on the small G protein Ras through the guanine nucleotide exchange factor (GEF), Sos. The adaptor protein Grb-2, directly or via another adaptor Shc, plays an important role in this process (represented in Fig. 1B). It forms a complex with Sos via its SH3 domain and with EGFR on phosphorylated Tyr1068 (or Tyr1148 and Tyr1173 for Shc) via its SH2 domain. This facilitates the localization of Sos closer to the plasma membrane where Ras resides[5]. Once Ras is bound to GTP, it undergoes a conformational change that favors binding to potent effector kinases like Raf and PI-3 kinase[22]. Activated Raf phosphorylates mitogen-activated-protein kinase (MAP)-kinase-kinase (MEK) on key Ser residues in the activation loop. MEK subsequently phosphorylates and activates the MAP kinase, extracellular signal-regulated kinase (ERK) on both threonine and tyrosine residues leading to its activation. ERK diversifies the signal by phosphorylating a large group of downstream effectors in the cytoplasm. Additionally, ERK rapidly translocates to the nucleus and phosphorylates a variety of transcription factors like Elk1 that increase transcription of response genes involved in cellular growth and proliferation[23, 24].

Phosphoinositol signaling

The prime activator of phosphoinositol metabolism, phospholipase C γ (PLCγ), is recruited through its SH2 domain to phosphorylated Tyr992 in EGFR (Fig. 1B). PLCγ subsequently hydrolyzes its substrate phosphatidylinositol bisphosphate, PtdIns(4,5)P_2, to form diacyl glycerol (DAG) and inositol trisphosphate, Ins(1,4,5)P_3.

Ins(1,4,5)P$_3$ stimulates the release of Ca^{2+} from intracellular stores which activates Ca^{2+}/calmodulin-dependent protein kinases and together with DAG activates protein kinase C(PKC)[25]. The phospholipid kinase PI3-kinase is the other prominent signaling molecule activated by EGFR. By phosphorylating membrane phospholipds it creates docking sites for PH domain containing Ser/Thr kinases PDK1 and PKB/Akt. These in turn activate major cellular survival and growth responses[26, 27]. Additionally, PI3K and PLCγ through the small GTPases Rho/Rac mediate the reorganization of the actin cytoskeleton that leads to formation of membrane ruffles, filopodia and lamellipodia. These changes are central to EGF induced cell motility[28-30].

Signal transduction and activators of transcription (STATs) signaling

STAT proteins get activated upon recruitment to phosphorylated tyrosines on EGFR leading to formation of STAT homo- or hetero-dimers. The dimers translocate to the nucleus and act as transcription co-activators of select target genes. Alternatively, c-Src mediated phosphorylation of EGFR at Tyr845 acts as a docking site for STAT5 that is subsequently activated. This pathway is central in promoting cell cycle progression, proliferation and survival[31].

It is of paramount importance to note that in response to EGF stimulation, most cells either proliferate or migrate but not both. This so-called proliferation-migration dichotomy is due to selective activation of MAP kinase/STAT5/c-Src (proliferation) and PI3K/PLCγ (migration) pathways. The precise mechanism how this occurs is still not clear[32].

1.1.5 Physiological functions of EGFR signaling

Prokaryotes do not have any homologues of EGFR or other RTKs. EGFR homologues first appeared in lower organisms, like the nematode *Caenorhabditis elegans*[33] and the fruitfly *Drosophila melanogaster*[34]. In *C. elegans*, the EGFR homologue, LET-23 is expressed in the three vulval precursor cells and together with its diffusible ligand LIN-3 (EGF-like) is essential for cell fate determination and induction of vulval development. Loss of function of LET-23 results in death. Interestingly, the major downstream signaling components are conserved as exemplified by the existence and action of the Ras like protein, *let-60ras* gene product[33].

In *D. melanogaster*, there is one homologue of EGFR, DER, but four ligands: Spitz, Gurken, Keren and Vein and the negative regulator Argos[34, 35]. DER plays roles at many instances during *D. melanogaster* development such as in oogenesis, embryogenesis, and brain, wing and eye development[36]. In mammals, EGFR and its ligands are important for embryonic development, tissue differentiation and cellular functions. Knocking out EGFR in mice has severe consequences depending on genetic background. In CF-1 and 129/Sv backgrounds, EGFR ablation was embryonic lethal whereas in CD-1 background mice survived till the 3rd week of life. In those pups that survived birth, defects were seen in multiple organs. There were major defects in the epidermis such as total lack of eyelids, low proliferation of gut epithelial cells and defective brain cortex[37]. All this shows that EGFR plays essential roles in development.

1.1.6 Pathological perturbations of EGFR and its signaling pathway

Aberrant expression and activation of ErbB receptors and various downstream components are implicated in tumorigenesis. Gene amplifications leading to receptor overexpression, excessive autocrine or paracrine production of EGFR ligands, deletions and point mutations leading to constitutive activation occur in many solid tumors like glioblastoma, non-small cell lung cancer (NSCLC) and colorectal cancer[38]. Point mutations are also reported granting the receptor resistance to tyrosine kinase inhibitors[39].

Hence, strategies to inhibit signaling through ErbB receptors have been developed and used with promising results. Humanized monoclonal antibodies can block binding of ligand to the receptor, induce receptor endocytosis or activate a type of antibody dependent cellular cytotoxicity (e.g. cetuximab). The other strategy, which is already approved to treat patients with colorectal and NSCLC, is the use of small molecule inhibitors of the EGFR kinase (e.g. gefitinib and erlotinib). Novel antibodies, antibody-chemotherapy conjugates and inhibitors with improved pharmacokinetic properties are now in clinical development[38, 40]. It is of interest to note that patients receiving EGFR tyrosine kinase inhibitors suffer from side effects that are directly related to the physiological function of EGFR in adults. These include acneiform

eruptions and other proliferative disorders of the epidermis where EGFR is highly active[41].

1.1.7 Mechanisms of EGFR signal attenuation

Activity of RTKs is tightly regulated to mount an appropriate and physiological response to a stimulus. In Drosophila, an antagonistic EGF-like ligand called Argos competes away a positive signaling ligand. In a classic negative feedback mechanism, gene expression of negative regulators like Argos is induced upon DER activation[42]. So far, however, no EGFR antagonist ligand has been reported in vertebrates. Phosphorylation of EGFR is generally activating, however phosphorylation on Ser and Thr residues in the juxtamembrane domain by protein kinase C (PKC) results in inhibition of its catalytic activity[43]. A major negative modulator of EGFR signaling is dephosphorylation of activated receptor and downstream effectors by protein tyrosine phosphatases (PTP). Several phosphatases have been implicated in dephosphorylating EGFR after ligand stimulation such as receptor-type protein-tyrosine phosphatase kappa (RPTPκ)[44].

However, the most important way of signal attenuation is by rapid endocytosis and degradation of both the receptor and the ligand. Ligand binding and activation induces clustering of the receptor in primarily clathrin-coated pits (CCPs) on the plasma membrane that pinch of to form clathrin-coated vesicles (CCVs). EGFR is trafficked through CCVs, early endosomes and multivesicular bodies and eventually degraded by lysosomal enzymes[45-47].

1.2 EGFR trafficking

1.2.1 Endocytosis

Endocytosis can be defined as the formation of internal membranes from the lipid bilayer of the plasma membrane leading to full internalization of membrane lipids, proteins and extracellular fluid. It can be considered the opposite of exocytosis where internal membranes fuse with the plasma membrane[48]. As imaging techniques improved, understanding of the process has come a long way from the initial description by Elie Metchnikoff that cells could phagocytose (literally "eat") foreign

particles[49]. Based on morphological and molecular characteristics of the endocytic structures and cargos transported, different pathways have been described. Classically, clathrin-mediated endocytosis (CME) has been the most extensively characterized. However, several clathrin independent endocytic pathways are now known to exist (depicted in Fig. 2).

1.2.1.1 Clathrin-mediated endocytosis (CME)

The defining feature of CME is the recruitment of soluble clathrin to the plasma membrane where it is assembled into pentagonal and hexagonal lattices that curve around membrane invaginations forming coated-pits (CCPs)[50]. The presence of clathrin alone is not enough for deforming and stabilizing the membrane fold. Adaptor proteins such as amphiphysin and endophilin that contain uniquely curved domains called BAR domain (Bin/Amphyphysin/Rvs) are important in bending the plasma membrane[51]. Additionally, cargo specific and non-specific adaptor proteins like AP2 (adaptor protein 2) link the cargo to the clathrin and aid in recruiting the GTPase dynamin[52]. Dynamin releases the CCP from the plasma membrane by scission of the neck region to form clathrin-coated vesicles (CCVs). Short linear stretches of amino acids in the cytoplasmic tail of receptors acts as sorting signals into early endosomes or lysosomes. These signals are tyrosine based as in NPXY or dileucine based as in DExxxLL. The AP-2 adaptor recognizes tyrosine based sequences whereas GGAs (Golgi localized gamma ear containing ARF binding proteins) recognize dileucine-based signals. Classic examples of receptors containing NPxY motif are EGFR and low density lipoprotein receptor (LDLR) whereas CD3γ and the glucose transporter GLUT4 contain DExxxLL motif[53].

Importantly, the membrane in these vesicles is far from being an inert media. Phospholipids like phosphatidylinositol-4.5-bisphosphate facilitate vesicle formation and budding by binding to adaptors. Subsequently, CCVs undergo uncoating to form naked vesicles that fuse with early endosomes (EEs). EEs are enriched in phosphatidylinositol-3-phosphate and FYVE (Fab1, YOTB, Vac1, EEA1) domain containing proteins that bind cargo and determine its destination. Hence, EEs are important molecular sorting stations. From here on, cargo can be directed into two

separate compartments, recycling endosomes (REs) or multivesicular endosomes (MVEs)[48, 49, 54].

A hotly debated area is how all of this change/transition of vesicular structures occurs. Basically, two schools of thought exist. In the "pre-formed compartment" model, vesicles transport cargo between two distinct and stable compartments. Endosomal carrier vesicles pinch of from early endosomes and fuse with late endosomes. Additionally, vesicles from the Golgi complex containing newly synthesized lysosomal enzymes fuse with this compartment converting it slowly to a lysosome. There is "vesicle shuttling" that denotes vesicles move in both directions to compensate for progressive membrane loss[55-58]. On the contrary, the "endosome maturation" model argues that there is gradual change in composition of a cargo containing vesicle[59, 60].

New imaging and fluorescent tagging of key proteins involved in assembly of these endocytic compartments is shedding light on their biogenesis and favors the maturation model. The GTPases Rab5 and Rab7 are key organizers of early and late endosomes respectively and act as compartmental identity markers. Dynamics of red fluorescent protein-Rab5 (RFP-Rab5) labeled single early endosomes were examined in real time. Images acquired by fast live-cell imaging were analyzed by a newly developed image analyses algorithm that is able to track single vesicles. Early endosomes progressively lost RFP-Rab5 signal and acquired GFP-Rab7. Remarkably, this Rab conversion coincided with changes in vesicle morphology (getting bigger), cargo content (getting brighter) and localization (coming closer to peri-nuclear area) which are all general features of late endosome formation. The other fundamental observation has been the visualization of the high dynamicity of the Rab5 machinery ranging from stable maintenance of identity to rapid loss of early endosomal identity[61].

The fate of cargo is decided at the level of early endosomes where cargo is destined either to be recycled back to the plasma membrane or to be degraded in lysosomes. Nutrient receptors such as the transferrin receptor and LDL receptor are uniformly recycled back to the membrane where as most RTKs are sorted for degradation[62]. Cargo destined for degradation ends up in late endosomes or multivesicular bodies (MVBs). Morphologically, MVBs have a characteristic appearance with accumulation of intraluminal vesicles (ILVs) containing cargo to be degraded[55, 60]. Sorting and ILV

formation proceed hand in hand and are dependent on sorting signals and machinery. Cargo Ubiquitylation is the major sorting signal[63]. Endosomal sorting complex required for transport (ESCRT) is a complex multi-protein sorting machinery on the limiting membrane of MVBs that recognizes this sorting signal and facilitates intraluminal budding of vesicles[64-66].

Additionally, phosphatidyl inositol 3- phosphate (PtdIns3P) and FYVE domain proteins are intimately involved in the formation of ILVs. PtdIns (3)P is found in early endosomes whereas PtdIns(3,5)P and the unconventional lipid lysobisphosphatidic acid (LBPA) are localized in late endosomes. These phospholipids are crucial components of the sorting machinery and function by recruiting the protein components of the sorting apparatus.

Hepatocyte growth factor regulated tyrosine kinase substrate protein (HRS) is the best characterized of the FYVE domain proteins involved in MVBs biogenesis. HRS is recruited by PtdIns3P and it in turn recruits clathrin. HRS also binds ubiquitylated cargo proteins through its ubiquitin interacting motif (UIM)[67, 68].

Polyubiquitylation through Lys-48 is a signal for proteasomal degradation. On the contrary, multiple monoubiquitylation and Lys-63 polyubiquitylation serve as signals for lysosomal protein degradation[69, 70]. In the endosomal membrane the ESCRT machinery recognizes the ubiquitylated cargo. Detailed genetic and biochemical analysis in the yeast *Saccharomyces cerevisiae* has led to the elucidation of components of this machinery that is conserved from yeast to humans. This complex apparatus consists of four complexes, ESCRT-0, I, II and III and several accessory components. ESCRT-0 consists of Hrs and STAM which function as the initial ubiquitin sensing subunits and help to concentrate cargo that will be sequentially passed onto the other complexes. ESCRT I and II also bind ubiquitin but primarily function to deform the endosomal membrane and recruit ESCRT III. ESCRT III causes prominent invagination and forms a circular array around the invagination to cause abscission that completes the formation of ILVs. ESCRT III also recruits deubiquitinating enzymes to recycle ubiquitin. Vps4 (vacuolar protein sorting 4) hydrolyses ATP to drive the disassembly of the ESCRT III complex and generation of individual subunits[62, 65, 66].

Subsequently, MVBs fuse with lysosomes in such a way that ILVs end up in the lumen that contains hydrolytic enzymes whereas the limiting membrane remains

intact. The ILV membrane is degraded by lipases and the cargo proteins are degraded by lysosomal proteases[71, 72]. Mechanistically late endosomes and lysosomes either permanently fuse to create a hybrid organelle or transiently fuse (kiss-and-run). Like other vesicular fusions, fusion occurs in three steps; tethering of the two vesicles via Rab7-recruited fusion complex, trans-SNARE (soluble N-ethylmaleimide sensitve factor [NSF] attachment protein receptor) complex formation between the opposing membranes and the final phospholipid bilayer fusion[73].
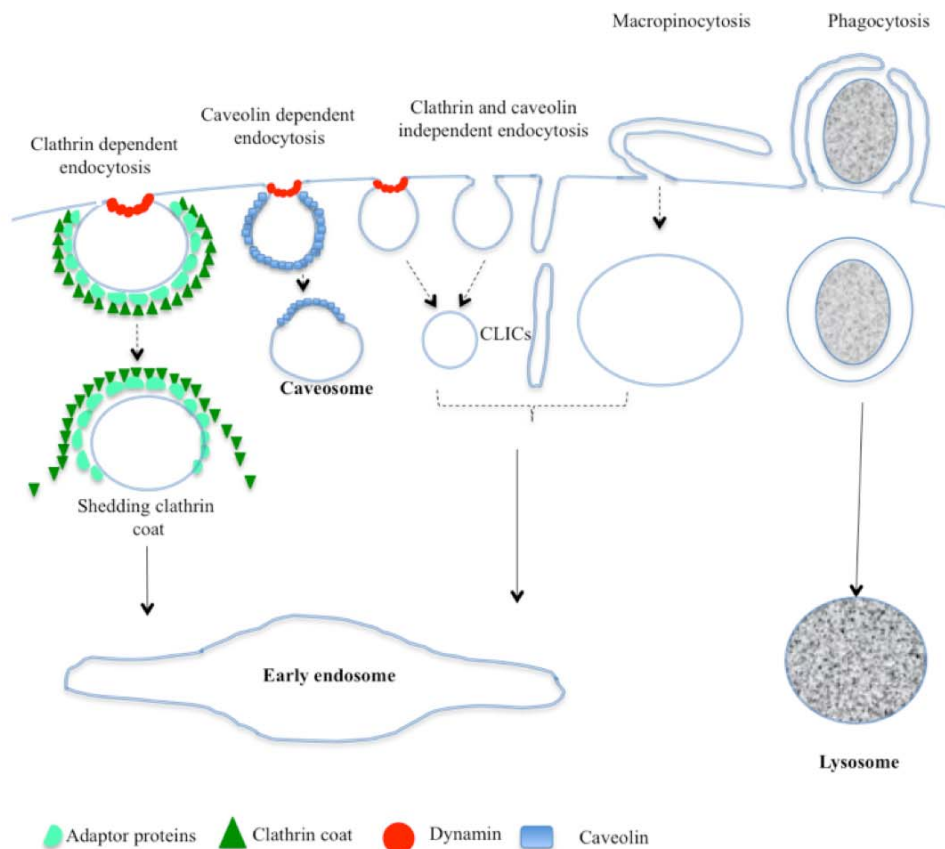
Figure 2. Entry into the cell. The simplistic rendition of major internalization pathways includes clathrin mediated (CME) and caveolin dependent (CDE) pathways that require the GTPase dynamin for the release of vesicles. The less well characterized clathrin and caveolin independent pathways may or may not require dynamin. Large particles are engulfed by phagocytosis, whereas fluid is taken up by macropinocytosis. These two routes involve extensive cytoskeletal rearrangement and encompass large areas of the cell membrane. Most pathways eventually lead to early endosomes, either through coated vesicles (clathrin or caveolin) or through clathrin and dynamin independent carriers (CLICS). In some cases of CDE, cargo may end up in caveosomes. Phagocytosed particles are usually terminated by fusion with lysosomes.

1.2.1.1 Clathrin independent endocytosis (CIE)

The existence of clathrin-independent modes of endocytosis is currently well established. The advent of novel techniques and markers has unraveled diverse

pathways of endocytosis[74, 75]. However, precise distinctions between some routes are still lacking. A recurring theme in clathrin independent endocytosis is the involvement of specialized microdomains of the plasma membrane called "lipid rafts". Lipid rafts are highly enriched in cholesterol and sphingolipid. Biochemically, they are isolated in low buoyant density and detergent–resistant membrane fractions [76, 77]. Their existence was once debated, as their specific composition seemed to defer widely depending on the type of detergent used for extraction. Currently though, research is focused on analysis of their biogenesis, size, stability, and lipid and protein composition[78].

1.2.1.1.1 Caveolin mediated endocytosis

Caveolae (literally "small caves") are flask-shaped invaginations in the plasma membrane enriched with the lipid raft resident protein caveolin-1. Furthermore, they contain high proportion of cholesterol and sphingolipids [79, 80]. Like CME, caveolae-mediated endocytosis requires scission by the GTPase dynamin. Caveolin is able to form oligomers and organizes caveolae by binding to cholesterol and fatty acids[81]. It is also able to bind to other components of "lipid rafts" such as the glycosphinoglipid GM1 and Gb3. Cargo in caveolae is endocytosed into caveosomes, which are large neutral pH vesicles, can end up in classical early endosomes[82] or can fuse with the Golgi complex[83, 84]. The number of markers shown to be endocytosed through caveolae is relatively few. These include simian virus 40 (SV40) and some glycosylphosphatdiylinositol (GPI)-anchored proteins. The best characterized is transport of cargo across endothelial barriers, so called transcytosis[85, 86].

Another obscure dynamin dependent CIE endocytic pathway is responsible for the endocytosis of interleukin-2 receptor β chain (IL-2R-β). IL-2R-β segregates into detergent-resistant membranes, like in other CIE pathways, and is dependent on both dynamin and the small GTPase RhoA for its internalization[87].

1.2.1.1.2 Dynamin-independent cdc42 regulated endocytosis

Unlike most other forms of endocytosis, one class of CIE endocytosis is also dynamin independent. Rather, this pathway requires the small GTPase cdc42. The primary

vesicles that bud from the membrane, also called clathrin and dynamin independent carriers (CLICs), have long and wide surface invaginations[88, 89]. CLICs end up in specialized endosomes known as glycosyl-phosphatidylinositol–anchored protein (GPI-AP) enriched early endosomal compartments (GEECs)[74, 88]. So far, no clear sorting signal or specialized adaptor proteins have been identified for this pathway. It is recently hypothesized that the nano-scale clustering of GPI-APs (at most four molecules per cluster), which is dependent on cholesterol might act as a sorting signal[90, 91]. Cholera toxin B, GPI-anchored receptors and fluid phase markers like dextran are transported through this pathway[92].

1.2.1.1.3 Internalization of large volumes of membrane – macropinocytosis and phagocytosis

Macropinocytosis is a large-scale internalization of fluids and membrane that involves transient plasma membrane protrusions. The eventual fusion of these membranes with themselves or the plasma membrane results in the uptake of extracellular particles caught between the protrusions. One of the classical upstream activators of this route of endocytosis is growth factor signaling that activates PI3K[93]. This process is rac1 and actin dependent[94]. Morphologically, macropinocytosis is similar to dorsal membrane ruffle formation after growth factor stimulation. Rac1 directly binds and activates p21-activated kinase-1 (PAK1) that is central to subsequent morphological alterations of the cytoskeleton and plasma membrane by phosphorylating several effectors[95]. The other role of rac1 is the recruitment of the actin polymerization complex Arp2/3 and N-WASP. The growth of actin polymer is the main driving force behind the membrane protrusions[96]. Macropinocytosis is also dependent on cholesterol that is involved in recruitment of active rac1[97].

Phagocytosis denotes the engulfment of particles that are larger than 0.5μm in diameter by specialized phagocytic cells like macrophages. Targets for phagocytosis could be invading pathogens, apoptotic cells or even inert foreign particles like beads[98]. Actin-driven protrusions of the plasma membrane, called pseudopods, engulf the target by repeated receptor-ligand interactions. This very much proceeds in a zippering mechanism. Phagocytosis leads to massive reorganization of the actin cytoskeleton by activating multiple signaling pathways that end up with the formation

of the phagosome. The primary purpose of the phagosome is to degrade the cargo and hence fuses with lysosomes to form a hybrid organelle, the phagolysosome[98, 99].

1.2.1.1.4 Pathogens and the endocytic pathway

Endosomes help in fighting infections through several ways. In the innate immune response, pattern recognition proteins of the Toll-like receptor (TLR) family sense the presence of pathogens and trigger inflammatory responses by activation of transcription factors such as nuclear factor (NF)-kB. Some of the TLRs, namely TLR3, TLR7 and TLR9, signal from endosomes[100]. Endosomes are also important for adaptive immune response. Antigen presenting cells take up and process extracellular antigens into peptides that are loaded onto major histocompatibility (MHC) class II complexes. These are sorted from the Golgi to the internal membranes of endosomes and the peptide-loaded complex is delivered by back fusion to the limiting membrane of the endosome. From here it is eventually delivered to the plasma membrane[101]. Endosomes are also actively involved in pathogen killing. After phagocytosis of microorganisms, the phagosome undergoes a series of maturation events to be competent in cell killing and digestion. This mature phagosome, also known as phagolysosome, contains lysosomal hydrolases and an active NADPH oxidase complex in a highly acid pH that are crucial for its microbicidal activity.

Intracellular pathogens, or their products, traverse through the plasma membrane mainly through the cell's pre-existing internalizing pathways (CME, phagocytosis or macropinocytosis). These opportunistic organisms have developed ingenious ways of avoiding entrapment in pathways that could lead to their degradation.

Anthrax toxin (AT) and enveloped vesicular stomatitis virus (VSV) are prototypic in using endocytosis to reach the cytoplasm. They are transported down the endocytic pathway, sorted into the intraluminal vesicles (ILVs) in MVBs and are finally released into the cytoplasm as the ILVs back-fuse with the limiting membrane[102, 103]. Bacteria such as *Listeria monocytogenes*, *Salmonella enerica* and *Shigella flexneri* are particularly good at manipulating normally non-phagocytic cells to take them up[104]. Bacteria not only use endocytosis to get into cells but have also come up with strategies to exit when necessary. Listeria, through its toxin listeriolysin O, forms

transmembrane pores that perforate the phagosome facilitating the bacteria's escape into the cytoplasm[105].

Another highly pathogenic organism, *M.tuberculosis* prevents the full maturation of the phagosome into a phagolysosome. It produces a highly glycosylated phosphatidylinositol (PtdIns) analogue, lipoarabinomannan and a PtdIns(3)P-phosphatase, SapM. These prevent the PtdIns(3)P-dependent recruitment of lysosomal enzymes and v-ATPases; hence the bacteria can persist in the early endosomal-like compartment of macrophages for extended durations[106-108].

1.2.3 EGFR endocytosis

At steady state conditions the majority of EGFR is localized to the plasma membrane with a minor pool in endosomes. This is achieved by the interplay between constitutive internalization at a slow rate that is comparable to basal rate of membrane recycling (rate constant Ke ~0.02-0.05 min^{-1}) and a much faster recycling rate (rate constant $K_r \geq 0.2$ min^{-1})[109-111]. Upon ligand binding, EGFR is internalized at a much faster rate (Ke ~0.2-0.4 min^{-1}), which incidentally is similar to internalization rate of transferrin receptors through clathrin-coated pits (CCPs)[112]. In addition to this finding, various experiments have conclusively shown that EGFR is primarily internalized through clathrin-mediated endocytosis. These include localization of EGF/EGFR in CCPs[113, 114] and inhibition of EGFR internalization either by expression of dominant-negative mutant of dynamin[115] or RNA interference mediated knockdown of clathrin heavy chain or dynamin[116]. Interestingly, it is reported that EGFR internalization through CCPs occurs only at low EGF concentration (1-2ng/ml). At higher EGF concentrations (100ng/ml) EGFR is internalized via clathrin independent and lipid-raft dependent pathway[114]. However in cells expressing low to moderate amount of EGFR, the receptor is primarily internalized through CME even at high ligand concentrations[112, 117]. In cells expressing very high amount of EGFR, like the human epidermoid carcinoma cell line A431, EGF stimulation leads to internalization of the receptor also through macropinocytosis[118].

Kinase activity is important for internalization of EGFR as shown by inhibition of endocytosis in a kinase-dead mutant and by small molecule kinase inhibitors[119-121]. Phosphorylation of several tyrosine residues in EGFR is also required for efficient

internalization. Tyr1068 and Tyr1086, which bind to Grb2 adaptor protein, are particularly important for CME[120]. Additional evidences such as severe inhibition of endocytosis by Grb2 siRNA knockdown and localization of Grb2-EGFR complex in CCPs point to the possibility of EGFR being primarily internalized via Grb2 dependent endocytosis[122, 123].
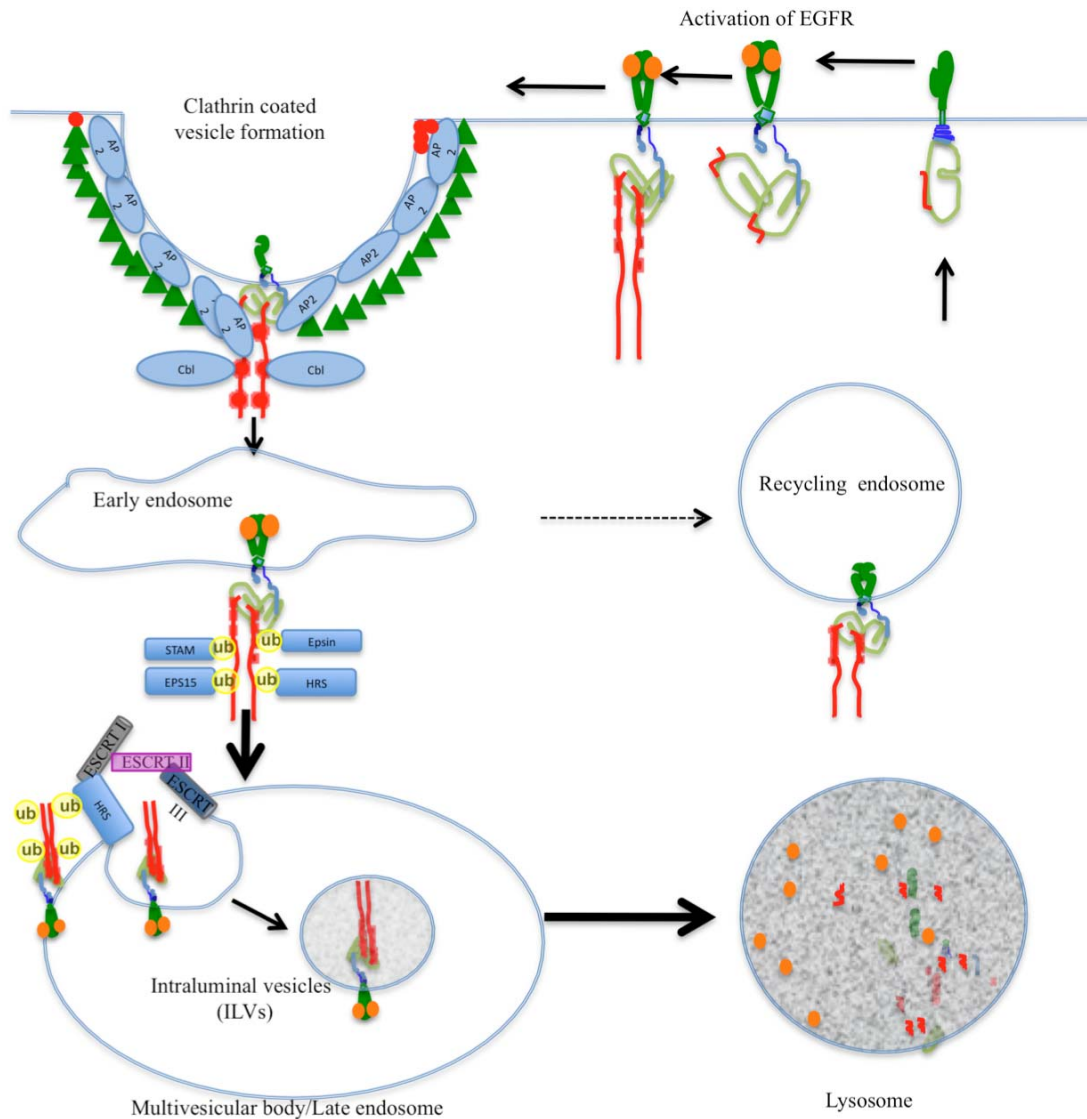
Figure 3. Salient features of EGFR trafficking. The binding of ligand, EGF, to its cognate receptor, EGFR, activates not only signaling pathways but also negative regulators of EGFR signaling. Ligand-induced internalization of EGFR occurs primarily through clathrin coated pits. Recruitment of the E3 ubiquitin ligase, cbl, to phosphorylated EGFR leads to multiple monoubiquitylation of the receptor. Ubiquitin is recognized by ubiquitin interacting motif containing proteins like HRS or epsin. In a process orchestrated by the ESCRT complex, ubiquitylation acts as the sorting signal to degradation. This proceeds via pinching off of small vesicles containing cargo from the limiting membrane of the late endosomes into the intravesicular space creating intraluminal vesicles (ILVs). This effectively terminates signaling from the C-terminus of the receptor. Finally, fusion of these multivesicular bodies/late endosomes with lysosomes results in both ligand and receptor degradation by proteolysis.

One of the major interactors of Grb2 is the Cbl family of E3-ubiquitin ligases. Additionally, all three members of Cbl family, c-Cbl, Cbl-b and Cbl-3, bind to EGFR directly via Tyr1045[124]. Cbl proteins are able to ubiquitylate EGFR; however, whether this ubiquitylation of EGFR is essential for internalization is still an unresolved issue. Knockdown of c-Cbl and Cbl-b or expression of dominant negative mutants leads to partial inhibition of EGFR internalization[70, 125, 126]. Importance of homologues of Cbl proteins in EGFR internalization and signaling is also shown by genetic studies in *Drosophila*[127] and *C.elegans*[128]. It is possible that Cbl proteins ubiquitylate other proteins in the endocytic pathway to mediate their effect on internalization of EGFR.

Subsequent to internalization through CCPs, EGFR containing vesicles rapidly (within a few minutes) shed their clathrin coat and fuse with early endosomes (Fig 3). Even though the pH of early endosomes is mildly acidic (6.0-6.5), EGF-EGFR complex is not dissociated and is still phosphorylated and signaling competent[129]. Interestingly, as opposed to earlier thoughts, early endosomes act not only as down-modulators but also function as platforms for activating downstream signaling pathways like ERK/MAPK[130].

As early endosomes mature, the vast majority of EGF-EGFR complex begins to accumulate in ILVs of MVBs[131]. At this junction, a "point of no return" is reached. Unlike nutrient receptors (like transferrin receptor) that are constitutively endocytosed and recycled, the fate of ligand bound EGFR is degradation. The crucial determinant in the sorting of the ligand-receptor complex is the ubiquitylation of the receptor by E3 ubiquitin ligases like c-Cbl and recognition of this ubiquitin moiety by adaptor proteins in the ESCRT complex[132]. In contrast to poly-ubiquitin chain formation in proteasomal degradation, mono-ubiquitylation (single or multiple) is the predominant degradation signal in endosomes[69]. Ubiquitin interacting motif containing proteins like HRS or STAM1/2 recruit ubiquitylated EGFR. This starts the cascade of ESCRT machinery leading to formation of ILVs within MVBs that end up in lysosomes[133, 134]. A number of proteins fine-tune the downregulation of EGFR, primarily by acting on Cbl activity. For instance, Sprouty 2 binds to Cbl and inhibits its ubiquitin ligase activity[135]. In contrast CIN85 (Cbl-interacting protein of 85kDa) is postulated to form multimeric protein complexes that enhance receptor internalization[136, 137].

In summary, ubiquitylation of EGFR by c-Cbl is a primary sorting signal for the lysosomal degradation of the receptor. Ubiquitylation targets lysine residues on its

substrate proteins. Another posttranslational modification that targets lysine residues is acetylation. This raises an interesting question. Can acetylation act competitively on the same lysine residues that are targeted by ubiquitylation?

1.3 HDAC6 and protein acetylation

1.3.1 Lysine acetylation as a post-translational modification

The study of protein lysine acetylation has come a long way from the first demonstration of correlation between acetylation of histones and RNA synthesis[138]. Two types of protein acetylation can be distinguished: a co-translational acetylation of N-terminal residues of most proteins and post-translational acetylation of the epsilon amino group of lysine residues[139, 140]. The description that follows is focused exclusively on lysine acetylation as a post-translational modification. Histones are generally acetylated on lysine residues of their N-terminal tails in a site-specific manner in transcriptionally active chromatin. The primary result of this acetylation is charge neutralization, which is hypothesized to weaken histone to DNA interactions and also change histone to histone interaction between close nucleosomes[141]. Modulating this acetylation are two groups of enzymes with opposing activities: acetyltransferases (HATs) and deacetylases (HDACs). Histone acetyltransferases transfer acetyl groups from acetyl coenzyme A (acetyl-CoA) onto the ε-amino groups of lysines whereas deacetylases remove this acetyl group[142, 143].

 Based on domain architecture, HATs can be classified into GNAT (Gcn5-related N-acetyltransferase), MYST (named after the founding members MOZ, Ybf2, Sas2 and Tip60) and p300/CBP families. They all share a common HAT domain containing binding site for acetyl-CoA but differ in other domains. Most of these HATs have been discovered as transcriptional co-activators[142]. Even though acetyltransferases are generally termed as histone acetyltransferase, their substrates are by no means limited to histones.

Currently, the list of acetylated proteins is rapidly increasing. Acetylation appears to occur predominantly in the nucleus where transcriptional co-activators and transcription factors are abundantly acetylated. Some of these include p53, estrogen receptor-α, nuclear factor-κB, c-Myb, androgen receptor and HMG (high mobility

group) proteins[140]. Interestingly, the number of reports of acetylated cytoplasmic proteins is also increasing. α-Tubulin is the quintessential cytoplasmic protein known to be acetylated[144, 145]. Moreover, functionally relevant acetylations of HSP90[146], cortactin[147], and STAT3[148] have been reported.

How does acetylation affect the function of proteins? Acetylation of transcription factors such as p53 and E2F1 increases binding to DNA where as acetylation of HMGI transcription factor abolishes DNA binding[140]. Furthermore, acetylation also influences protein-protein interactions, either positively or negatively. For instance acetylation of HSP90 increases its interaction with its client protein glucocorticoid receptor[146]. It is also important to note that there is a highly conserved domain of 60 amino acids that specifically recognizes acetylated lysines, the bromodomain. Located in various transcription factors, co-activators and co-repressors the bromodomain is involved in building large transcriptional and chromatin remodeling complexes[149]. So far no cytoplasmic acetyllysine binding domain/motif has been described. Acetylation also regulates stability of proteins; acetylated E2F1 is for example more stable than it's non-acetylated form[150]. Interestingly, acetylation of Smad7 by p300 competes against ubiquitylation on the same lysine residue and rescues it from degradation[151].

1.3.2 Deacetylases

Lysine deacetylases are highly conserved proteins found from yeast to higher mammals. As the first deacetylases to be described are from the yeast *Sacharomyces cerevisiae,* deacetylases are generally classified into three classes based on their similarities to the yeast HDACs. Class I HDACs (HDAC1, 2, 3, 8 and 11) are related to yeast RPD3[143, 152] whereas Class II HDACs (HDAC 4, 5, 6, 7, 9 and 10) share more similarities to yeast Hda1[153]. The third class known as SIR2 (sir2 yeast founder protein) family of NAD^+- dependent HDACs are very distinct from the previous two classes of HDACs in sequence and catalytic mechanism[154].

Class I HDACs are exclusively localized in the nucleus and their physiological targets are histones and transcription factors. They are classical transcriptional repressors and are active only in large chromatin remodeling complexes, hence the catalytic inactivity of recombinantly produced proteins. Phosphorylation slightly increases

their enzymatic activity but are primarily regulated by interactions with co-repressors[155] .

Class II HDACs are able to shuttle between the nucleus and the cytoplasm. However, HDAC6 is almost exclusively localized in the cytoplasm[156]. HDACs 4, 5, and 7 are important in fine-tuning repression of gene expression as they readily respond to signaling cues by changing their sub-cellular localization via binding to 14-3-3 proteins. Furthermore they are phosphorylated and depend on other co-repressors[157].

The enzymatic action of these two classes of HDACs is similar. The catalytic deacetylase domain is composed of about 390 amino acids. The active site is a tubular pocket comprising of two aspartate-histidine charge-relay systems that activate a water molecule. This water molecule launches a nucleophilic attack on the carbonyl carbon of the acetyllysine that is polarized by the critical zinc ion. An additional tyrosine residue is required to stabilize the intermediate, which yields acetate and lysine[158]. There are various structural groups of HDAC inhibitors but act in related fashion by chelating the zinc, removing the water molecule and closing the entrance to the active site pocket. The most potent of HDAC inhibitors belongs to the hydroxamic acids such as the fungal fermentation product trichostatin A (TSA) while short chain fatty acids like sodium butyrate and valproic acid are weak inhibitors[143].

The SIR2 family of deacetylases is completely resistant to all the above HDAC inhibitors due to their unique catalytic mechanism. They deacetylate lysines by consuming nicotinamide adenine dinucleotide (NAD^+) to generate 2`-O-Acetyl-ADP-ribose, nicotinamide and the deacetylated substrate. They deacetylate histones and transcription factors involved in metabolism, stress response and survival[154, 159]. Recently, SIR2 deacetyases have garnered immense interest, as they appear to be major regulators of life span of organisms. Their activation leads to longer and healthier life in model organisms, in a manner remarkably similar to caloric restriction[160, 161].

1.3.3 Histone deacetylase 6 (HDAC6)

HDAC6 is a unique deacetylase as it is the only deacetylase with two catalytic domains[153]. It contains ubiquitin binding zinc-finger domain of the type Zn-UBP[162], and is almost exclusively localized in the cytoplasm[163]. HDAC6 was initially cloned

by searching the GenBank/expressed sequence tag database for homologues of the yeast deactylase Hda1[153]. A single 5kb transcript was highly expressed in heart, liver, kidney, brain, pancreas and testis. Overexpressed and immunoprecipitated HDAC6 is capable of deacetylating histones in vitro. Both deacetylase domains are functional and can act independently of each other, at least *in vitro*. Like the other class II HDACs, HDAC6 shares sequence similarity to yeast Hda1 only in the deacetylase domain. However, in higher eukaryotes from *C.elegans* to humans these HDACs are well conserved[153]. The discovery of α-tubulin as an in vivo and in vitro substrate of HDAC6 established it as the first full-fledged cytoplasmic lysine deacetylase[156, 164]. Interestingly, HDAC6 can not deacetylate free α/β-tubulin dimers but only polymerized microtubules[156]. HDAC6 binds to β-tubulin through its deacetylase domains and deacetylates α-tubulin on lysine-40[164].

The generation of HDAC6 null mice by targeted ablation confirmed that HDAC6 is the physiological deacetylase of α-tubulin. Even though these mice are viable and lack gross defects, they show massively increased acetylation of α-tubulin in various tissues[165].

What are the cellular functions of HDAC6 then? The major cellular roles of HDAC6 for which reliable evidence has been provided are outlined in Figure 4. HDAC6 mediated deacetylation of α-tubulin enhances chemotactic motility towards serum. Acetylated microtubules are known to be highly stable and are absent from leading edge of motile cells where the cytoskeleton is very dynamic. It is hypothesized that HDAC6 increases fibroblast motility by destabilizing microtubules[156].

Shortly after this finding, numerous substrates of HDAC6 have been identified. HDAC6 interacts with the F-actin binding protein cortactin. Cortactin is multiply acetylated on the F-actin binding site. Acetylated cortactin is not able to bind to actin and is not recruited to the cell periphery where active actin polymerization is taking place. In a Rac1 dependent fashion, HDAC6 deacetylates cortactin enabling it to translocate to the cell periphery, interact with actin and the actin polymerizing machinery. Thus deacetylated cortactin facilitates actin polymerization that is associated with ruffle formation and cell movement[147]. Heat shock protein 90 (HSP90) is involved in maturation of various signaling molecules like the glucocorticoid receptor. HSP90 is acetylated on a single lysine, K294, which is important in client protein and co-chaperone binding[166].

HDAC6 down modulation, either by inhibitor or siRNA, results in hyperacetylation of HSP90. This leads to the dissociation of HSP90 from the co-chaperone p23 and the client protein glucocorticoid receptor that in turn inhibits proper nuclear receptor maturation and signaling[146, 167].
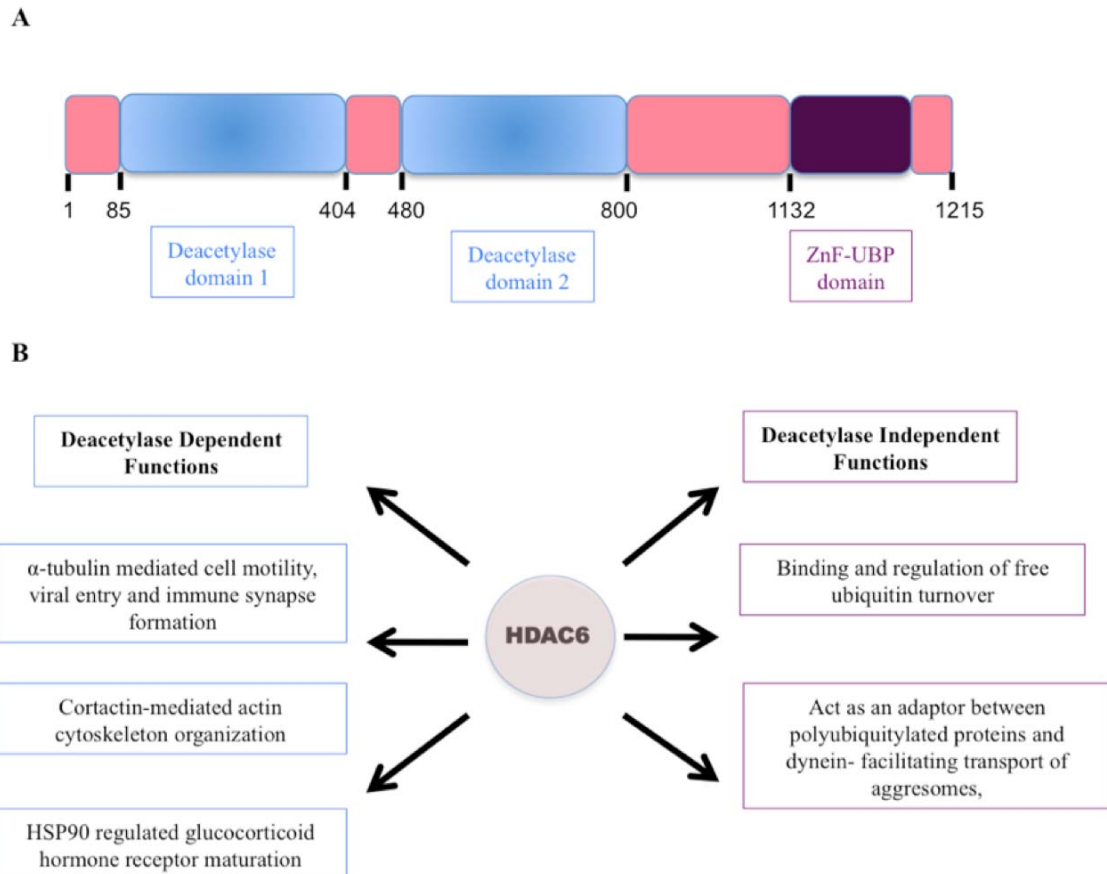
Figure 4. **Domain architecture and functions of HDAC6**. (**A**) HDAC6 is unique among all deacetylases in having two active deacetylase domains. It also contains a ZnF-UBP domain capable of binding to the C-terminal diglycine motif of ubiquitin. So far no 3-D structure of HDAC6 has been solved. Even isolated domains have proven to be poorly suited to structural studies. (**B**) Major substrates and biological functions of HDAC6. Deactylation of -tubulin is important for chemotactic cell motility, HIV-1 viral fusion to cell membrane and formation of immune synapse. Effect on the actin cytoseleton is mediated via cortactin, actin polymerization nucealtion protein. Cortactin needs to be deacetylated for its function. Proper level of acetylation of HSP90 needs to be maintained for functional interaction to its cochaperone and client proteins. TSA inhibition of HDAC6 abolishes these functions. On the other hand, HDAC6 also functions as an adaptor. It binds to free mono-ubiquitin with high affinity and can regulate cellular pool of free ubiquitin. The other well described role of HDAC6 is its interaction with polyubiquitylated misfolded proteins (via ZnF-UBP domain) and dynein. This helps in the clearance of misfolded proteins and aggressomes.

Interestingly, HDAC6 also has cellular functions independent of its enzymatic activity. This is primarily by acting as an adaptor protein by virtue of its ability to bind to ubiquitin[162] and the motor protein dynein[168]. Upon misfolded protein stress,

HDAC6 simultaneously binds polyubiquitylated proteins through its ubiquitin binding zinc finger and dynein through a short stretch of amino acids adjacent to the second catalytic domain. It thus participates in the transport of cytotoxic aggregates to a single prominent juxtanuclear storage structure termed the aggresome[168]. Additionally it is known that inhibition of the ubiquitin proteasome system (UPS) leads to the induction of an alternative degradative pathway called autophagy that removes protein aggregates. In an elegant fly model of neurodegeneration, in which UPS is inhibited, the induction of autophagy was demonstrated to be HDAC6 dependent. In fact, ectopic expression of HDAC6 alone was sufficient to prevent retinal degeneration in flies with impaired UPS[169].

Intriguingly, a recent report using microtubules (MTs) purified from *Tetrahymena thermophila* showed that the recruitment of the molecular motor kinesin-1 to MTs is dependent on acetylation of α-tubulin K40. Acetylation of MTs also increased the motility of kinesin-1 on a lawn of MTs as measured by in vitro gliding assays. This was found to be replicated also in vivo where acetylation induced by HDAC inhibition increased the proportion of neurites receiving the cargo through MT dependent transport[170]. These findings were further extended when acetylated MTs were shown to bind dynein more efficiently by Dompierre et al[171]. Furthermore, it was demonstrated that acetylation stimulates anterograde transport of brain-derived neurotrophic factor (BDNF) containing vesicles in cortical neurons for secretion into the striatum. Using dual color live-cell imaging, GFP-BDNF is trafficked more slowly in cells expressing a non-acetylatable mCherry-tubulin K40R mutant compared to mCherry-tubulin wt. Interestingly, postmortem staining of brains from patients who suffered from Huntington disease showed a dramatic decrease in acetylated MTs. It is important to note that MT based trafficking is known to be impaired in Huntington disease[172].

1.4 Microtubule dependent intracellular trafficking

Microtubules are long filamentous entities that are important for organelle trafficking and localization, cell motility, segregation of chromosomes during cell division and cytokinesis. Movement on MTs is relatively faster than on actin, and can occur over longer distances. The role of MTs in the endocytic pathway is well established. MTs

are essential for trafficking from early endosomes to late endosomes and hence for degradation of cargo[173-175]. Importantly, the early internalization events are largely independent of MTs but are rather orchestrated by the actin cytoskeleton whereby small vesicles are propelled by a "comet tail" of F-actin[176, 177].

The driving forces behind these cytoskeleton-based movements are the various molecular motor proteins. The three classes of motors - myosin, kinesin, and dynein derive energy from ATP hydrolysis and undergo conformational changes that generate a `step` on the cytoskeleton track[178]. In order to carry cargo over long distances, motor proteins need to move on their tracks without dissociating, a feature known as processivity. Classical processive motor proteins achieve this by acting as dimers; the monomers keep the ATPase cycles out-of-phase and when one is attached to the track the other is stepping towards the next binding site[178].

In endocytic trafficking, motor proteins are able to interact with the membrane of the organelle through the transmembrane cargo protein either directly or via adaptor proteins. For instance, some motors can bind to membrane lipids through their lipid binding plekstrin homology (PH) domains. An example for the use of an adaptor protein is the dynein-dynactin complex that is the prime organizer for early to late endosome movement[179].

An important property of motor proteins is directionality and the choice of cytoskeleton apparatus. Myosins generally move along actin filaments whereas dyneins and kinesins use MTs[180]. Although the picture is much more complicated than initially appeared, dyneins are generally credited for movement towards the slow-growing minus-end of MTs in the juxtanuclear microtubule-organizing center (MTOC). In contrast, members of the kinesin and myosin superfamilies can move to either the plus- or minus-end[178].

1.5 Membrane based yeast two-hybrid screening (MYTH)

Inspired by the revolution in molecular genetics of the last decades, understanding of the functions of proteins on a global scale, and not only as single molecules, is becoming a pressing issue. Similar to genomics, this nascent field of science (termed proteomics) owes its existence largely to advances in technology. Proteomics aims to systematically study protein expression, structure, modifications and protein-protein

interactions at a global level[181]. The complexity of the study subject can encompass a signaling pathway, a macromolecular complex, a cellular organelle, a cell or even a whole tissue[182]. Some of the tools in proteomics include mass spectrometry (MS), protein-protein interaction screening platforms and high throughput structural determinations[183]. As expected, each technology has its own strength and limitation that must be taken into account when applying it to investigate a particular system.

Protein-protein interaction studies have contributed immensely to the study of signal transduction pathways. One of the most versatile tools for this purpose is affinity purification followed by mass spectrometry. MS relies on the digestion of protein samples into peptides by sequence specific proteases such as trypsin followed by separation of these peptides by high-pressure liquid chromatography. Next, these peptides are injected into an ionizer forming highly charged peptides. The core of the MS, the mass analyzer then measures the mass to charge ratio, *m/z* and a detector determines the number of ions at each *m/z value.* Further fragmentation by gas collision and measurement gives a tandem mass spectrum (MS/MS). The spectra generated are then matched against protein sequence database giving identity of the peptide and hence the proteins it is derived from[184].

Other tools to study protein-protein interaction include array based formats like protein microarrays and yeast-two hybrid screens (YTH). YTH has been extensively used to screen protein-protein interactions since its development in 1989 by Stanley Fields and Ok-kyu Song[185]. The investigators made use of GAL4, a yeast transcription factor (TF), whose DNA binding domain and transactivation domain can be separately fused to two independent proteins. A genetic readout is switched on only when these two proteins can locate to the nucleus, bind to each other and bring the two domains of GAL4 into such close proximity that they can activate expression of their target genes. Some of the important limitations of YTH are the high rate of false positives and the need for the interacting proteins-TF fusion to translocate to the nucleus to activate gene expression. Unfortunately, this precludes the use of a conventional YTH to identify interacting partners of integral membrane proteins.

To circumvent this problem and study integral membrane proteins, a split-ubiquitin based modified membrane yeast two hybrid (MYTH) screening technique has been developed. The founding principle for this technique was one of the many seminal works of Alexander Varshavsky on ubiquitin[186]. It was observed that ubiquitin can be

expressed in cells as two separate fragments, N-terminus (Nub, aa 1-34) and C-terminus (Cub, aa 35-76), and that these fragments can spontaneously re-associate to form a "quasi-native ubiquitin". Importantly, if Nub and Cub are fused to the C-terminus of different proteins they can still associate with each other and this was sufficient for ubiquitin specific proteases to recognize the re-associated "ubiquitin" and cleave it off. However, when ubiquitin Ile13 was mutated to Gly in the Nub fragment (henceforth called NubG), NubG and Cub were not able to re-associate spontaneously. Importantly, when NubG and Cub were fused to proteins that interact with each other, the "quasi-native ubiquitin" entity was formed and can be cleaved off. Later on, Igor Stagljar and Stanley Fields developed a technique that could be used to screen for interaction partners of integral membrane proteins in the yeast *Saccharomyces cerevisae*[187].

The central features of this technique are drawn in Figure 5. Cub and NubG were attached individually to two different transmembrane proteins and could validate that the two proteins interact with each other. The ubiquitin fragments need to be fused to the cytosolic part of the proteins as UBPs are exclusively found in the cytosol and not in the endoplasmic reticulum (ER) lumen. An artificial transcription factor (ATF) made up of a fusion of the bacterial LexA-DNA binding domain and the *Herpes simplex* VP16 transactivator domain was used. The cleaved ATF activates expression of *HIS3* and *LacZ* reporter genes that incorporate LexA binding sequences in their promoters. *HIS3* encoded expression of imidazoleglycerol-phosphate dehydratase (an enzyme involved in histidine synthesis) enables the yeast to grow in selective media lacking histidine while β-galactosidase encoded by the *LacZ* gene gives the characteristics blue coloration upon exposure to the substrate X-Gal (5-bromo-4-chloro-β-D-indolyl-galactopyranoside).

It is important to note that at least one of the two interacting proteins should be anchored to a membrane to prevent translocation of the non-cleaved fusion protein to the nucleus and activation of reporter genes without any specific interaction. So far the MYTH has been used to screen for transmembrane proteins like ion channels, G-protein coupled receptors, and membrane transporters[188-191].
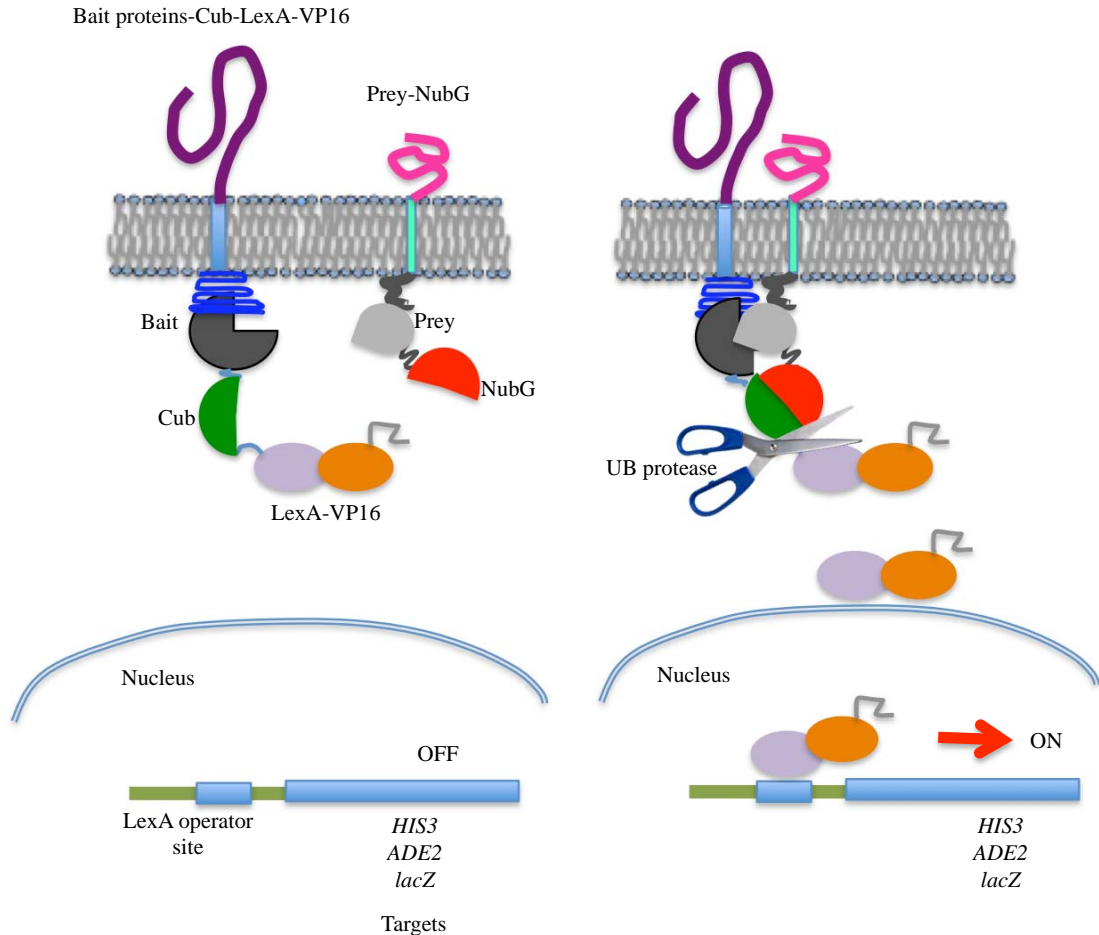
Figure 5. Split-ubiquitin based membrane yeast--two-hybrid system. Membrane anchored bait protein is fused to Cub and LexA-VP16 artificial transcription factor. Prey could be either membrane bound or cytosolic fused to NubG. LexA operator sites in the promoter of reporter genes are unoccupied and no transcription is going on (left panel). If bait and prey interact in the extracellular, intra-membrane or cytoplasmic regions, NubG and Cub will get into enough proximity to permit reconstitution into "native " ubiquitin. Ubiquitin specific proteases recognize this and cleave C-terminus to it. The released transcription factor binds to LexA operator sites and activate expression of reporter genes like *His3, ADE2* or *lacZ* (right panel).

1.6 Related original work- a Cbl-CIN85 complex in EGFR endocytosis

Before moving into the main topic of my thesis, I was involved in characterizing the formation of a complex of proteins necessary for the downregulation of EGFR. As described before, the ubiquitin ligase c-Cbl and its binding partner CIN85 are prominent regulators of the endocytosis of EGFR. The E3 ubiquitin ligase c-Cbl incorporates ubiquitin on select lysines in the cytoplasmic domain of EGFR. These ubiquitin moieties are recognized by ubiquitin binding domain containing proteins in the ESCRT complex[132]. CIN85 is recruited to the EGFR complex after ligand induced activation by binding to c-Cbl. CIN85 is constitutively associated with the BAR

domain containing protein endophilin[192]. Endophilin and closely related proteins like amphyphysin are important for bending of the plasma membrane[193]. Hence, the complex initiated by c-Cbl acts at multiple levels of the downregulation of EGFR. c-Cbl, through a proline rich region containing the PxxxPR motif interacts with the SH3 domains of CIN85. CIN85 contains three SH3 domains, which are all capable of interacting with c-Cbl. It has thus been proposed that CIN85 can act as a scaffold to recruit c-Cbl molecules[124, 136].

Together with our collaborators, Katrin Rittinger (London) and Jeronimo Bravo (Spain), we studied in detail the CIN85-Cbl interaction. In order to understand more about the complex formation between c-Cbl and CIN85, a peptide containing a PxxxPR motif of c-Cbl was co-crystallized with the first SH3 domain of CIN85. Interestingly, the Cbl peptide interacted simultaneously with two molecules of SH3 domains. This was in sharp contrast to other PxxxP-SH3 domain interactions that occur in 1:1 ratio. The crystallographic observation was reproducible in solution. Additionally, the formation of a trimeric complex between two SH3 domains from CIN85 and Cbl was confirmed in vivo by using co-immunoprecipitation of differentially tagged SH3 domain and full length CIN85 with Cbl[137]. In a similar fashion, a crystal structure of SH3 domain of a CIN85 related protein, CMS, was shown to interact with Cbl in a 2:1 stoichiometric ratio. Again, this was corroborated by in vivo work[194]. The relevance of such a trimeric complex on downregulation of EGFR was analyzed by using Cbl mutants that selectively abolish formation of trimeric complex while keeping 1:1 binding. Both Cbl and CIN85 are able to homo-dimerize.

These two works identified crucial residues in Cbl that are involved in the formation of a large complex endocytic machinery that is important for efficient clearance of the receptor from the plasma membrane. In these two reports, I contributed to characterizing the interaction of Cbl and CIN85 or CMS in vivo. Taken together, the fact that Cbl can interact with two SH3 domains, and that CIN85 can bind more than one Cbl molecule via its three SH3 domains shows that a large complex of the two proteins can form. The precise composition of the complex in vivo is still not understood and should be investigated further.

1.7 Aims of the current study

There are a number of proteomic investigations that described the list of proteins that interact with EGFR[195, 196]. These studies have looked primarily at the activated receptor following ligand binding. However, to the best of our current knowledge, a systematic approach to identify proteins that bind to EGFR in the absence of ligand stimulation has not been reported. Interestingly there are isolated reports of proteins that interact with the inactive receptor. For instance, it is known that the zinc finger containing protein ZPR1 binds to EGFR in the absence of ligand but dissociates from the receptor and translocates to the nucleus upon ligand binding[197].

Hence, one of the primary objectives of the current study is to identify the group of proteins that bind to EGFR in a ligand-independent manner using the MYTH screening system. Even though the MYTH has been used with success to study various transmembrane proteins, so far it has limited success with single pass TM proteins like RTKs. The lack of success is primarily due to problems with the proper folding of the bait receptor fusion protein and resulting degradation (*unpublished personal communications with Igor Stagljar*).

Hence the first objective of the present study is to optimize the screening strategy. Next validation of putative interactors as true EGFR binders will be performed by one-to-one yeast retransformation, co-immunoprecipitation in mammalian cells and supporting bioinformatic analysis. Furthermore, this study also seeks to address the molecular functions of select binding partners on EGFR function. In as much as signaling by EGFR is important, its proper regulation is of paramount significance. Hence, the interplay between the putative interactor and EGFR will be studied in terms of effect on EGFR signaling, trafficking and degradation.

Moreover, the influence of EGFR on the interactor will be investigated. This pertains primarily to the study of the phosphorylation status of the novel binder and to ascertain whether it is a target for the kinase activity of the receptor.

2. MATERIALS and METHODS

2.1 MATERIALS

2.1.1 Chemical compounds

All chemicals were, unless otherwise stated, purchased from Roth (Karlsruhe, Germany), Sigma-Aldrich (Taufkirchen, Germany), Merck (Darmstadt, Germany) or Baker (Deventer, the Netherlands).

Reagent	Source
Trichostatin A	Cell Signaling Technology (Beverly, MA USA)
Cycloheximide	Sigma-Aldrich ((Taufkirchen, Germany)
Taxol	Cytoskeleton Inc (Denver, CO, USA)
Phenylmethylsulfonyl fluoride (PMSF)	Roth (Karlsruhe, Germany)
Leupeptin	BioMol (Lörrach, Germany)
Aprotinin	Sigma-Aldrich
Sodium vanadate	Sigma-Aldrich
Bovine serum albumin (BSA)	Roth
1,4-diazabicyclo (2,2,2) octan (DABCO)	Fluka (Neu-Ulm, Germany)
Mounting medium	Biomeda (Foster city, CA, USA)
Ampicillin	Roth
Kanamycin	Roth

2.1.2 Recombinant proteins and speciality reagents

Reagent	Source
EGF (human, recombinant)	BD Biosciences (Bedford, MA, USA)
EGF-Alexa Fluor 488	Invitrogen (Karlsruhe, Germany)
EGF-Alexa Fluor 555	Invitrogen
GST-EGFR kinase domain (human, recombinant)	Abcam (Cambridge, UK)
HDAC6 (human, recombinant)	BioMol
Microtubules (bovine)	Cytoskeleton Inc.
^{125}I-EGF (human, recombinant)	Perkin Elmer (Jügesheim,

	Germany)
Lyticase	Sigma-Aldrich
ProteinA- agarose beads	Santa Cruz Biotech (Santa Cruz, CA, USA)
Mission® shRNA lentivirus	Sigma-Aldrich
Calf intestinal phosphatase	New England BioLabs (Ipswitch, MA, USA)
Restriction enzymes	Fermentas (St.Leon-Rot, Germany)
Pfu-Ultra polymerase	Roche (Mannheim, Germany)
Pwo polymerase	Roche
Precisionplus Dual stained protein marker	BioRad (Richmond, CA, USA)

Basic cell culture

Reagent	Source
Dulbecco`s modified Eagle`s medium (DMEM)	Gibco®, Invitrogen
Fetal calf serum	PAA Laboratories (Austria
Penicillin/Streptomycin	Gibco®, Invitrogen
Trypsin	Gibco®, Invitrogen
Puromycin	Roth
Geneticin	Gibco®, Invitrogen
Lipofectamine™	Invitrogen
FugeneHD™	Roche
Effectene™	Qiagen (Hilden, Germany)

Kits

Kit	Source
QIAfilter® plasmid Mini kit	Qiagen
QIAfilter® plasmid MIDI kit	Qiagen
QIAfilter® plasmid MAXI kit	Qiagen
Luminol chemiluminescence reagent	Santa Cruz Biotech (Santa Cruz, CA, USA)

2.1.3 Antibodies
Primary antibodies

Antibody	Source species	WB	IP	IF	Supplier
EGFR (RK2)	R	1:1000	1:100	-	*Home-made*
EGFR (528)	M	-	1:100	1:50	Santa Cruz
HDAC6 (227)	R	1:1000	1:100	1:100	*Home-made*
HDAC6 (H-300)	R	1:1000	1:100	1:50	Santa Cruz
Phospho-tyrosine (Py99)	R	1:1000	-	-	Santa Cruz
Tubulin Acetyl-Lys40	M	1:1000	-	-	Sigma-Aldrich
α-tubulin	M	1:1000	1:100	-	Sigma-Aldrich
Acetyllysine	M	1:1000	-	-	Cell signalling technology
Phospho-ERK1/2	M	1:500	-	-	Santa Cruz
ERK 1/2	R	1:1000	-	-	Santa Cruz
Phospho-Akt-Ser473	R	1:500	-	-	Cell signalling technology
Akt	R	1:1000	-	-	Cell signalling technology
Phospho-EGFR (Tyr1045)	R	1:1000	-	-	Cell signalling technology
FLAG M2	M	1:10000	1:500	-	Sigma-Aldrich
EEA1	R	-	-	1:100	*Home-made*
LAMP1	M	-	-	1:100	*Home-made*
Phospho-GSK3 Ser9		1:1000	-	-	Cell signalling technology
Phospho-PTEN Ser380		1:1000	-	-	Cell signalling
HA epitope tag	M	1:1000	1:100	-	Santa Cruz
His epitope tag	R	1:2000	-	-	Santa Cruz
MAP3K12	R	1:500	-	-	Abcam
α-adaptin	M	1:1000	-	-	BD Biosciences (San Diego, USA)

(M = mouse, R = rabbit, WB = Western blot, IF = Immunofluorescence, IP = Immunoprecipitation, HRP = horseradish peroxidase)

Secondary antibodies

Antibody	Source species	WB	IF	Supplier
Rabbit-HRP	Goat	1:2000	-	Dako (Glostrup, Denmark)
Mouse-HRP	Goat	1:5000	-	Dako
Rabbit-Cy3	Goat	-	1:500	Jackson Immunoresearch (Suffolk, UK)
Mouse-Cy5	Donkey	-	1:500	Jackson Immunoresearch
Rabbit-FITC	Goat	-	1:500	Jackson Immunoresearch

2.1.4 Buffers, solutions and media for routine use

Solution	Composition
SDS loading buffer	50mm TrisHcl, pH6.8, 2% SDS, 10% glycerol, 0.1% bromophenolblue 25mm DTT
SDS running buffer	192mm glycine 25mm Tris base 0.1% SDS
WB transfer buffer	192mM glycine 25mM Tris 20% methanol
WB blocking solution	5% BSA in 1x TBS-Tween

TBS-Tween	10mM Tris, pH 7.4
	100mM NaCl
	0.05% Tween 20
PBS	20mm NaH_2PO_4, pH 7.4
	150mm NaCl
Luria-Bertoni (LB) media	10g/L tryptone
	5g/L yeast extract
	10g/L NaCl
Z buffer (for X-gal test)	60mM Na_2HPO_4,
	40mM NaH_2PO_4,
	10mM KCl
	1mM $MgSO_4$.
Polyethyleneglycol (PEG)-lithium acetate master mix for yeast transformation per µg of DNA	240µl 50% PEG-4000
	36µl 1M Lithium acetate
	50µl single strand DNA (2mg/ml)
	34µl ddH_2O
YPAD medium	20g/L peptone
	10g/L yeast extract
	18g/L agar (for plates)
	2% glucose
Selective drop-out (SD) media	46.7g/L minimal SD agar base for plates or 46.7g/L minimal yeast nitrogen base + 1.4g/L yeast synthetic drop-out media supplement (-His, -leu, -Trp,- Uracil as needed)

2.1.5 Plasmids

EGFR encoding plasmid in the pRK5 vector background was made in the lab of Joseph Schlessinger (Yale University, CT, USA). The plasmids, pcDNA3 FLAG-HDAC6 wt and deletion mutants were kindly provided by Prof Tso-Pang Yao (Duke University, NC, USA). The yeast two-hybrid screen bait vector, MFα pAMBV, and the prey library (human fetal brain cDNA) were from Dualsystems Biotech

(Schlieren, Switzerland). FKBP38-HA is a kind gift of Keiichi Nakayama (Kyushu University, Japan). mCherry-tubulin wt was received from Frederic Saudou (Institut Curie, Paris), under permission from the creator, Roger Tsien (University of California at San Diego, CA, USA).

2.1.6 Oligonucleotides

Primer name	Sequence
MFα pAMBV for	GCACAATATTTCAAGCTATACCAAGCATACAATCAA CTCCAAGCAAAAATGAGATTTCCTTCAATTTTTACTG CAG
MFα pAMBV rev	GCCACTGGTTCGGCCCGGGCGAGCGAGTTTGGCCTG AATGGCCGGCTCTTTTATCCAAAGATACCCCTTCTTC
HDAC6 S568E for	AGTTCCAACTTTGACGAGATCTATATCTGCCCCAGT
HDAC6 S568E rev	ACTGGGGCAGATATAGATCTCGTCAAAGTTGGAACT
HDAC6 S568A for	AGTTCCAACTTTGACGCCATCTATATCTGCCCCAGT
HDAC6 S568A rev	ACTGGGGCAGATATAGATGGCGTCAAAGTTGGAACT
HDAC6 Y570E for	AACTTTGACTCCATCGAGATCTGCCCCAGTACC
HDAC6 Y570E rev	GGTACTGGGGCAGATCTCGATGGAGTCAAAGTT
HDAC6 Y570F for	AACTTTGACTCCATCTTTATCTGCCCCAGTACC
HDAC6 Y570F rev	GGTACTGGGGCAGATAAAGATGGAGTCAAAGTT

2.1.7 Cell lines, bacterial and yeast strains

The *E.coli* strain DH5α is from Invitrogen (Karlsruhe, Germany) and *E.coli* BL21 is from Promega (Madison, WI, USA). The *S.cerevisea* strain THY.AP40 is from Dualsystems Biotech (Schlieren, Switzerland). The cell lines used in the study, HEK293T, HeLa, A549 and A431 are derived from American Type Culture Collection (ATCC) in Rockville, MD, USA.

2.2 METHODS

2.2.1 Basic molecular biology techniques

2.2.1.1 Plasmid DNA transformation into *E.coli*

Plasmid DNA was transformed into competent *E.coli* strain DH5α by heat-shock treatment. Basically, 1μl of a 0.1μg/μl solution of DNA was incubated with freshly thawed bacteria for 15 minutes on ice, heat-shocked at 42°C for 45 seconds and chilled on ice for 2 minutes. 250μl of LB media added to the bacteria that were then incubated at 37 ^{o}C for one hour and plated on LB+Agar plates containing respective antibiotic (100μg/ml Ampicillin or 25μg/ml kanamycin). Twelve to sixteen hours later, bacterial colonies were picked and inoculated into desired amount of LB media with antibiotic.

2.2.1.2 Plasmid DNA extraction from bacteria

Plasmid purifications were done using Qiagen® Miniprep or Midiprep kits. For minipreps for instance, an overnight culture of DH5α was spun down at 4000g and resuspended in 250μl of resuspension buffer (50mM TrisHCl, pH 8.0, 10mM EDTA, 100 μg/ml RNase A). Bacteria were then lysed in 250μl of lysis buffer (200mM NaOH, 1% SDS) and neutralized with 350μl of 3M potassium acetate at pH 5.5. Precipitate was removed by centrifugation at 13,000g and supernatant loaded onto DNA binding columns. Columns were washed with   and ethanol. Finally, DNA is eluted with 10mM TrisHCl, pH 8.0, 1mM EDTA).

2.2.1.3 Plasmid DNA transformation into *S.cerevisae* using the lithium acetate method

A single colony of yeast strain is inoculated into 5ml of YPAD media and grown overnight at 30^{0}C with shaking. Next day, the optical density was measured at 600nm (OD_{600}) and diluted with appropriate amount of liquid YPAD media to reach final OD_{600} of 0.3. The yeast are then grown to an OD_{600} of 0.8, pelleted at 700g, then resuspended and washed in 10ml of sterile 1xTE, pH 8.0 (10mM Tris, 1mM EDTA). Yeast were pelleted again at 700g and resuspended in sterile H_2O in such a volume that each transformation will utilize 2ml of culture. 300μl of PEG-lithium acetate

master mix is then added to each transformation mix. 50μl of yeast are added to the transformation mix and vortexed vigorously for 1 min. Yeast are then heat-shocked at 42^0C for 15 min, pelleted at 700g, resuspended in 100μl H_2O and plated onto SD-Leu plate (for bait transformation) or SD-Trp (for prey transformation). Plates are incubated for 2-4 days at 30^0C to monitor growth.

2.2.1.4 Plasmid DNA extraction from yeast- the lyticase approach

5ml of yeast grown in liquid SD-Leu or SD-Trp media are pelleted at 4000g and resuspended in 30μl lyticase solution (in 0.9M sorbitol, 10mM TrisHCl pH 8, 0.1mM EDTA, 4,5 units/μl) and incubated at 37^0C for 1hr. Then 200μl yeast lysis buffer (2% TritonX-100, 1%SDS, 100mM NaCl, 10mM TrisCl pH8 and 1mM EDTA) added. After 5min, mixture centrifuged 12,000gfor 15min and supernatant loaded onto DNA binding columns of Qiagen Miniprep. The rest done basically as described for plasmid DNA isolation from bacteria.

2.2.1.5 Site-directed mutagenesis

C-terminal deletion constructs of pcDNA3-FLAG-HDAC6 and other point mutations were generated by site-directed mutagenesis using the specific character of the restriction enzyme DpnI to cleave only the methylated template DNA produced in bacteria. Basically, an oligonucleotide pair containing the desired nucleotide substitution is used as a primer set to amplify the template plasmid in a 50μl reaction volume with the high-fidelity polymerase, Ultra-Pfu. Later, the reaction mixture is incubated with 1μl of the enzyme DpnI and 10μl was transformed into competent DH5α bacteria. Colonies surviving on plates with appropriate antibiotics were used to purify plasmids that were sequenced to confirm the successful introduction of the desired mutations.

2.2.1.6 PCR amplification and restriction digestion of DNA

PCR reactions for amplification of cDNAs were performed in a Biometra thermocycler using Pfu or Pwo DNA polymerases. Typical conditions include 15ng of template, 10pmol of sense and antisense primers with 1μl of dNTPs, 5μl of PCR reaction buffer, 0.5μl enzyme to a final volume of 50μl. Restriction digestion of

plasmid DNA was performed in 25µl volume using diluted DNA with buffer and temperature as suggested by the manufacturer.

2.2.1.7 Preparation of MFα-EGFR-C-T construct

MFα-EGFR-C-T construct was generated by in vivo recombination in yeast. Briefly, cDNA encoding human EGFR was amplified by PCR with 60-mer primers having 5` ends (40 nucleotides) that are identical to the vector, thus allowing cloning into the vector by homologous recombination in yeast, and 3` 20 nucleotides specific to EGFR. Primers were designed in such a way that they amplify EGFR starting only from amino acid 25, and thus exclude the signal peptide. The PCR product and an empty and HindIII linearized MFα pAMBV vector were then transformed into the yeast strain THY.AP40. The yeast directs the homologous recombination and gap repair, resulting in the MFα-EGFR-C-T bait construct that imparts growth in selective media lacking leucine. Further confirmation of successful generation of bait construct was tested by colony PCR, where a loop full of yeast colony was boiled in PCR reaction solution and amplified with primers recognizing vector and bait.

2.2.2 Membrane-based yeast two-hybrid screen

For this screen the yeast reporter strain THY.AP40 (*MATa trp1 leu2 his3 LYS2::lexA-HIS3 URA3::lexA-lacZ*) was used. This strain has its *trp*, *leu* and *his* genes deleted and substituted with *LYS2*, *HIS3* and *lacZ* under control of lexA responsive promoter elements. For the large-scale screen, THY.AP40 was transformed with 1.5µg of the plasmid construct MFα-EGFR-C-T bait using the lithium acetate protocol to generate the bait-strain. Later, this bait strain was transformed with 28 µg of prey library using the above mentioned transformation protocol. The prey library was derived from fetal brain cDNA library and is fused C-terminally to NubG (NubG-X orientation).

Yeast were streaked on 30, 15cm plates containing highly selective media (SD Leu⁻Trp⁻His⁻Ade⁻) with 5 mM 3-aminotriazole (3-AT). Transformation efficiency was measured by streaking serially diluted amounts on SD Leu⁻Trp⁻ medium and was about 3 x 10^6 TRP^+ LEU^+ transformants. After 5 days of growth at 30^0C a total of 300 colonies were picked and transferred to SD Leu⁻Trp⁻His⁻Ade⁻ and SD Leu⁻Trp⁻ plates. The yeast growing on SD Leu⁻Trp⁻ plates were tested for activation of the *lacZ*

reporter (β-galactosidase) by X-gal filter lift-off assay. A 3MM Whatmann filter paper is layed on top of yeast growing on a plate. Yeast are "lifted-off" onto the filter paper which is briefly immersed in liquid nitrogen. The filter paper is then put in a plate and carefully covered with X-gal substrate solution. This is composed of Z-buffer, 0.3mg/ml X-Gal (20mg/ml stock diluted in Dimethylformamide) and 0.27% β-mercaptoethanol. Development of blue colour on the Whatmann paper up to 8 hrs was scored as positive.

Of the 300 colonies picked, 295 turned positive on X-gal test and also grew on SD Leu⁻Trp⁻His⁻Ade⁻. Plasmid DNA was extracted from all "positives" using the lyticase method. As plasmid DNA isolated from these yeast is of low quality and quantity, one more round of amplification was done by transforming into *E. coli* DH5 using standard protocols.

These library plasmids were individually retransformed into THY.AP40 expressing EGFR-C-T, TFRC-C-T or empty bait vector for the so-called "one-to-one" test. The transformants were again analysed for the activation of the *lacZ* reporter by X-gal filter lift-off assay and growth on SD Leu⁻Trp⁻His⁻Ade⁻ plates. Plasmids that activated the *HIS3* and *lacZ* reporters in combination with the EGFR-C-T bait were selected for sequencing and further studies.

2.2.3 Cell culture methods

2.2.3.1 Cultivation of mammalian cells

Mammalian cells were grown in an incubator (Heraeus) with 5% CO_2, 95% humidity at 37^0C. All the cells used in the study were grown in Dulbecco`s Modified Eagle Medium (DMEM) with 4.5g/l glucose, supplemented with 10% fetal calf serum, 5μg/l penicillin and 5mg/l streptomycin. Cell passage was facilitated by trypsinization (2-3min, 37^0C) with 0.05% (w/v) trypsin, 0.53mM EDTA in PBS. Growth media for A549 cells stably expressing HDAC6 shRNA is supplemented with puromycin (3μg/ml) and A431 cells expressing GFP-Rab5 with G418.

2.2.3.2 Transfection of mammalian cells

The transfection reagents used are Lipofectamine™ (Invitrogen) for HEK293T cells, Effectene™ (Qiagene) for HeLa and FugeneHD™ (Roche) for A549 cells. Briefly,

3×10^5 cells were seeded in each well of a 6-well dish one day before transfection. Plasmid DNA (from 0.1μg to 1μg) was diluted in serum free DMEM and then mixed with recommended amount of transfection reagent. Generally, 3μl of Lipofectamine™ or FugeneHD™ and 8μl of Effectene™ enhancer with 15μl of Effectene™ were used per 1μg of DNA. After 20min incubation, the DNA/reagent complex was added drop-wise onto cells. Adequate expression of desired protein was achieved within 24 hours.

2.2.3.3 Lentivirus transduction and stable shRNA expression cell line generation

Mission® Lentivirus transduction particles expressing four different shRNA sequences targeting the coding sequence of human HDAC6 and one shRNA against the 3`untranslated region (UTR) in the vector bacbone of pLKO.1-PURO were purchased from Sigma. These sequences were selected by a proprietary algorithm developed by the supplier and detailed information is sadly unavailable. Viral particles with shRNA sequence non-existent in the human genome were used as negative control. A549 cells were seeded in 24-well format and 24 hours later hexadimethrine bromide added to final concentration of 8μg/ml to increase transduction efficiency. Viral particles were added at 5, 10 and 20 multiplicity of infection (MOI). 72 hours later cell lysates were analysed for expression of HDAC6. However this transient transduction resulted in only minor knockdown of HDAC6. Hence, the experiment was repeated and 48 hours after transduction, puromycin (3μg/ml) was added to select for stable clones. After two weeks of propagation in selective media, cell lysates were prepared and tested for expression of HDAC6 by immunoblotting. Only one shRNA sequence transduced at 20 MOI resulted in marked knockdown, two in moderate knockdown of HDAC6 whereas the two other sequences failed to suppress expression of HDAC6.

2.2.3.4 Real time cell analysis (RTCA)

The real time cell analysis (RTCA) from Roche was made possible by the xCelligence device that uses electrodes to detect minor perturbations in current flow caused by cells. A549 parental and knockdown cells were seeded in the provided gold coated 96-wells at 1250, 2500, 5000, 10000 and 20000 cells per well in DMEM with only 0.3% fetal calf serum. After 16 hours, EGF (100ng/ml) was added and cells were

continually monitored for change in cell index (representing cell attachment or number) for 72 hours.

2.2.4 Biochemical assays

2.2.4.1 SDS-PAGE and Western blot

Separation of proteins in one dimension by electrophoresis was performed essentially according to standard protocols in 5-15% SDS polyacrylamid gels with 1mm thickness. Vertical mini-Protean® system (BioRad, Munich) was used in running buffer (25mM Tris, 250mM glycine pH 8.3, 0.1% SDS), at low constant 80V (initially, for the stacking gel) and 120V (for separation gel). Gels were then either stained with Comassie brillian blue R250/G250 or electroblotted using the wet system onto nitrocellulose membranes (0.45μm pore-size). Transfer was done at 200mA constant current for 60 to 120 min in transfer buffer (25mM Tris, 192mM glycine, 20% methanol, freshly added). Nitrocellulose membranes were stained with Ponceau S to assess transfer quality and blocked in blocking buffer (5% BSA in TBS-Tween) for 2 hours at room temperature or overnight at 4^0C. Blots were incubated with primary antibody in 5% BSA for 1 hour room temperature or overnight at 4^0C and then washed four times in TBS-Tween or Tx100, 10 min each. Afterwards, species-specific Horseradish peroxidase (HRP) conjugated secondary antibody was added in 5% milk in TBS-Tween for 40 min at room temperature. Blots were again washed four times in TBS-Tween or TBS-Tx100. Bound antibody was visualized by chemiluminescence using Western Blotting Luminol reagent (Santa Cruz), whereby an iridescent light is emitted during oxidation of luminol by HRP.

When re-probing with additional set of antibodies is required, blots were stripped of primary and secondary antibodies by incubating in 0.2M NaOH solution for 10 min.

2.2.4.2 Immunoprecipitation

HEK293T cells were transfected with the needed constructs. After 24 to 48 hours, cells were lysed for 20 min on ice in lysis buffer (50 mM HEPES, 150 mM NaCl, 1 mM EDTA, 1 mM EGTA, 10% glycerol, 1% Triton-X-100, 25 mM NaF, 10 M ZnCl$_2$, pH 7.5) containing protease inhibitors (2μg/ml aprotinin, 1μg/ml leupeptin, and 1mM PMSF) and the phosphatase inhibitor sodium vanadate. Cell lysates were

collected, centrifuged for 15 min (13,000 x *g*) to remove the insoluble fraction. Supernatant was incubated with the respective antibodies for 2 to 4 h at +4 °C followed by 1 hr incubation with 20μl of ProtA-Sepharose beads. The sepharose matrix was then washed three times either with RIPA buffer (50 mM TrisCl pH 7.4, 150 mM NaCl, 2 mM EDTA, 1% NP-40, 1% sodium deoxycholate, 0.1% SDS plus inhibitors) or with lysis buffer depending on downstream application. The final wash was removed via insulin needle to minimize loss of beads, which were then boiled in SDS loading buffer. The immunoprecipitated proteins were analysed by SDS-PAGE and immunoblotting using antibodies against other proteins to determine co-immunoprecipitation or with the antibody used for immunoprecipitation.

To detect acetylation, cells were treated with trichostatin A (TSA, 1μM) for 2-4 hrs to inhibit deacetylases, lysed, and immunoprecipitation was performed with the antibody against the protein of interest followed by immunoblotting with acetyllysine specific antibody.

2.2.4.3 GST-GATE16 purification and GST pull down assay

GST-GATE16 expressing plasmid was transformed into E.coli BL21 strain which were inoculated into 20 ml starter LB media with ampicillin overnight. Next day, the starter culture was used to inoculate 500ml media, and bacteria were induced at OD of 0.4 with 0.5mM IPTG. After 4 hours of growth, bacteria were spun down, washed in chilled PBS and frozen in -20^0C. They were thawed in buffer 1 (20mM Tris-HCl, pH 7.5, 10mM EDTA, 5mM EGTA, 150mM NaCl, 1mM PMSF, 0.1% β-mercaptoethanol), and broken by sonication. After centrifugation at 10,000g, supernatant was incubated with 500μl glutathione beads for 90 min at 4^0C. The beads were then washed with buffer 2 (buffer 1 plus 0.05% triton X100) to remove unbound proteins and resuspended in buffer 3 (20mM Tris-HCl, pH 7.5, 0.1% NaN$_3$). Purity was assessed by running 5 to 10μl of sample on SDS-PAGE and staining with Comassie. 10μl of beads bound to GST-GATE16 or GST were incubated with A431 cell lysates and washed in cell lysis buffer. Beads were boiled in SDS loading buffer, loaded on SDS-PAGE and Western probing done with EGFR antibody to detect if EGFR is pulled down specifically by GST-GATE16.

2.2.4.4 In vitro kinase assay

Recombinant full length human HDAC6 expressed and purified from Sf9 insect cells and GST-EGFR kinase domain were purchased from Biomol and Abcam respectively. An in vitro kinase assay was setup in kinase assay buffer (8mM MOPS, pH 7.0, 0.2mM EDTA, 10mM $MnCl_2$, 0.8M ammonium sulfate). Typical reactions (total volume 50μl) included 4μM of HDAC6, 2 to 20nM of EGFR kinase domain, 100μM ATP, incubated for 30 min at 30^0C. Control reactions were set up by eliminating ATP, EGFR or HDAC6. Reaction was stopped by boiling in SDS loading buffer and run on SDS-PAGE. Immunoblotting using phosphotyrosine (Py99, Santa Cruz) was used to detect presence of phosphorylated tyrosine residues.

2.2.4.5 Deacetylase assay

$2x10^6$ HEK293T cells were seed into 10cm plates and transfected with 5μg of FLAG-HDAC6. A day later, cells were lysed in 1ml of mammalian cell lysis buffer. FLAG-HDAC6 was immunoprecipitated by 4μg of M2-FLAG antibody followed by stringent washing in lysis buffer. While HDAC6 was still bound to ProteinA-sepharose beads, calf interstinal phosphatase was added in PIPES buffer (5mM PIPES pH 8.0, 85mM KCl), and washed away after incubation for 1 hr at 37^oC. Taxol stabilized microtubules (50 μg) were then added to the beads in 10 mM Tris-HCl, pH 8, 10 mM NaCl buffer and incubated for 2 h at 37^oC and chilled for 15 min on ice. Subsequently, the reaction mixtures were spun down, beads and supernatant separated, boiled in SDS loading buffer and subjected to western blot. Probing is done with HDAC6 antibody for the bead fraction and with acetyllysine antibody against the supernatant where free α and β-tubulin dimers are located.

2.2.4.6 Ligand induced EGFR degradation

$3x10^5$ A549 cells were seeded in each well of a 6-well dish. 24 hours later, they were transfected with 1μg of FLAG-HDAC6, deacetylase dead HDAC6 or HDAC6 deltaHEBD constructs. A day later, serum starvation started by growing the cells in DMEM supplemented with 0.3% fetal calf serum. After 16 hours, cells were pre-treated with cycloheximide (40μg/ml) for two hours and then stimulated with EGF (100ng/ml) for 0, 20, 40, 60, 120 or 180 minutes. Cells were lysed and centrifuged.

Total protein concentration of the supernatant was measured by a nano-spectrophotometer (Implen) at 280nm wavelength, and 30μg of protein loaded per lane in an SDS-PAGE. Total cellular levels of EGFR were then probed by EGFR antibody.

2.2.4.7 EGFR internalization assay using ^{125}I-labelled EGF
 as performed and described by Mirko Schmidt, Edinger Institute of Neurology, Goethe universitaet Frankfurt

 Chinese hamster ovary (CHO) cells were transiently transfected with EGFR together with wt or deacetylase dead HDAC6 constructs or with GFP vector as a negative control. Forty-eight hours later, 50 ng/ml EGF was added to induce receptor trafficking at 37°C for 10, 20, 30 and 60 min and transferred on ice. Subsequently, the amount of EGFR molecules still left at the cell surface was determined by removal of receptor bound EGF by mild acidic treatment and incubation with 1ng/ml ^{125}I-labelled EGF for 1.5 hours. Following vigorous washing, cells were lysed and samples analyzed with a gamma-counter (1470 Wizard, Perkin Elmer). The percentage of surface receptor was calculated by comparison to samples challenged with EGF on ice only.

2.2.4.8 Mass spectrometry sample preparation
$1x10^7$ A549 cells were grown in 15cm dishes, serum starved for 16 hours and left untreated or stimulated with EGF (100ng/ml) for 30 min. Cells were lysed and immunoprecipitation done using α-tubulin antibody. Samples were run on SDS-PAGE, Comassie stained and a band corresponding to tubulin was cut out. Similarly, FLAG-HDAC6 was transfected in HeLa cells, immunoprecipitated from lysates, run on an SDS-PAGE, Comassie stained and bands corresponding to estimated size were cut of of the gel and subjected to mass spectrometry to identify phosphorylated residues.

(Mass spectrometric analysis - as performed and described by Blagoy Blagoev, University of Southern Denmark, Odense, Denmark)- Tubulin containing gel bands were cut out from the SDS-PAGE and subjected to reduction and alkylation with 10 mM dithiothreitol and 55 mM iodoacetamide (Sigma–Aldrich), respectively. Bands were subsequently washed with 50 mM ammonium bicarbonate and in-gel digested

with endoproteinase Asp-N (Roche, Penzberg, Germany) for 16 h at 37°C. Samples were analyzed by online C18-reverse-phase nanoscale liquid chromatography tandem mass spectrometry essentially as described. Briefly, analysis were preformed on an Agilent 1200 nanoflow system (Agilent Technologies, Boeblingen, Germany) connected to a LTQ-Oribitrap XL (ThermoFisher, Bremen, Germany) equipped with a nanoelectrospray ion source (Proxeon Biosystems, Odense, Denmark). The MS/MS spectra were centroided and searched with Mascot (MatrixScience, London, UK) against the human IPI protein database. Search parameters included mass tolerance of 6 ppm for peptides and 0.6 Da for fragments, Carbamidomethyl (C) as fixed modification and Oxidation (M) and Acetyl (K) as variable modifications. The intensities of the acetylated Lys40-containing peptide derived from the non-stimulated and EGF stimulated cells were used to calculate a ratio reflecting the relative levels of Lys40 acetylation between the two samples. The intensity ratios of seven distinct non-modified Tubulin peptides were used for normalization.

2.2.5 Cell imaging studies

2.2.5.1 Immunofluorescence microscopy

1×10^5 A549 cells (parental and HDAC6 knockdown) were grown on cover slips for one day before starting starvation by changing media to DMEM with only 0.3% serum. After 16 hours, cells were pulsed with Alexa488-EGF (100 μg/ml) for 30 sec and chased for 0, 1, 2, 3, 5, 7, 10, 20, 30, and 60 min with unlabelled EGF. Cells were fixed with 4% paraformaldehyde for 15 minutes and permeabilised for 10 minutes in permeabilization and blocking buffer (0.1% saponin w/v, 0.2% gelatin w/v, 0.02% sodium azide, 5mg/ml BSA). Cells were then incubated with EEA1 and LAMP1 primary antibodies in saponin/gelatin buffer (0.01% saponin w/v, 0.2% gelatin w/v, 0.02% sodium azide) for one hour. After three, five-minute washes with PBS; secondary antibodies (Cy3 anti-rabbit, Cy5 anti-mouse) in saponin/gelatin buffer were added and incubated in the dark for one hour. Following washing steps as above, DAPI (1:1000) was added and coverslips were mounted in Dabco/Moviol mounting media. Four channel images (EGF- channel 488, EEA1- channel 563, LAMP1- channel 668, Nucleus- UV channel) with Z-stacks were taken by Carl-Zeiss 510 UV confocal microscope. All cover slips were imaged at the same laser output and in a

single batch to minimize laser fluctuations, with at least 10 representative fields having a minimum of 10 cells per experimental point. After image acquisition, with the help of manual inspection parameters and cut-off points for MotionTracker® program were determined. All images were then analysed by the software for position, size, signal intensity and overlap. The data generated was fed into the Supercomputer service at the Technical University of Dresden for data crunching. Afterwards, desired parameters were statistically analysed and graphed by the in-built application in MotionTracker®.

2.2.5.2 Live cell imaging

$1x10^5$A431 cells stably expressing GFP-Rab5 were seeded in glass bottom dishes. One day later, they were transfected with 100ng of plasmid encoding mCherry-tubulin wt or the dominant negative mCherry-tubulin K40A. 24 hours later, cells were imaged in a live cell chamber (CO_2 and temperature regulated). Imaging was done using a custom assembled microscope at the Max-Planck-Institute for Cell Biology and Genetics in Dresden, Germany. The microscope uses spinning-disc technology for laser beam focusing and connected with a high-speed camera for image acquisition. Cells were imaged for 5 minutes (4 images per Z-stack, 2 stacks per second). Z stacks were collapsed by maximum projection and minimum of 10 cells were followed for each experimental condition. Individual endosomes were identified and tracked for the duration of the imaging. Fluorescence tracing with intensity were quantified for individual GFP-Rab5 endosomes by MotionTrack® software. Statistical analysis was done to arrive at cumulative average speed and processive movement of vesicles essentially as in Rink et al.

2.2.6 Bioinformatic analyses
(detailed analysis by Igor Jurisica, University of Toronto, Toronto, Canada)

All proteins from MYTH screen were mapped into SwissProt identifiers, and integrated with protein-protein interactions (PPIs) in Interologous Interaction Database (I^2D) version 1.71 (http://ophid.utoronto.ca/i2d). Mapping was done using the source databases: the International Protein Index version 3.36 (IPI, http://www.ebi.ac.uk/IPI/), SwissProt version 51.5, Unigene Hs.208, and Entrez Gene 2007-02-08. Interactions in I^2D integrate interactions from human curated sources, high-throughput mammalian experiments, and predicted PPIs using orthologs from

model organism protein interaction data sets, as previously described [198, 199]. Computational evidence provided support to the experimentally-derived PPIs using the following procedure, performed essentially as previously described [198]. First, a domain-domain co-occurrence matrix was constructed by extracting all InterPro domains from UniProt version 9.5, and enumerating the number of times each domain pair occurs between proteins known to interact, or those that have not been experimentally demonstrated to interact. Domain pairs that occur more frequently between interacting proteins were identified using the hypergeometric distribution with a Bonferroni-corrected alpha level of 0.05. The resulting domain-domain co-occurrence set included 10,391 domain pairs significantly enriched in known human PPIs. Second, gene co-expression was calculated using the Pearson correlation between genes encoding the interacting proteins from the GeneAtlas expression compendium [200], which profiles gene expression on 79 human tissues. Finally, functional similarity was computed for all PPIs using Gene Ontology (GO) annotations [201]. Briefly, GO terms were retrieved from the UniProt database (version 9.5) for each of the interacting proteins, and the semantic similarity [202] was computed.

In order to establish a threshold above which the aforementioned evidence was statistically significant, 65,535 random protein pairs were selected from the set of proteins that comprise the known human interactome. Each evidence type was computed for every random protein pair, and the threshold for statistical significance was derived from the 95% confidence interval of the resulting distributions.

Protein-protein interaction network was visualized using NaViGATor ver. 2.02 (http://ophid.utoronto.ca/navigator).

3. RESULTS

3.1 MYTH based screening of ligand-unoccupied EGFR.

3.1.1 Generation of bait EGFR-Cub-TF construct

The first step in any yeast two-hybrid screen is the generation of a suitable bait construct expressing the desired protein fused in-frame with the appropriate transcription factor. For this study the full length human EGFR was initially fused to the Cub-TF moiety that comprises of the C-terminus of ubiquitin plus an artificial transcription factor composed of the DNA binding domain of LexA and the transactivation domain of VP16. Unfortunately, expression of this fusion protein in yeast caused a strong self-activation phenotype and the protein was markedly degraded in vivo (Fig. 6B and 6C) rendering it unsuitable for screening purposes. Therefore, a modification was necessary. In order to facilitate insertion of the heterologous human protein into yeast membrane, the signal peptide of human EGFR (comprising aa 1-24) was deleted and substituted with the first 85 amino acids of the yeast mating factor α (MFα) pheromone followed by the Cub-TF fragment (Fig. 6A). Subsequently, various experiments were undertaken to verify transformation, expression and localization of the bait protein in yeast.

Immunoblotting analysis using crude protein extracts from the yeast strains showed that a major single band representing the MFα-EGFR-C-T fusion protein at approximately 180 kDa is seen (Fig. 6B, lane 3), but not in the case of the full length receptor fusion protein, EGFR-C-T (Fig 6B, lane 2) showing it is a stable protein. Next a genetic assay was done to ensure that the MFα-EGFR-C-T bait protein is properly inserted into the membrane (the so-called NubI test) and not self-activated (NubG test) [188, 189]. For this purpose, the MFα-EGFR-C-T bait was analyzed in the presence of two non-interacting yeast integral membrane proteins, the ER membrane protein Ost1p and the plasma membrane protein Fur4p, fused to either NubI (Ost1-NubI and Fur4-NubI) or NubG (Ost1-NubG and Fur4-NubG) (Fig. 7A). The constructs Ost1-NubI and Fur4-NubI are designed to activate the yeast reporter system constitutively (positive controls) because of the high affinity of NubI to associate with Cub into active ubiquitin irrespective of a protein-protein interaction[187].
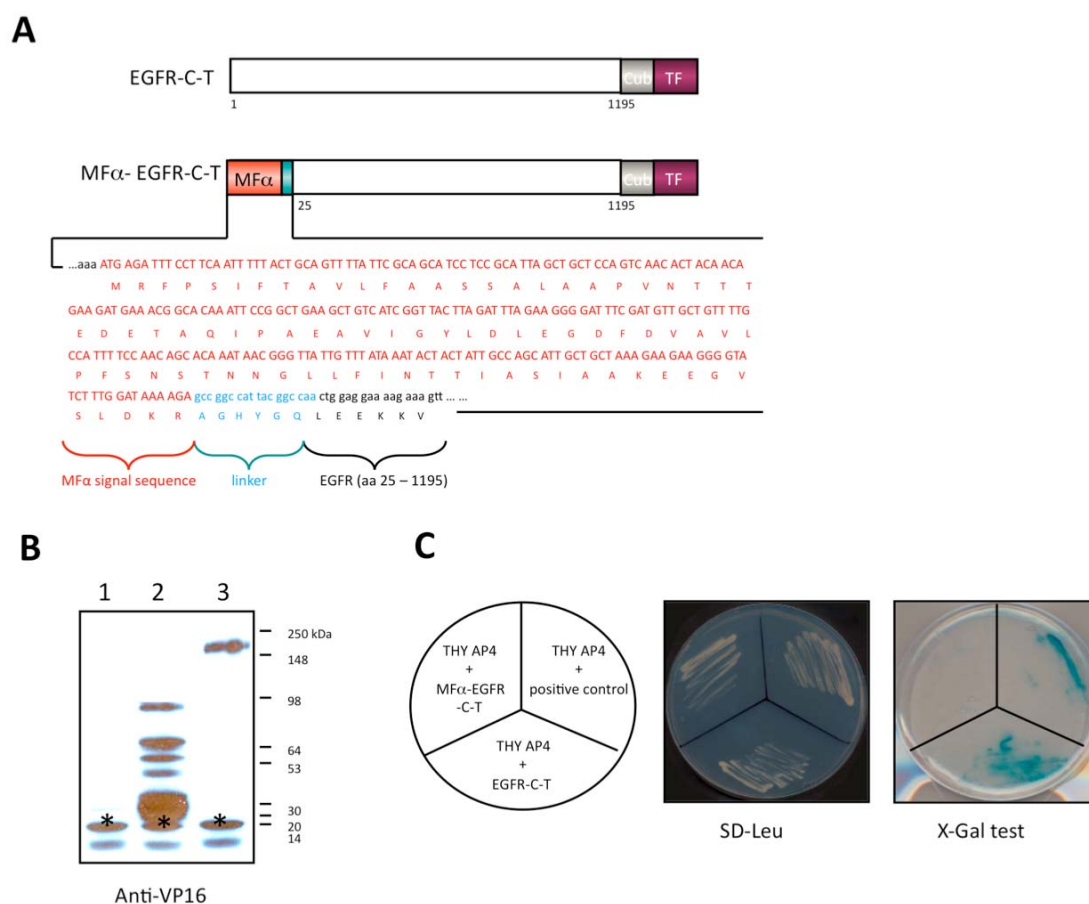
Figure 6. MFα-EGFR-C-T is a stable and non-self-activating bait for use in MYTH screens.
(**A**) Design of the EGFR bait construct for MYTH screening. The EGFR-C-T construct encodes its endogenous signal sequence and the full-length EGFR protein (aa 1-1195) fused at the C-terminus to Cub-TF (C-T). The second construct, MFα-EGFR-C-T, was modified to include the yeast mating factor α pheromone precursor (MFα) signal sequence (aa 1-85) and amino acids 25 through 1195 of the EGFR protein fused at the C-terminus to C-T. (**B**) Western blot of total protein of yeast THY.AP4 cells transformed with empty bait vector (pMFα-AMBV.4, lane 1), the EGFR-C-T construct (lane 2), or the MFα-EGFR-C-T construct (lane 3), probed with an α-VP16 polyclonal antibody. (*) in lanes 1-3 indicate the presence of unspecific proteins. (**C**) Self-activation test for the EGFR bait constructs. THY.AP4 cells were transformed with a positive control vector (pLexA-VP16) and the two EGFR bait constructs, EGFR-C-T and MFα-EGFR-C-T. Yeast were grown on SD-Leu and Xgal plates. MFα-EGFR-C-T construct is not self-activating.

The MFα-EGFR-C-T bait protein showed a positive signal in the presence of both NubI membrane protein fusions, indicating that it is properly inserted into the ER and plasma membranes. On the other hand, expression of the MFα-EGFR-C-T bait fusion with the non interacting Ost1-NubG and Fur4-NubG protein fusions (negative controls) did not lead to activation of the reporter system, showing that the MFα-EGFR-C-T bait is not self-activating (Fig. 7A).

Furthermore, membrane targeting of the MFα-EGFR-C-T bait was analyzed in yeast lysates after sequential high-speed centrifugations. The endogenous yeast ER membrane protein Wbp1p and a cytosolic Gpd1p were included in this assay to validate the cell fractionation procedure. As shown in the Fig. 7B, the MFα-EGFR-C-T bait was found exclusively in the membrane and not in the cytosolic fraction of yeast lysates. Another important parameter checked was whether the expressed MFα-EGFR-C-T is phosphorylated on tyrosine residues and thus activated. By using anti-phosphotyrosine antibodies, the EGFR or other yeast proteins were not detected to be tyrosine phosphorylated in yeast lysates expressing MFα-EGFR-C-T bait (Fig. 7C). In summary, the results of these biochemical and genetic experiments strongly suggest that the above-mentioned N-terminal modification of the human EGFR yields a non-phosphorylated EGFR-C-T bait protein that is properly inserted into the yeast membrane, thereby minimizing its self-activation problems. Furthermore, MFα-EGFR-C-T bait localization was analyzed by immunofluorescence and was found predominantly in the plasma membrane of yeast cells (Fig. 7D).

3.1.2 MYTH screening using MFα-EGFR-C-T

To identify EGFR-interacting partners, the MFα-EGFR-C-T construct was used as a bait protein in large-scale MYTH screens. A cDNA library derived from human fetal brain tissue fused to NubG in the orientation NubG-X was used as the prey library. From approximately 3×10^6 yeast transformants tested in total, 300 grew in selective media lacking histidine and adenine. Further X-Gal test narrowed down the positives to 295 colonies. Subsequently, the specificity of these interactions was evaluated through the bait-dependency test. This test is designed to rule out false positive prey clones by retransforming each prey cDNA into yeast together with either the bait, a negative control protein that is known to have distinctly different localization or the empty vector. This is particularly helpful if the prey clone has a propensity to non-specifically bind to parts of the fusion protein like the transcription factor or simply self-activates the expression of reporter genes.
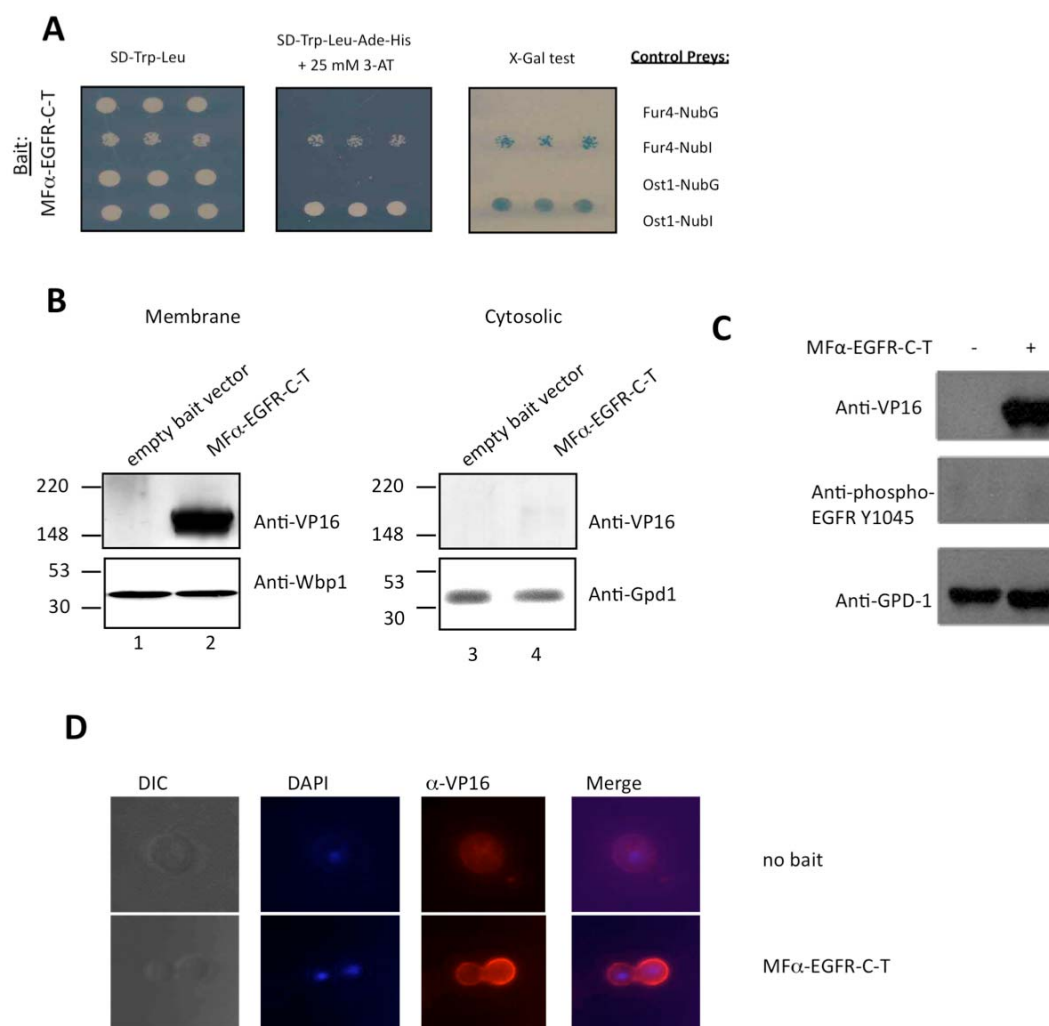
Figure 7. MFα-EGFR-C-T is properly inserted into membranes and is not tyrosine phosphorylated. (A) NubG/NubI assay. THY.AP4 cells were co-transformed with the bait construct, MFα-EGFR-C-T, and the testing vectors as listed (Fur4-NubG/I and Ost1NubG/I). Growth was assayed by spotting three independent transformants on SD-Trp-Leu-Ade-His and X-gal plates with two different yeast integral membrane proteins fused to NubG confirms that MFα-EGFR-C-T is not self-activating. Growth on the same plates with NubI constructs indicates that the modified construct is expressed and the protein is properly inserted into the membrane. **(B)** Western blot of yeast lysates harboring either an empty vector (lanes 1 and 3) or the MFα-EGFR-C-T bait construct (lanes 2 and 4) were subjected to two consecutive ultracentrifugations to segregate the cytosolic (lanes 3 and 4) from the detergent-soluble membrane fractions (lanes 1 and 2). Bait protein was detected by a α-VP16 polyclonal antibody. Controls used are the endogenous yeast ER membrane protein Wbp1p and the cytosolic Gpd1p. **(C)** MFα-EGFR-C-T bait protein is not phosphorylated in yeast. Lysates from yeast transformed with either an empty vector (lane 1) or MFα-EGFR-C-T bait construct (lane 2) were subjected to Western blotting and probed with phospho-EGFR 1045 to determine if the receptor is phosphorylated in yeast. Gpd1p antibody was used as a loading control.

(D) Fluorescence images were taken by confocal microscopy exhibiting the localization of the MFα-EGFR-C-T bait in yeast. Yeast cells expressing bait or empty vector were fixed, and acetone-treated spheroblasts were probed with rabbit anti-VP16 antibody and visualized by Cy3-conjugated anti-rabbit antibody (red). DAPI staining (blue) located the nucleus of yeast cells.
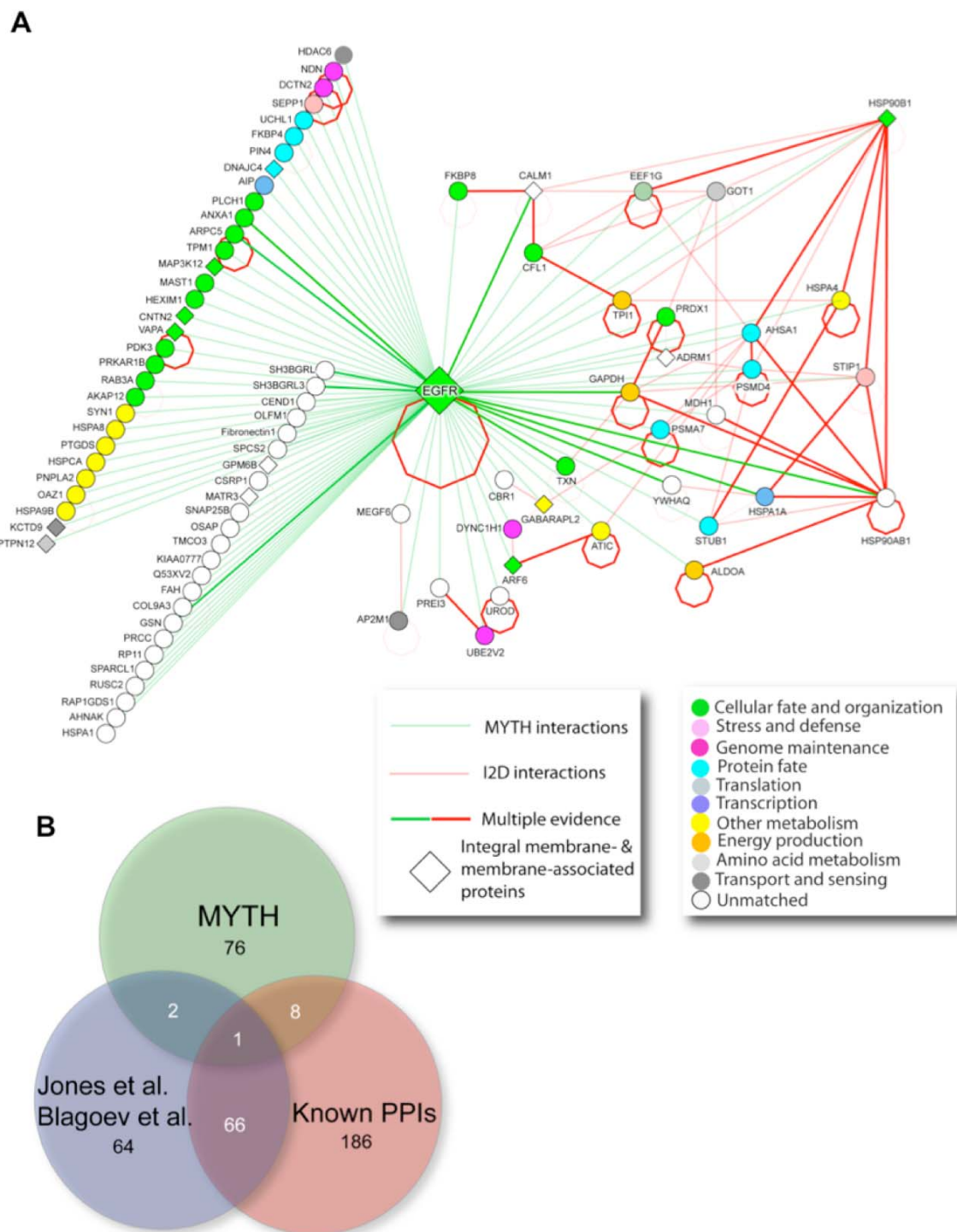
Figure 8. Application of a modified MYTH system to the human EGFR.
 (**A**) EGFR-interactome identified using a modified MYTH. All proteins from MYTH screen were mapped into SwissProt identifiers, and integrated with interactions in I^2D version 1.71 (http://ophid.utoronto.ca/i2d). The interactions identified are rendered using NAViGaTor 2.02 (http://ophid.utoronto.ca/navigator). Node color corresponds to the GeneOntology, as shown in the legend. Diamond nodes represent membrane-associated and integral membrane proteins. Edge color corresponds to source of interaction; green represents MYTH interactions, while red corresponds to I^2D interactions. Thicker edges signify multiple sources for a given interaction.
(**B**) Venn diagram showing the intersection of 402 EGFR interactions from the three main sources – two published reports (*5, 6*) known interactions from I^2D version 1.71 (http://ophid.utoronto.ca/i2d), and MYTH.

In this case, using human transferrin receptor (TFRC) as a negative control, it was ensured that the prey proteins interacted specifically with EGFR due to their affinity for the original bait (MFa-EGFR-C-T). The bait dependency screen refined the number of EGFR-interacting proteins to 87 that were further evaluated by bioinformatics, biochemical and functional tests.

The proteins comprising the EGFR-MYTH-interactome fall into multiple GeneOntology biological function groups as depicted in Fig 8A. These include those that play a role in cell fate and organization (green nodes), metabolism (yellow and green nodes), protein degradation (light blue nodes) and proteins with yet undefined functions (white nodes). Fourteen of the EGFR-interacting partners are annotated as either integral membrane or membrane-associated proteins thus clearly demonstrating the utility of the modified MYTH system for the identification of membrane proteins as EGFR binding partners. To see how this screen fares in relation to other approaches, the data was compared with data from other studies. The venn diagram in Fig 8B shows the comparison of the MYTH isolated proteins with previous proteomic studies on EGFR[195, 196]. There were only 3 common proteins between these two studies and the MYTH where as 8 more overlapping interactions were documented in the manually curated protein-protein interaction database.

To further annotate and support observed protein interactions, computational tools were used. With the help of the bioinformatician Igor Jurisca (University of Toronto, Canada), significant domain-domain co-occurrences, gene co-expressions, and computed functional similarity of interacting protein pairs were identified.

The proteins from the MYTH screen were compared with protein-protein interactions described in protein binding databases that represent experimentally verified interactions (both low- and high-throughput assays in mammalian and other organisms). These computations yield more support for the validity of the screen. First, domain pairs that occur in proteins that interact were compared to domains that occur in non-interacting proteins creating the so-called domain-domain co-occurrence matrix[198]. Application of this matrix to the MYTH result supported 34 of the interactions identified (Fig. 9). Secondly, functional similarity was computed for all protein-protein interactions using Gene Ontology (GO) annotations [201] by taking about 65000 random protein pairs from the human genome. Of the novel interactions

identified, 62 fall within the 95% confidence interval of the resulting distribution. Take together, the above investigations in yeast and *in silico* provide more support for the validity of the MYTH. However, in order to see if the results are relevant in the context of mammalian cells, further assays were done.
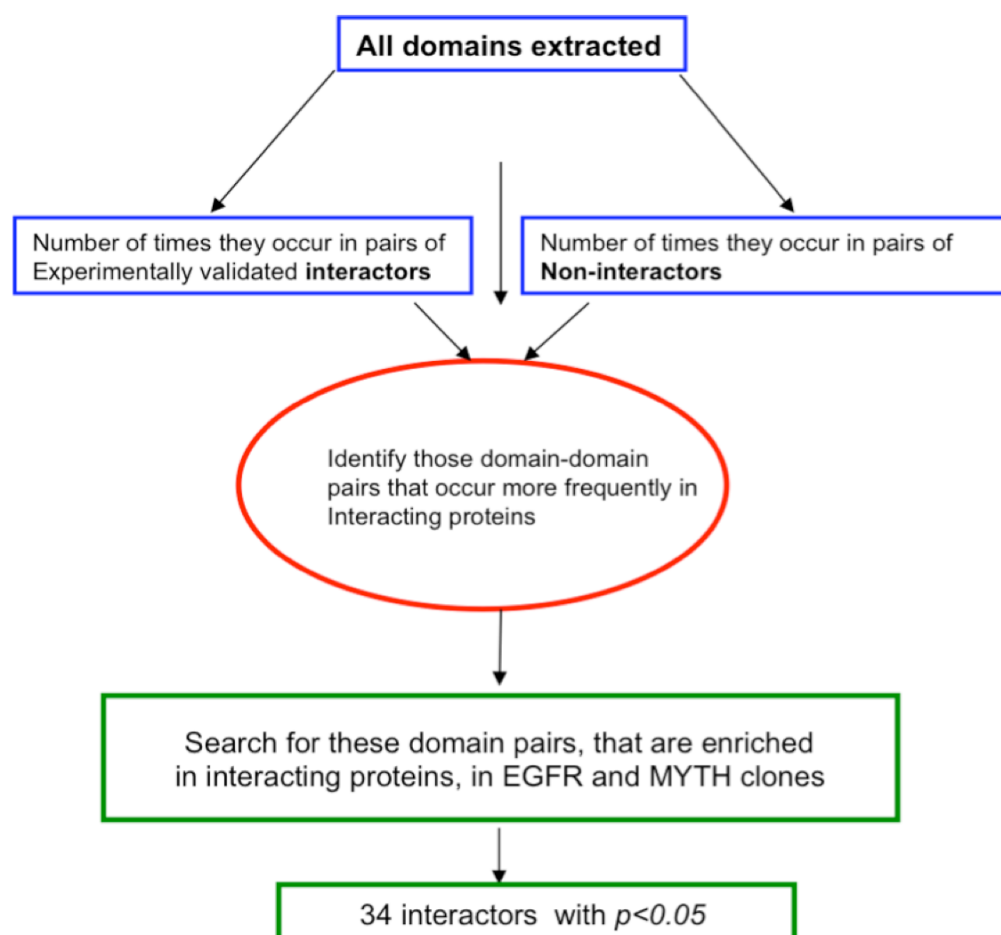
Figure 9. Flow chart of bioinformatic analysis of putative MYTH interactors. Domain pairs that occur more frequently between interacting proteins were identified by generating domain-domain co-occurrence matrix. This was done by taking all reported protein-protein interactions (PPIs) and for every interacting protein pair, each domain from protein A was connected to the domains in protein B. The frequency of these domain pairs was determined for all interacting protein pairs ($n = 16\ 107$), as well as all non-interacting pairs (i.e. all proteins not reported to interact in PPI databases; $n = 1.8 \times 10^7$). Statistical analyses was used to determine which domain pairs were enriched in interacting protein pairs compared to the non-interacting pairs. Finally, a search was done for these domain pairs between EGFR and MYTH clones.

3.1.3 Biochemical validation of putative interactions

To demonstrate specific binding of the MYTH clones to EGFR in mammalian cells several approaches were used. To assess whether the isolated clones are found in

complex with EGFR and whether this association was in any way affected by ligand binding A431 cells were used. This cell line is derived from human epidermoid carcinoma, expresses sufficient amount of EGFR and has been used extensively in studying EGFR signalling[203]. Cells were grown in normal growth medium for 24 hours followed by 24 hours of serum starvation. Subsequently cells were stimulated with EGF (100ng/ml) for 5, 15, 60 minutes or left unstimulated. Cell lysates were subjected to immunoprecipitation with antibody to EGFR. Resulting blots were probed with antibodies to the respective proteins identified in the screen. It is important to note that the lack of good antibodies for many of the less characterized proteins hampered the effort to study most of them.

Nonetheless, several putative interactors were validated for their ability to bind to EGFR in these cells. Histone deacetylase 6 (HDAC6), α-adaptin, HSP70, and MAP3K12 were co-immunoprecipitated with endogenous EGFR in non-stimulated cells (Fig. 10A). The results showed that HDAC6 is constitutively bound to the receptor before and after ligand stimulation. On the contrary, the interaction with -adaptin was progressively increased upon receptor stimulation, whereas that of MAP3K12 and HSP70 transiently increased after five minutes only to decline to the basal level after one hour.

For those proteins whose endogenous study was not successful, overexpression and co-immunoprecipitation was done. EGFR, along with 14-3-3θ-His or FKBP38-HA, was expressed in HEK293T cells. 14-3-3θ is co-immunoprecipitated by EGFR antibody (Fig 10B, right panel). Similarly, immunoprecipitation with either EGFR or HA antibody showed that FKBP38 and EGFR can associate together (Fig. 10B, lower panel). In a different approach, the bacterially expressed and purified GST-GATE-16 fusion protein efficiently pulled down EGFR whereas GST alone did not (Fig. 10C).

Taken together, it was possible to show that several of the novel putative EGFR interactors were indeed EGFR binders in mammalian cells. Furthermore, the combination of studies in yeast, cell culture and supporting bioinformatics strengthen the conviction in the quality of data generated from the membrane yeast two hybrid screen.
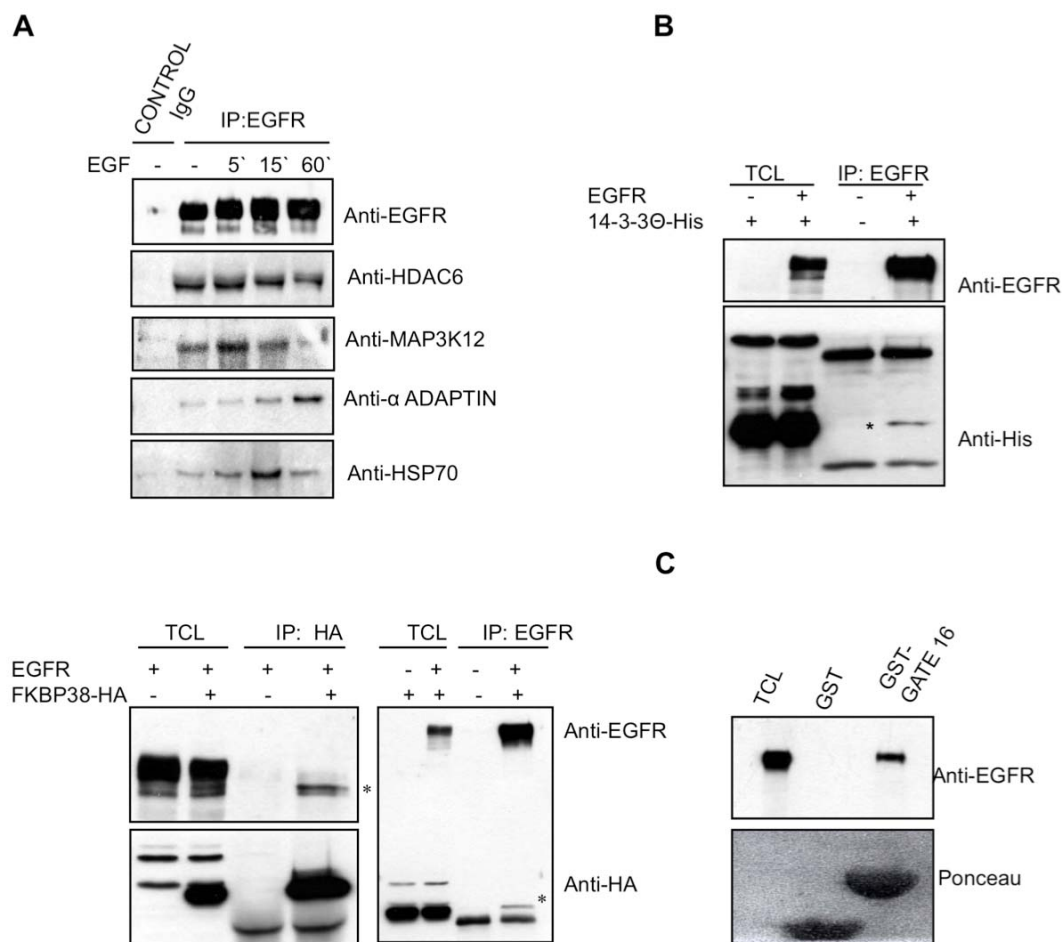
Figure 10. Several putative EGFR interactors identified by MYTH bind to the receptor in mammalian cells. (A) HDAC6, MAP3K12, α-adaptin, HSP70 associate with endogenous EGFR. A431 cells were serum starved overnight and left non-stimulated or stimulated with EGF for 5, 15 or 60 min. Immunoprecipitation (IP) was done using EGFR antibod and probed with indicated antibodies. Probe with EGFR antibody after stripping membrane shows equal efficiency of immunoprecipitation. **(B)** 14-3-3θ and FKBP38 interact with EGFR. HEK293T cells were transfected with plasmids encoding EGFR and 14-3-3θ-His (upper panel) and FKBP38-HA (lower panel). Cell lysates were subjected to IP by anti-His, anti-HA or EGFR antibody and probed as shown. Total cell lysates (TCL) indicate expression of each protein analysed. (*) indicates co-IPed proteins. **(C)** For GST- pulldown assay, GST-GATE16 fusion protein was purified from bacteria, coupled to Sepharose beads and incubated with lysate of A431 cells. Blot was probed using EGFR antibody.

3.2 Interaction between the cytoplasmic deacetylase HDAC6 and EGFR

One of the interesting proteins identified in the screen was histone deacetylase 6 (HDAC6). As its initial cloning was based on domain similarity search with already established yeast histone deacetylase[153], it is stuck with the rather misleading name of

"histone" deacetylase. However, its localization and so far described functions clearly show it to be a cytoplasmic lysine deacetylase[146, 156, 165].

Hence, the identification of HDAC6 in the MYTH screen opened the door to a number of speculative thoughts. EGFR undergoes a number of post-translational modifications that regulate its function such as phosphorylation and ubiquitylation. In the same context, could acetylation be an additional modification in EGFR? Or is there another protein in complex with EGFR that is acetylated? These highly provocative ideas encouraged the rest of the work to be focused on the study of the interplay between HDAC6 and EGFR.

3.2.1 HDAC6 binds to EGFR

In order to confirm the initial observations from the screen, NubG-HDAC6 construct was transformed into yeast expressing MFα-EGFR-C-T or transferrin receptor Cub-transcription factor (TFRC) as bait proteins. Strongly positive X-gal test and growth on highly selective media showed that HDAC6 interacts with MFα-EGFR-C-T (Fig. 11A, left panel) but not with TFRC (Fig. 11A, right panel). Positive interactions of both MFα-EGFR-C-T and TFRC with the plasma membrane resident yeast protein (Fur4-NubI) show that they are properly expressed and inserted into the plasma membrane. In this assay, the known EGFR interactor glyceraldehyde-3-phosphate dehydrogenase (GAPDH) acted as positive control. Fur4-NubG and GABA1β1A are negative controls showing the specificity of EGFR-HDAC6 binding.

To see if this apparent interaction is also evident in mammalian cells, FLAG-HDAC6 and EGFR were overexpressed in HEK293T cells. Co-immunoprecipitation clearly showed that HDAC6-FLAG and EGFR are able to interact (Fig. 11B). Furthermore, similar observation can be reproduced at endogenous levels. Lysates from A431 cells growing at steady state (Fig. 11C) or starved and stimulated with EGF (Fig. 10A) were immunoprecipitated with HDAC6 or EGFR antibody. In both cases antibodies to EGFR and HDAC6, but not a rabbit pre-immune serum, were able to co-immunoprecipitate HDAC6 and EGFR respectively. Interestingly, the interaction between HDAC6 and EGFR is not modulated by ligand stimulation to any discernible extent (Fig. 10A). Importantly, HDAC6 was able to co-immunoprecipitate

catalytically dead EGFR mutant, EGFR K721A (Fig. 11D), showing activation or tyrosine phosphorylation of EGFR is not required for efficient interaction.
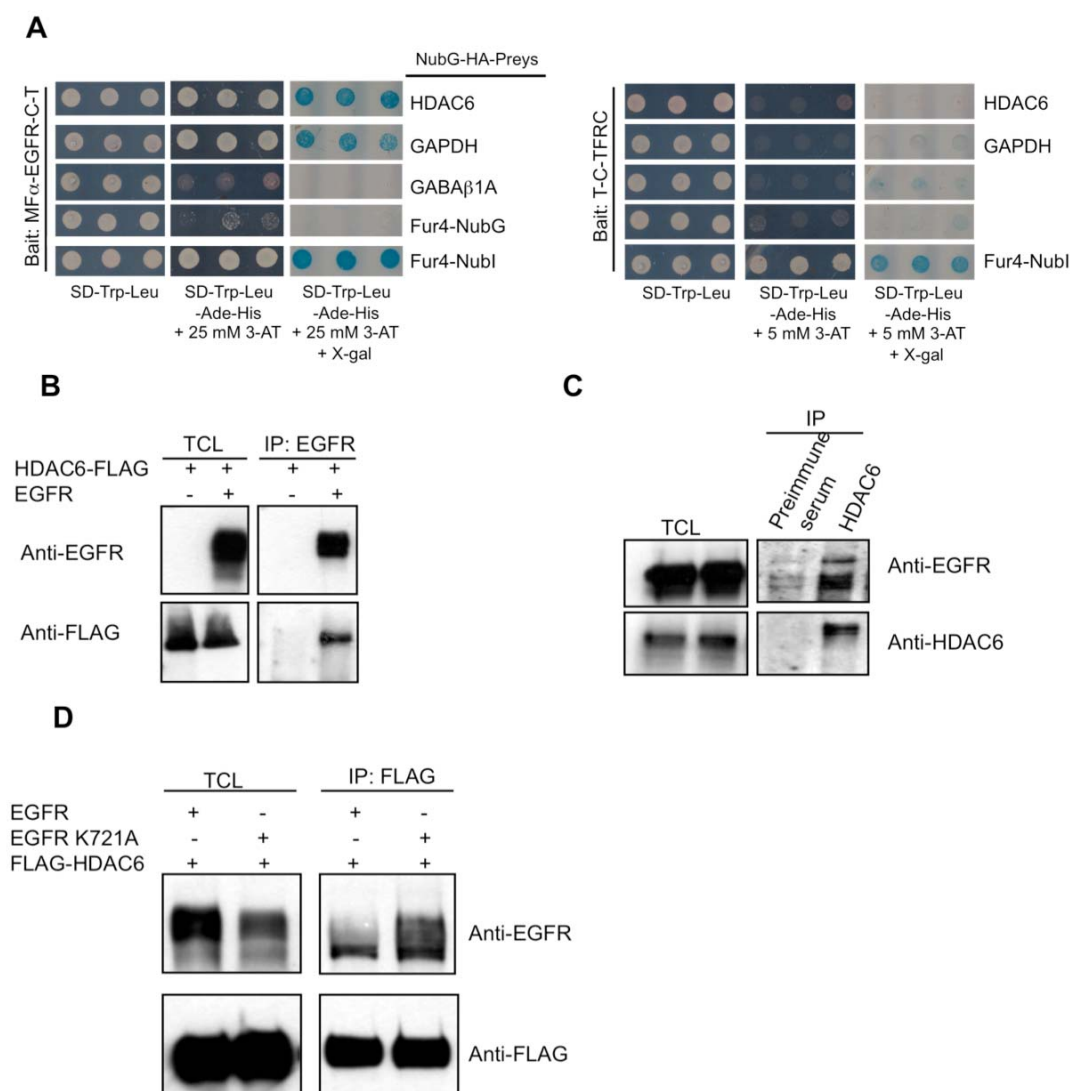
Figure 11. HDAC6 is a novel EGFR interactor. (**A**) Bait-dependency test. The isolated NubG-HDAC6 prey plasmid was transformed into the THY.AP40 strain expressing MFα-EGFR-C-T (left panel) and human transferrin receptor (T-C-TFRC fusion, right panel). Yeast growth was assayed on SD-Trp-Leu-Ade-His + 25 mM 3AT media, and for blue colour on X-gal plates.NubG-GAPDH was used as a positive control and NubG-GABAβ 1A as a negative control. Cells co-transformed with Fur4-NubI serve as a positive control for growth on selective plates. (**B**) EGFR overexpressed in HEK293T cells was IPed and blot probed with FLAG antibody to detect the co-expressed HDAC6-FLAG. (**C**) Lysates of A431 cells was IPed with HDAC6 anitserum and blot probed with EGFR. Stripped blot was reprobed with HDAC6 antibody. (**D**) Wt EGFR or EGFR K721A and FLAG-HDAC6 were transfected in HEK293T cells, and IP done using FLAG antibody. Blots were probed with EGFR and later reprobed with FLAG antibody.

3.2.2 Mapping of EGFR and HDAC6 binding regions

In order to map the binding site of EGFR on HDAC6, FLAG-tagged HDAC6 wt, HDAC6 deacetylase dead (DD), HDAC6 N-terminal deletion (dN), HDAC6 lacking the ubiquitin binding domain (dBUZ) or HDAC6 with stop codon at residue 840 (1-840) were co-expressed with EGFR in HEK293T cells (Fig. 12A). Immunoprecipitation using FLAG antibody showed that all constructs, except HDAC6 1-840, were able to efficient bring down EGFR, thus narrowing down the interaction surface on HDAC6 to the region between amino acid residues 840 and 1132 (Fig. 12A). The minimal binding domain of HDAC6 was further defined using the MYTH system. Five prey constructs comprising of different C-terminal HDAC6 fragments were generated and transformed in to yeast expressing MFα-EGFR-C-T. As seen by growth on selective media and blue coloration on X-gal test, the interaction was maintained in the short fragment containing HDAC6 amino acids 1010 to 1050, which denotes the minimal interaction domain between the two proteins (Fig. 12B).

Further analyses to determine the binding surface of HDAC6 on EGFR and whether HDAC6 can also bind to other transmembrane receptors was done by Jasna Curak in the lab of Igor Stagljar on a collaborative basis. Since it is helpful for the discussion of the work presented here, these findings are briefly described below.

Using the MYTH approach the HDAC6 binding surface of EGFR was determined. The deletion mutants reveal that the juxtamembrane region of EGFR (corresponding to amino acids 645-672 of mature EGFR) is responsible for its interaction with HDAC6.

Furthermore, binding of HDAC6 to other ErbB family members was detected including binding to ErbB2, ErbB3, and ErbB4. However, HDAC6 did not interact with a wide variety of mammalian integral membrane proteins such as the mouse transporters NHE3, NaPi-IIa, and MAP17, as well as the human ion channels SLC989 and SLC22A4. This excludes the possibility that HDAC6 associates with any integral membrane protein that is internalized via clathrin-coated pits.
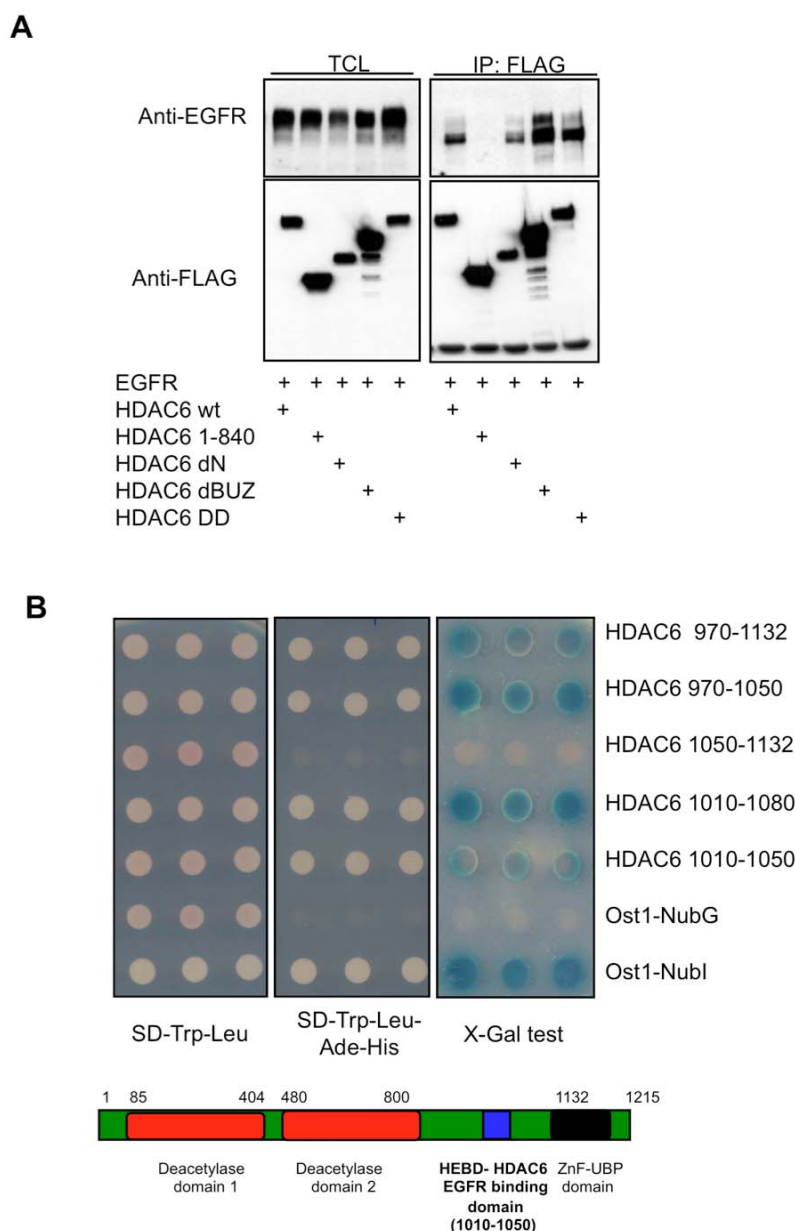
Figure 12. Mapping of EGFR binding site on HDAC6.
(A) HEK293T cells were transfected with EGFR and FLAG-HDAC6 wild-type or deletion constructs containing the first 840 amino acids (HDAC6 1-840), lacking the N-terminus (dN, 439-1215), lacking the zinc-finger domain (dBUZ, 1-1132), or a full-length HDAC6 lacking deacetylase activity (DD, HDAC6-H216A/H611A). IP done using M2-FLAG antibody, followed by probing first with EGFR antibody and then with FLAG antibody. Total cell lysates (TCL) show comparable levels of expression of the proteins.
(B) HDAC6 amino acid residues 1010 to 1050 bind to EGFR.
Yeast THY.AP40 cells were co-transformed with MF -EGFR-Cub-TF and the various HDAC6 prey constructs as indicated. Three independent colonies from each co-transformation were tested for growth on Trp⁻Leu⁻, Trp⁻Leu⁻Ade⁻His⁻, and X-gal containing media. A non-interacting membrane protein, Ost1p, fused to NubG was used as a negative control and the same protein fused to NubI was used as a positive control. Schematic representation of HDAC6 domains and HEBD (HDAC6 EGFR binding domain) shown.

3.2.3 HDAC6 colocalizes with EGFR on the plasma

To strengthen the above biochemical observations, the sub-cellular localizations of EGFR and HDAC6 were investigated. HeLa cells were grown in cover slips, serum starved and stimulated with fluorescent-labelled EGF (EGF-Alexa 555). The fixed cells were then stained with anti-HDAC6 antibody and confocal images were acquired. As expected, HDAC6 is primarily localized in the cytoplasm. However, a minor fraction is seen to partially co-localize with EGF/EGFR complex at the membrane (Fig. 13A
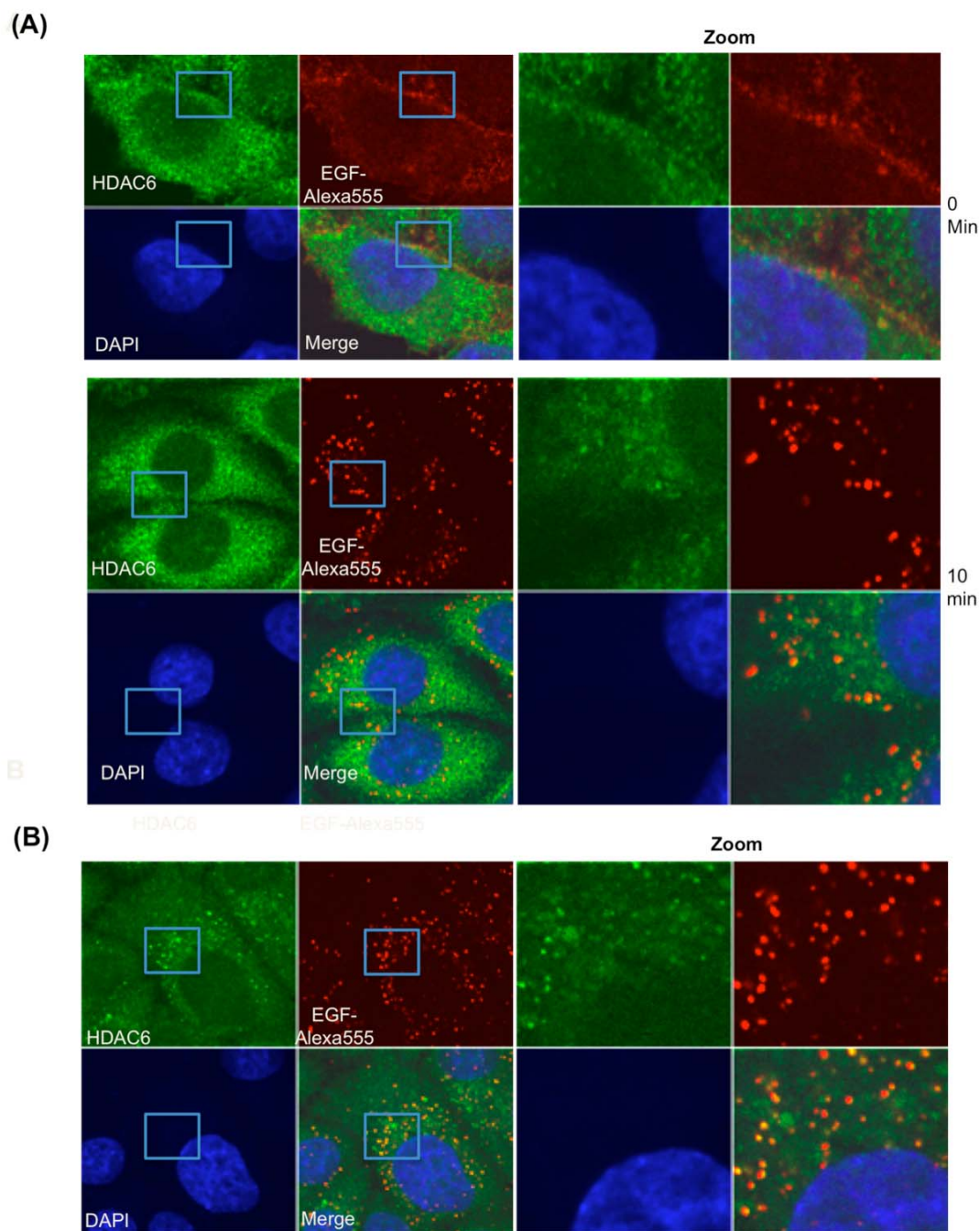
Figure 13. HDAC6 partially colocalizes with EGFR
(**A**) HeLa cells were starved and pulsed with EGF-Alexa555 (red) for 45 seconds. Then were immediately fixed (0 min) or chased for 10 minutes. Cells were later immunostained with HDAC6 antibody (green) and visualized by confocal microscopy. (**B**) HeLa cells transfected with Rab5 Q79L were starved, pulsed with EGF-Alexa555 and immunostained as in (A). Nucleus stained with DAPI and images in zoom shows a close up of representative vesicular signals.

upper panel). After 10 minutes of stimulation, EGF/EGFR is internalized and located in intracellular vesicles. Importantly, HDAC6 was again seen to partially co-localize with EGFR in these vesicular structures (Fig. 13A lower panel). The extent of colocalization was however weaker than can be expected from the co-

immunoprecipitation experiments. This could be due to a rapid on-off interaction between the two proteins. Hence in order to unequivocally demonstrate that HDAC6 is localized on endosomes carrying EGF/EGFR, the formation of enlarged early endosomes was induced by transfection of the GTPase-deficient mutant Rab5 Q79L. This mutant has the ability to increase the size of endosomes by facilitating homotypic fusions[204]. As depicted in Fig. 13B, a remarkably enhanced co-localization of HDAC6 is observed in these endosomes together with EGFR showing HDAC6 can travel with the receptor from the plasma membrane along endocytic vesicles.

3.3 HDAC6 regulates ligand-induced degradation of EGFR

While studying the interaction between HDAC6 and EGFR it was noted that over-expression of HDAC6 enhanced the levels of EGFR in HEK293T cells (Fig. 14A). As can be seen in lanes 2 and 4 the basal levels of the receptor are markedly enhanced upon transfection of HDAC6.

On the other hand downmodulation of HDAC6, either pharmacologically using an inhibitor or genetically by shRNA mediated knock down has the opposite effect. The inhibition of deacetylase activity of HDAC6 by trichostatin A (TSA) in A549 cells led to reduced expression of EGFR (Fig 14B). But more prominently the knockdown of HDAC6 using shRNA in these cells resulted in much lower expression of EGFR (Fig 13C). Degradation of EGFR in lysosomes, primarily due to ligand binding and to a lesser extent due to constitutive internalization, is a prominent regulatory mechanism[110, 112]. Hence, the effect of HDAC6 on ligand-induced degradation of endogenous EGFR was investigated next.

3.3.1 HDAC6 overexpression slows ligand-induced degradation of EGFR

Experiments to assess ligand-induced degradation of EGFR were performed in A549 cells. These cells, derived from human non-small cell lung carcinoma, are suitable for studying dynamics of ligand induced EGFR as they express decent amount of the receptor, are tightly adherent and amenable to plasmid or oligonucleotide transfection.

Cells grown in normal growth media were transfected with a control EGFP vector, FLAG-HDAC6 or a FLAG-HDAC6 mutant lacking deacetylase activity (HDAC6-H216A/H611A). One day later, cells were serum starved for 16 hours and *de*
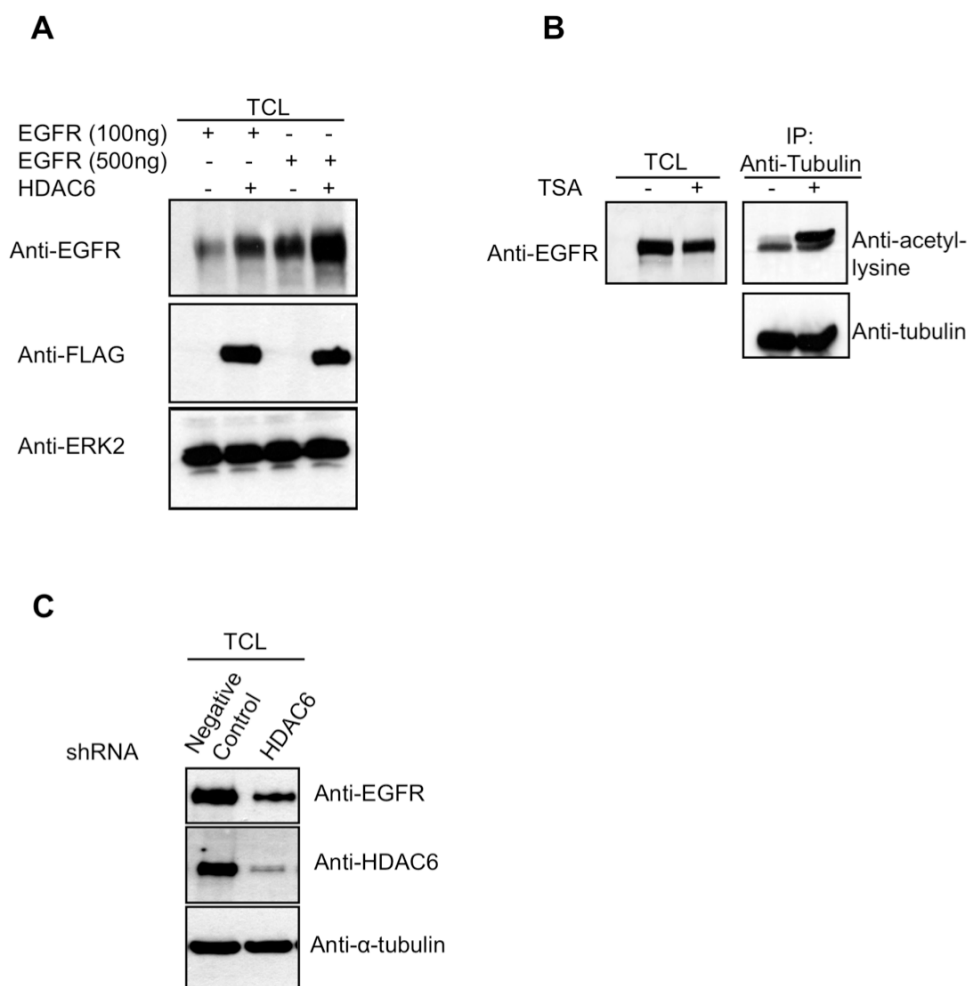
Figure 14. Expression level of HDAC6 affects total cellular levels of EGFR.
(A) HEK293T cells were transfected with 100ng (lanes 1 and 2) or 500ng (lanes 3 and 4) of a plasmid encoding EGFR, alone (lane 1 and 3) or with FLAG-HDAC6 (lane 2 and 4). Cell lysates were run on SDS-PAGE and immunoblotted with EGFR and FLAG antibodies. **(B)** A549 cells were treated with the inhibitor TSA (1μM) for 12 hours. TCL probed for EGFR. IPed tubulin shows increased acetylation, serving as control for efficienct inhibition of deacetylase activity. **(C)** A549 cells were transduced with Lentivirus expressing a scrambled or HDAC6 specific shRNA. Stable clones were established and tested for expression of EGFR and HDAC6. Tubulin blot show loading of comparable amount of cell lysates.

novo protein synthesis was inhibited by cycloheximide treatment. The cells were then stimulated with EGF for 20 to 180 minutes and lysates were probed for levels of EGFR. Wt HDAC6, but not HDAC6-H216A/H611A or control EGFP, led to

stabilization of EGFR in non-stimulated and EGF stimulated cells (Fig. 15A). Whether this stabilization was dependent on the ability of HDAC6 to bind to the receptor was tested next by using an HDAC6 deletion mutant that does not bind to EGFR (termed HDAC6-DelHEBD). This mutant is still catalytically competent and able to bind ubiquitin (data not shown). A similar assay as above was done to compare the ligand-induced degradation of EGFR upon overexpression of wt HDAC6 or HDAC6-DelHEBD. Importantly, HDAC6-DelHEBD had a weaker stabilization effect on ligand-induced EGFR degradation as compared to wild-type HDAC6 (Fig. 15B). It is worthwhile to notice that abolishing EGFR binding did not completely abrogate stabilization effect of HDAC6-DelHEBD, indicating the possibility of direct interaction independent effects of HDAC6 on EGFR.

3.3.2 HDAC6 knockdown accelerated the degradation of EGFR

In order to complement the above gain-of-function studies, a loss-of-function experiment using shRNA-mediated knockdown of HDAC6 was performed. For this purpose, A549 cells were transduced with lentiviruses encoding shRNA against HDAC6 and stable clones were established. A549 parental and knockdown cells were serum starved, EGF stimulated and lysates were subjected to Western blotting and probed with EGFR antibody. In control cells, receptor degradation was initiated slowly and progressively continued to 3 hours, whereas in HDAC6 knockdown cells, degradation of EGFR started much earlier and accelerated dramatically within the next hours (Fig. 15C). Again, it is important to note that the knockdown of HDAC6 caused a much more pronounced effect on EGFR degradation compared to the overexpression of HDAC6. This could very well be due to the high level of expression of endogenous HDAC6 in these cells whereby gain of function will have comparatively lower effect than loss-of-function as a result of near saturation of HDAC6-utilizing apparatus.

3.4 HDAC6 modulates the kinetics of EGFR intracellular trafficking

How is HDAC6 stabilizing the receptor from ligand-induced degradation? It is well established that the primary mechanism of EGFR regulation is ligand-induced

receptor internalization followed by endosomal trafficking, and subsequent degradation in lysosomes [54]. The question is whether HDAC6 affects any of these processes, for example internalization, or whether it influences the post-endocytic trafficking of EGFR.
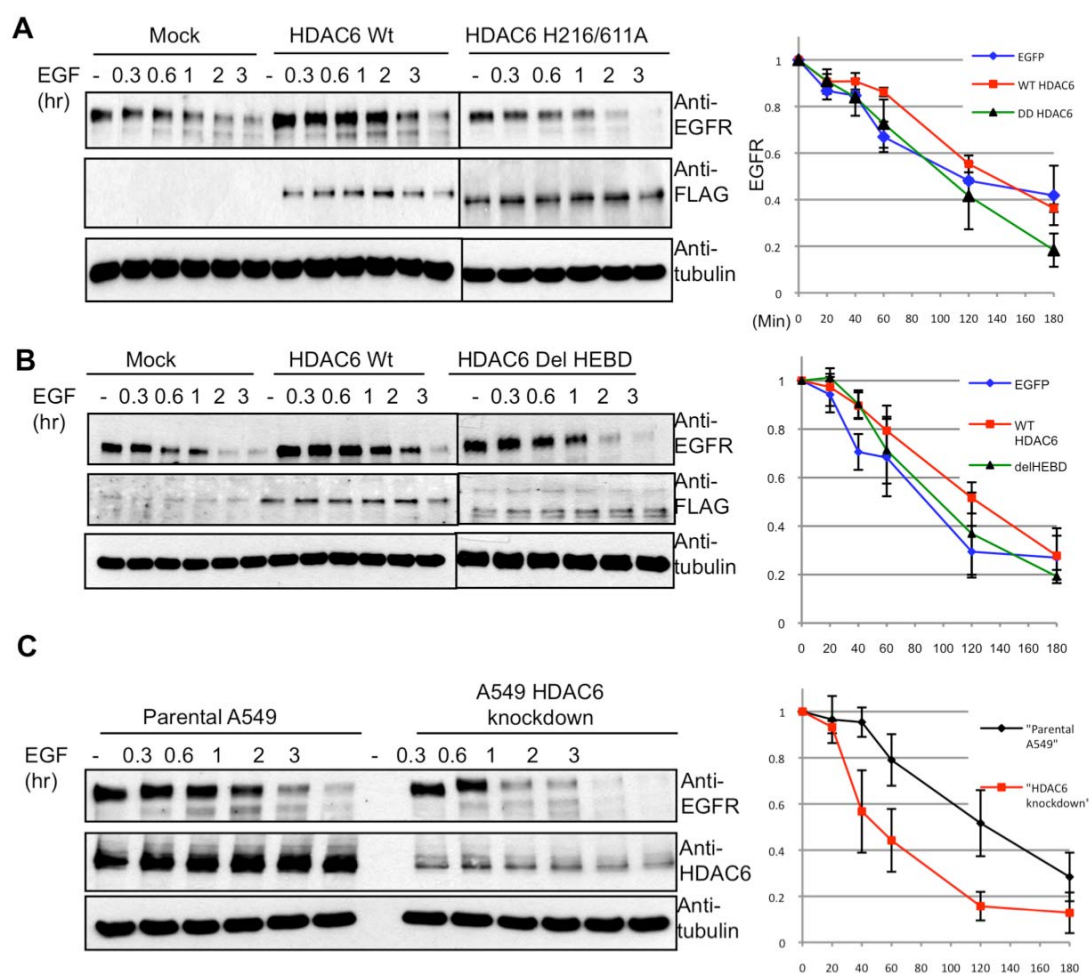
Figure 15. HDAC6 regulates ligand-induced EGFR degradation.
(A) A549 cells were transfected with an EGFP vector as control, FLAG-HDAC6 wild type or FLAG-HDAC6 H216A/H611A. Cells were then serum starved for 16 hours and pre-treated with cycloheximide. Subsequently, they were stimulated with EGF for the durations shown. Cell lysates were run on SDS-PAGE and blots probed with EGFR antibody to follow its degradation. Control probes were done to show the efficiency of knockdown and equal loading. EGFR signals from the several Western blots were quantified with ImageJ® and plotted, taking EGFR level before stimulation as 100% Cells were serum-starved and ligand induced EGFR degradation monitored as in. **(B)** A549 cells were transfected with an EGFP vector as control, FLAG-HDAC6 wild type or FLAG-HDAC6 DelHEBD. EGFR degradation was monitored as above. **(C)** Parental A549 and HDAC6 stable knockdown cells were serum starved and ligand-induced EGFR monitored essentially as in (A).

3.4.1 HDAC6 has no effect on EGFR internalization

To answer these questions, first a receptor internalization assay was done by labelling surface EGFR with radioactive iodine (^{125}I)-conjugated EGF. Interestingly, no remarkable difference in the rate of receptor internalization was observed in cells overexpressing wild type or a deacetylase-deficient mutant of HDAC6 relative to control cells (Fig. 16A). It is thus possible that HDAC6 might influence the post-endocytic trafficking and sorting of the receptor along the endocytic.

3.4.2 Knockdown of HDAC6 accelerates the delivery of EGF late endosomes

In order to further dissect the spatio-temporal influence of HDAC6 on the kinetics of EGFR trafficking *in vivo*, a pulse-chase experiment using Alexa488-labelled EGF as a ligand was performed. Parental A549 cells or cells expressing shRNA against HDAC6 were pulsed with Alexa488-EGF for 30 seconds and chased for various periods of time. The endocytic marker proteins EEA1 (early endosomal marker 1) and LAMP1 (late endosomal marker 1) were visualized by immunostaining (Fig. 16B). Four-channel laser confocal microscopy images were acquired from at least 10 fields per experimental setup with an average of 10 cells per field to get adequate numbers for statistical analyses. Images were then analysed by MotionTracker® software. This algorithm was developed to identify vesicular structures by analysing their localization in respect to other structures, size and intensity in three axes, much like human motion tracking algorithms being developed for security purposes[61]. Once vesicles marked with Alexa488-EGF, EEA1 or LAMP1 were identified, various parameters such as endosome number, size, intensity and co-localizations between the different markers were quantified. Comparing the results to known endocytic kinetic measurements validated the experimental setup.

First, measurement of the colocalization of EGF with EEA1 (as a proxy for internalization) showed that EGF is very rapidly taken into cells peaking after 15 minutes of starting the chase. Interestingly, as in the radioactive iodine based assay, no difference in internalization of EGF was noted between control and HDAC6 knockdown cells (Fig 17A). Additionally, as reported before by Rink et al[61], increasing the chase time to an hour resulted in progressive increase of the size of endosomes (Fig. 17B). Down-regulation of HDAC6 expression markedly accelerated
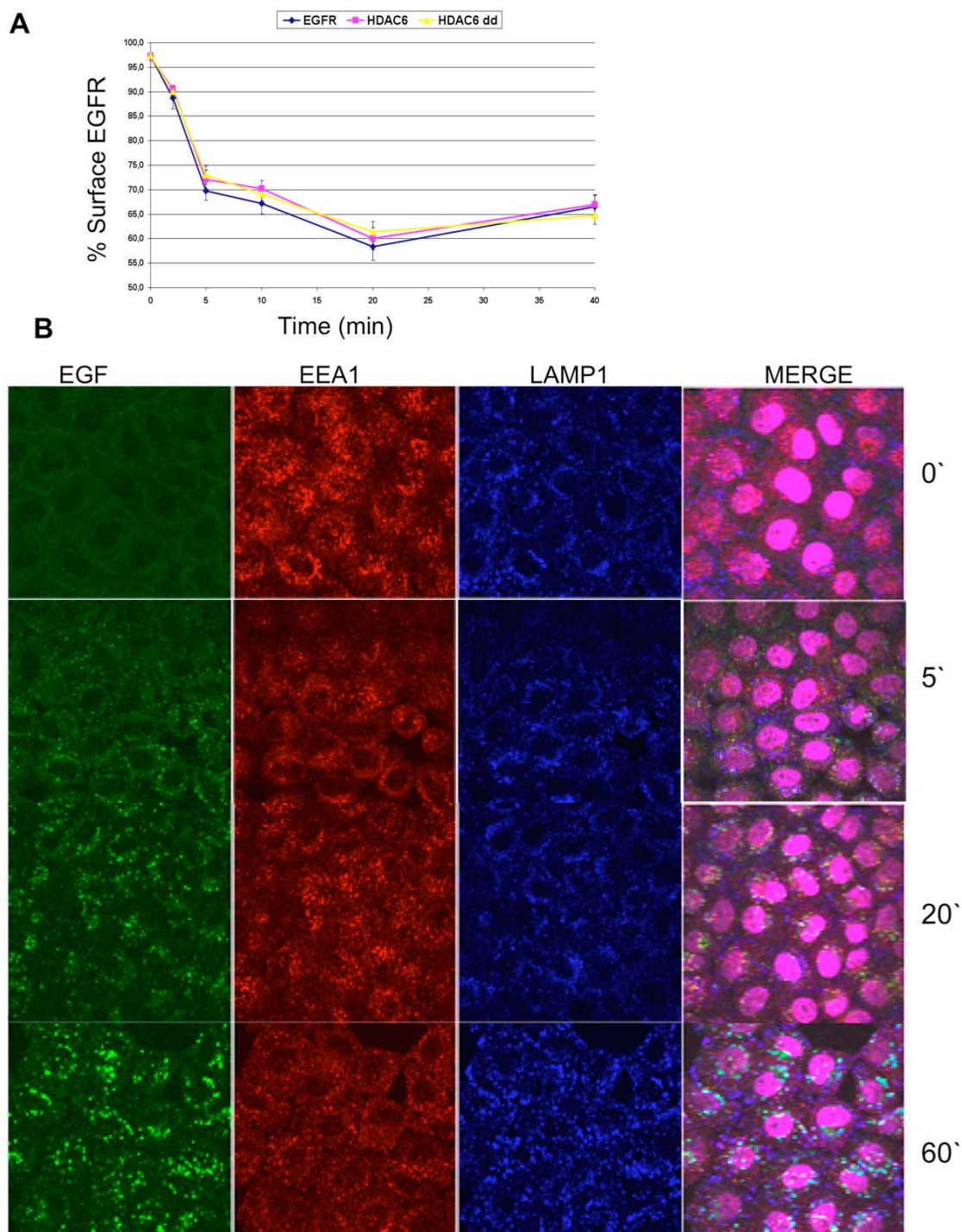
Figure 16. Dynamics of EGFR trafficking. (A) No influence of HDAC6 expression on the rate of internalization of EGFR. CHO cells were transfected with EGFR and EGFP, wild type HDAC6 or deacetylase-dead HDAC6- H216A/H611A (DD). After 16 h of serum starvation, cells were stimulated with 50 ng/ml EGF for the durations shown. The amount of radioactive EGF/EGFR complex left at the cell surface was measured quantified by ligand labelling, normalized to the amount of EGFR at time point 0. **(B)** Representative images for EGFR trafficking dynamic measurment. Parental and HDAC6 knockdown cells were pulsed for 45sec with EGF-Alexa488, and chased for the shown durations. Fixed cells were immunostained with EEA1 and LAMP1 antibodies and DAPI.A minimum of 100 cells were imaged for every experimental time point and condition. Images analysed later with MotionTracker®.

the delivery of EGF into LAMP1 positive late endosomes, as visualized by increased co-localization of EGF with LAMP1 (Fig. 18A). Furthermore, the distance between the EGF-containing endosomes and the nucleus decreased much faster in the knockdown cells indicating an increase in velocity of travel towards the centre of the cell (Fig. 18B).

These observations are consistent with the accelerated degradation of EGFR in HDAC6 knockdown cells by Western blotting (Fig. 15C). In addition, the integral vesicular intensity of EEA1 positive vesicles was increased in knockdown cells, demonstrating the accumulation of more content in these endosomes (Fig. 18C). Prior observations have shown that early endosomes progressively increase in size, concentrate cargo destined for degradation and adopt a more central location in cells prior to conversion into late endosomes and before fusing with lysosomes [61]. In conclusion, the increased co-localization of EGFR with LAMP1, decrease in endosome-nucleus distance and the increased content of endosomes in HDAC6 knockdown cells is consistent with a model of faster transport of EGFR carrying endosomes towards the peri-nuclear area where receptor degradation is known to occur [54, 71].
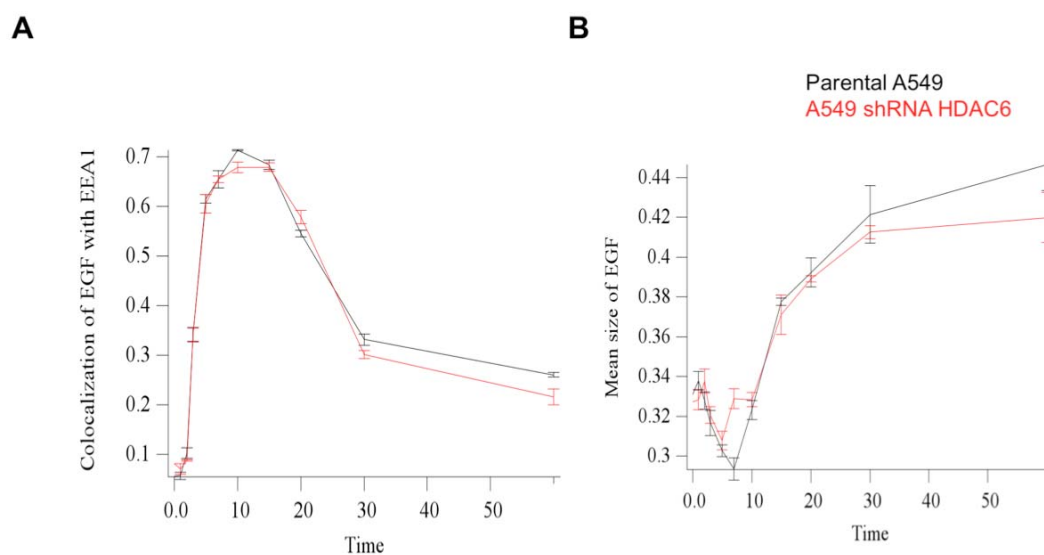
Figure 17. Validation of EGF Alexa488 pulse-chase experimental setup by measuring previously described parameters. Images from Fig. 16B were analyzed by MotionTracker. **(A)** The colocalization of vesicles staining positive for both EGF and EEA1 was quantified as a function of time. A rapid increase with gradual decrease shows the entry and exit of EGF in early endosomes. **(B)** The progression in the mean size of EGF positive vesicles over one hour of EGF stimulation.

3.5 Acetylation and receptor trafficking

How is HDAC6 able to modulate the trafficking of EGFR and endosomes? As the stabilization of EGFR required HDAC6 deacetylase activity (Fig. 15A), EGF induced acetylation/deacetylation of the receptor itself or a certain protein involved in trafficking might be involved. In order to test this hypothesis, it was important to identify an acetylated protein that is deacetylated by HDAC6 in the endocytic
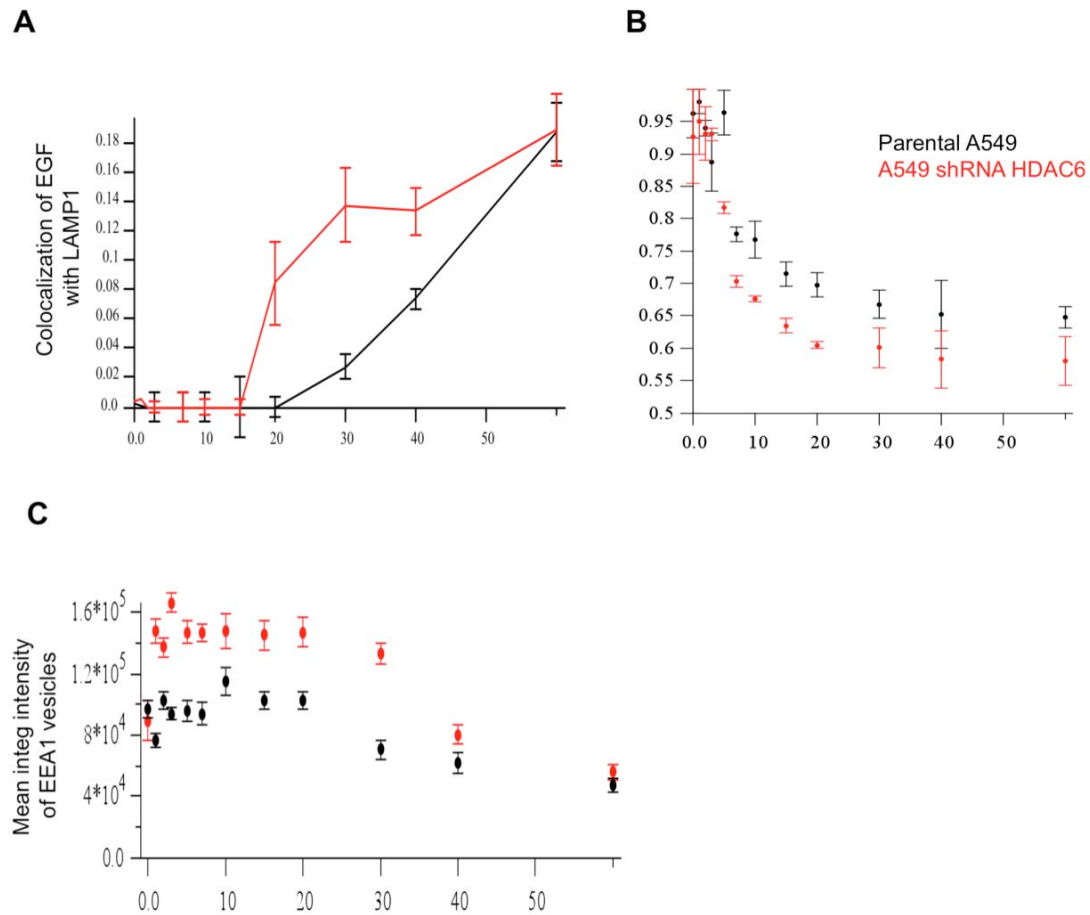
Figure 18. Downregulation of HDAC6 accelerates intracellular trafficking of EGFR. (A) EGF delivery to late endosomes is accelerated in HDAC6 knockdown cells. Serum starved A549 cells were pulsed with EGF-Alexa488 and chased for the indicated times. Following immunostaining with EEA1 and LAMP1 antibodies, images as in Fig. 16 were quantified. Graph shows percent of EGF co-localized with LAMP1 positive vesicles versus time for parental (black) and HDAC6 knockdown cells (red). **(B)** Internalized EGF approached the perinuclear area rapidly in HDAC6 knockdown cells. Data generated in EGF pulse-chase experiment were analysed to quantify distance of EGF positive vesicles from the nucleus in units of nuclear size in both parental (black) and HDAC6 knockdown cells (red). (C) The mean integral intensity of EEA1 vesicles was measured and plotted. This measurement corresponds to the content of endosomes.

machinery. Hence, a systematic search was done by immunoprecipitating major regulators of EGFR trafficking (including c-Cbl, CIN85, HRS, STAM, epsin, EPS15) and probing by acetyllysine specific antibodies.

A
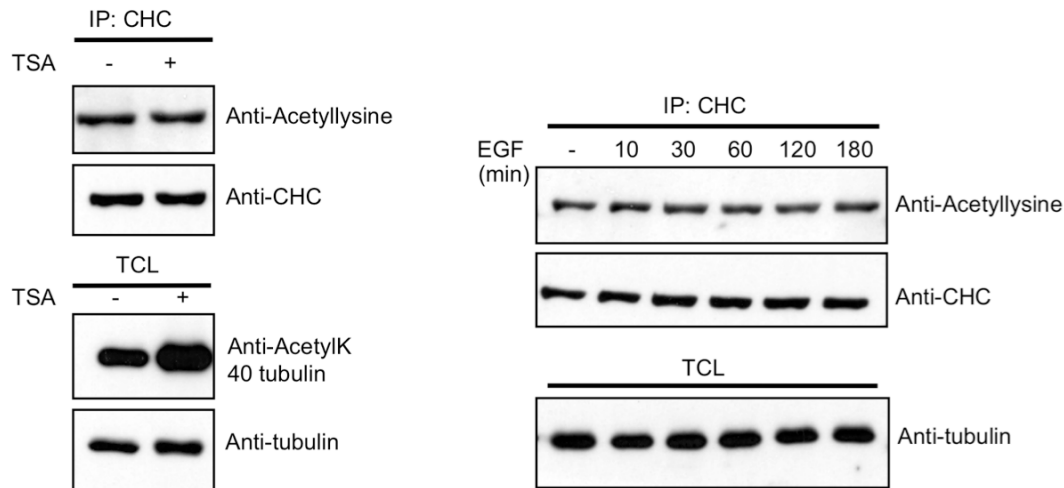
B
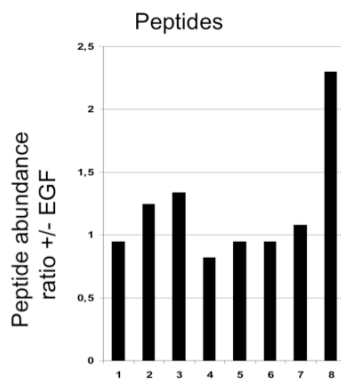
Figure 19. Searching for a target: (A) Clathrin heavy chain (CHC) is acetylated but is not a substrate of HDAC6. Cell lysaes from TSA treated cells were probed with acetyllysine antibody (left panel). Lysates from EGF stimulated cells were IPed with clathrin heavy chain antibody (CHC) and probed with acetyllysine antibody (right panel). **(B)** Acetylation of tubulin increases in response to EGF stimulation. Mass spectrometric determination of Lys40 acetylation of tubulin after EGF stimulation. HeLa cells were serum-starved for 16 hours and stimulated with EGF. Lysates were subjected to immunoprecipitation with tubulin antibody. Samples were run on SDS-PAGE, tubulin bands were cut out, proteolytically digested and analysed by mass spectrometry. Graph shows ratio of peptide abundance from each sample with EGF stimulation compared with peptides from non-stimulated cells. DK*TIGGGD denotes the peptide containing the acetylated Lys40**.** The peptides analysed are **1-** DGQMPSDKTIGGGD, **2-** DKTIGGG, **3-** DKTIGGGD, **4-** DKTIGGGDDSFNTFFSETGAGKHVPRAVFV, **5-** DLEPTVI, **6-** DCAFMVDNEAIY, **7-** DICRRNL, 8- D**K***TIGGGD

Additionally, immunoprecipitated EGFR and associated protein complex was subjected to mass spectrometry to identify acetylated peptides. However, no lysine acetylation of EGFR could be demonstrated. Of the established regulators of endocytosis, only clathrin heavy chain was identified to be acetylated on a single lysine residue, K456. However, to our dismay, this acetylation is not at all modulated by HDAC6 or EGF stimulation. Inhibition of HDAC6 by TSA (Fig. 19A left panel) or stimulation with EGF for various durations (Fig. 19A right panel) has no effect on the acetylation of CHC, effectively ruling out clathrin as a potential mediator of HDAC6 function.

In this search for potential targets we also included HSP90. HSP90 is a known substrate of HDAC6 that is involved in maturation of various signaling molecules [146]. HSP90 affects maturation of ErbB family members such as ErbB2. Importantly, however, wild type or mature EGFR is not influenced by HSP90 activity [205-207]. In order to unequivocally rule out that HSP90 does not play a role in our system, we have tested its significance in regulating ligand induced EGFR degradation. Serum starved A549 cells were cycloheximide treated to inhibit new protein synthesis, then left untreated or treated with HSP90 inhibitor geldanamycin for four hours. After addition of EGF for different durations cells were lysed and levels of EGFR were detected. Inhibition of HSP90 had no remarkable effect on the normal ligand induced degradation of EGFR (data not shown). In conclusion, it is highly unlikely that the effect of HDAC6 on trafficking of the mature and signaling competent membrane located receptor could be explained by its action on HSP90.

3.5.2 Acetylation of α-tubulin is increased upon EGF stimulation

In stark contrast to the above results, the mass spectrometric (MS) analyses detected an increase in the acetylation of -tubulin on lysine residue 40 (Lys40) following EGF stimulation (Fig. 19B). This was done by immunoprecipitating -tubulin with stringent washing and subjecting a band cut from an SDS-PAGE to MS. The intensity of the peptide containing acetylated Lys40 (labelled 8) was 2.3-fold higher in EGF-stimulated cells as compared to the basal level of acetylation of -tubulin in non-stimulated cells. The abundance of alternative non-modified peptides was also compared between the two samples. As shown in Fig. 19B, the ratio of the EGF

stimulated versus non-stimulated intensities of these control peptides (labelled 1 to 7) is approximately one, indicating equivalent amounts of total -tubulin analysed.

3.5.3 Acetylation of α-tubulin Lys40 is important for efficient motility of endosomes

At this point, an important question is whether -tubulin acetylation plays any regulatory role in intracellular trafficking.
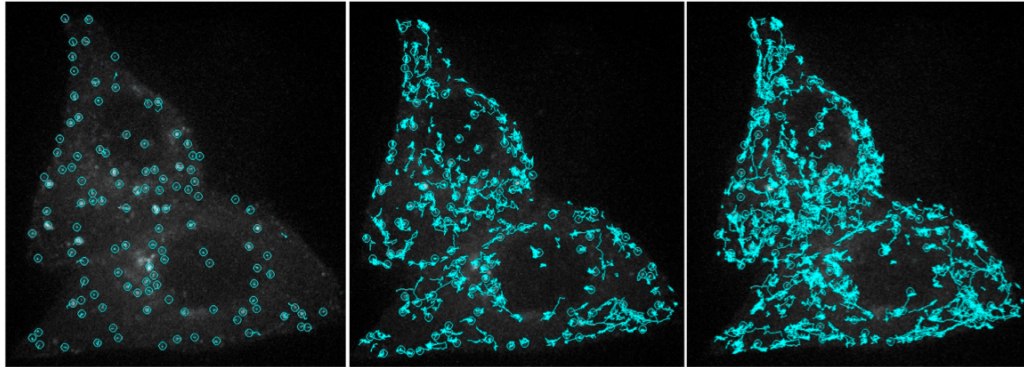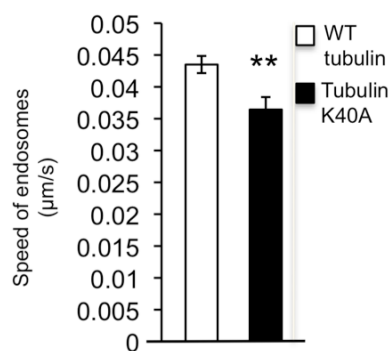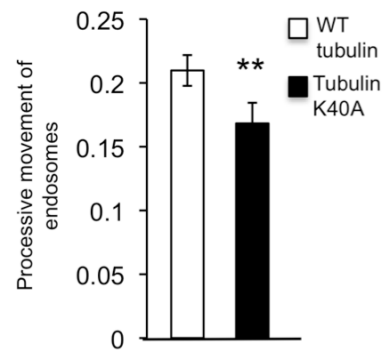
Figure 20. Acetylation of tubulin on lysine 40 is important for efficient motility of endosomes.
Fast live cell imaging and individual endosome tracking was performed in A431-GFP-Rab5 cells overexpressing wt and K40A-mutant mCherry-tubulin. Imaging parameters include image sequences (4 images per Z stack, 2 stacks/second) with observation time of 5 minutes and were rendered by maximum projection of GFP-Rab5 endosome dynamics in mCherry-tubulin expressing cells.**(A)** Snap shots from video microscopy showing endosomes identified (green circles) and being tracked during their motility (green line) **(B)**.The speed of GFP positive early endosomes was computed and depicted in the graph. GFP-Rab5 endosomes moved slowly in cells expressing the dominant negative Lys40Ala tubulin. Student's *t*-test for statistical significance performed, with *p*<0.05. **(C)** Efficient processive movement of endosomes depends on Lys40 of tubulin. Similar to (B) K40A mutation led to impaired processive movement of endosomes.

Two recent reports have shown that acetylation of Lys40 in -tubulin enhances the interaction between microtubules and the motor proteins kinesin and dynein, thus accelerating the transport of cargo proteins in the secretory pathway [170, 171].

To test whether acetylation of -tubulin Lys40 similarly affects movement of early endosomes along microtubules, live cell imaging by spinning disc microscopy was performed. This microscope, together with the associated high-speed camera, is suited for imaging fluorescently tagged intracellular vesicular structures with reduced photo bleaching compared to conventional confocal microscopy. mCherry- -tubulin and a mCherry- -tubulin-Lys40Ala were expressed in A431 cells stably transfected with low amount of GFP-Rab5. Expression of either mCherry -wild type or Lys40Ala -tubulin constructs is known to lead to an adequate incorporation of -tubulin in microtubules [171]. Additionally, it has been demonstrated that Lys40Ala acts in a dominant negative manner to reduce acetylation of endogenous microtubules [208]. Again, using the MotionTracker® software, single GFP-Rab5 endosomes were identified and tracked for five minutes (Fig. 20A). The speed and number of processive movements of these individual endosomes were calculated. Cells expressing -tubulin- Lys40Ala mutant displayed a statistically significant reduction in speed (Fig. 20B) and processivity of Rab5 endosomes (Fig. 20C), as compared to cells expressing wild-type -tubulin. Taken together these results show that an increased acetylation of tubulin, which can be induced by EGFR activation, is important in regulating the kinetics of trafficking of the receptor via early endosomes to late endosomes.

3.6 Phosphorylation of HDAC6 modulates enzymatic activity

3.6.1 HDAC6 is phosphorylated on serine and tyrosine residues

The next important question is how EGFR activation leads to the increase in acetylation of -tubulin. Acetylation is a result of the interplay between acetyltransferases and deacetylases. Hence, an increase in acetylation denotes either increase in activity of acetyltransferase or decrease in deacetylase activity. However, the molecular identity of tubulin acetyltransferase is so far unclear. Hence, a focus on this activity at this juncture is impractical. On the other hand, there is a high basal

activity of HDAC6 in cells and several members of the HDAC family are regulated by phosphorylation [209-211], therefore it is reasonable to hypothesize that phosphorylation of HDAC6 could also be an important regulatory mechanism.

To study this, a comprehensive mass spectrometric analysis of HDAC6 was performed. Following tryptic digestion of HDAC6, two phosphorylated peptides were identified. One contains Tyr570 and the other comprises of three serines, Ser563, Ser564, and Ser568 (any one of them can be phosphorylated, but not all).
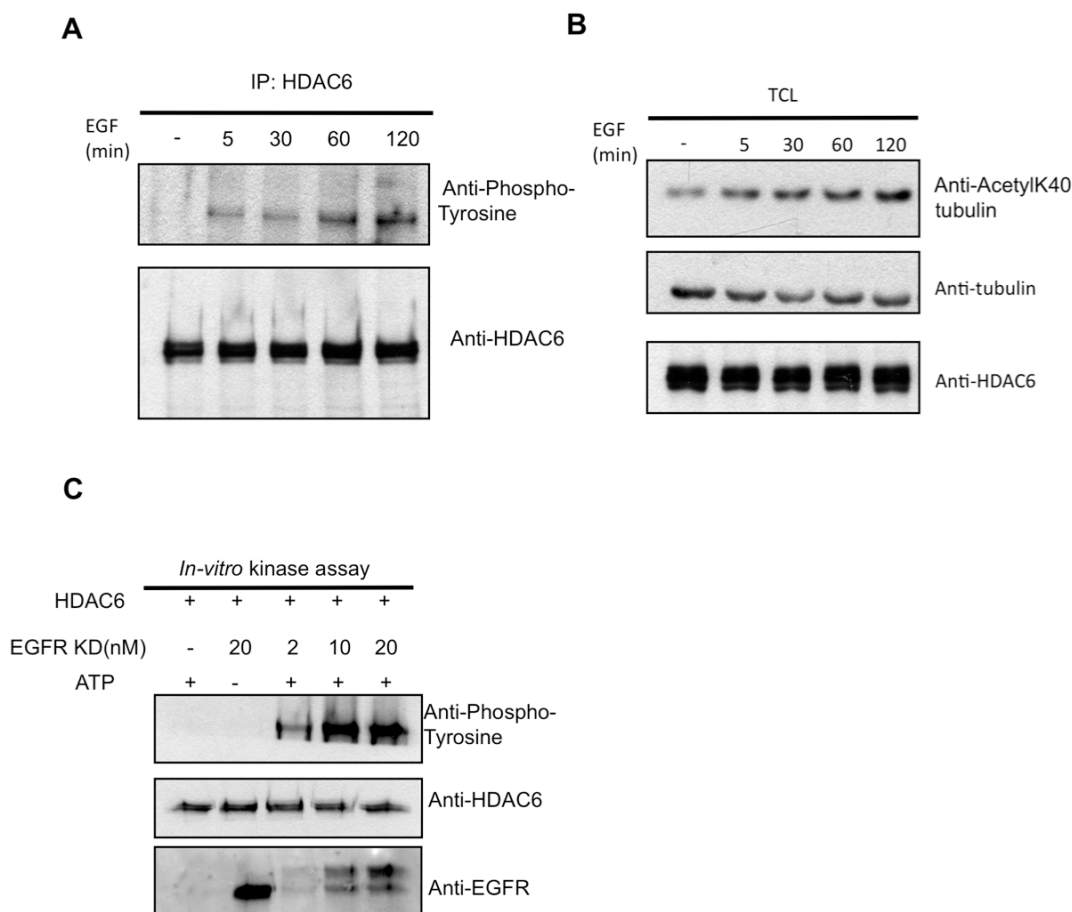
Figure 21. HDAC6 is phosphorylated by EGFR. (A) HDAC6 is tyrosine phosphorylated following EGF stimulalation. Serum starved HeLa cells were pretreated with sodium orthovanadate and EGF stimulated for indicated durations. After IP with HDAC6 antibody and stringent washes, blots were probed with anti-phospho-tyrosine and HDAC6 antibodies. **(B)** Acetylation of α-tubulin lysine 40 progressively increased after EGF stimulation.Total cell lysates from EGF stimulated HeLa cells as in (A) were subjected to Western blotting and probed with anti-acetyllysine 40 tubulin and anti-tubulin antibodies. **(C)** EGFR kinase domain is able to phosphorylate HDAC6. *In vitro* kinase assay was set up with purified recombinant HDAC6 (4μM) and GST-EGFR kinase domain protein (2, 10 and 20 nM) with and without ATP. Reaction mix was loaded on SDS-PAGE and blots were probed with phosphotyrosine, HDAC6, and EGFR antibodies.

To determine which of these phosphorylation sites is indeed modulated by EGFR activation, HeLa cells were serum starved and subsequently stimulated for various time points with the EGF ligand. HDAC6 was immunoprecipitated, washed in RIPA

buffer and blots were probed with phosphoserine or phosphotyrosine antibodies. A marked increase in phosphotyrosine signal that progressed over time was detected, suggesting HDAC6 Tyr570 is modulated by EGFR activation (Fig 21A). Probing with phosphoserine antibodies was inconclusive due to poor quality of antibodies.

3.6.2 Phosphorylation of HDAC6 by EGFR inhibits deacetylase activity

Interestingly, probing lysates from EGF stimulated HeLa cells for acetylation of α-tubulin on Lys40 showed a gradual increase in acetylation that correspond to increase in HDAC6 tyrosine phosphorylation. This indicates that phosphorylation might indeed have an inhibitory role on the activity of HDAC6 (Fig. 21B).
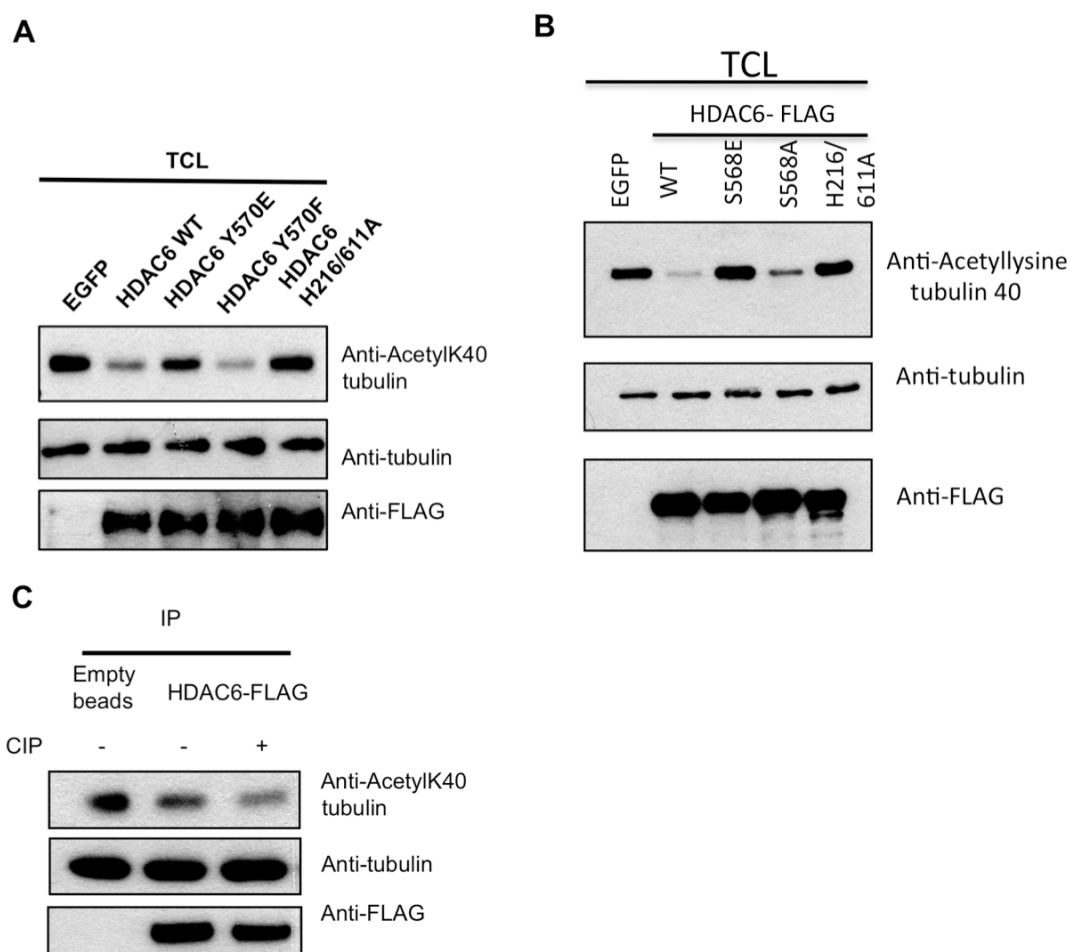
Figure 22. Phosphorylation of HDAC6 on Tyr570 abolished its deacetylase activity. **(A)** An EGFP vector, FLAG-HDAC6 wt, FLAG-HDAC6 Tyr570Glu and FLAG-HDAC6 Tyr570Phe and FLAG-HDAC6 His216/611Ala plasmids were transfected in HEK293T cells. Cell lysates were probed with acetyl Lys-40-tubulin, FLAG and tubulin antibodies. **(B)** FLAG-HDAC6 S568E and FLAG-HDAC6 S568A and indicated constructs were transfected in HEK293T cells basically as in (A). **(C)** Dephosphorylation of HDAC6 increased its deacetylase activity. Purified and polymerized microtubules were incubated with empty agarose beads (lane 1), immunopurified HDAC6 (lane 2), or HDAC6 treated with calf intestinal phosphatase, CIP, (lane 3). Blots were probed for tubulin acetylated on Lys40, total tubulin and FLAG-HDAC6.

Importantly, HDAC6 was tested whether it can be a substrate for EGFR kinase activity using *in vitro* kinase assay. It was found that purified recombinant HDAC6 was phosphorylated by EGFR in a concentration dependent manner by purified GST-EGFR kinase domain, only in the presence of ATP (Fig. 21C). To directly show that HDAC6 Tyr570 plays a crucial role by regulating its enzymatic activity, a phospho-mimicking mutant, Tyr570Glu and a non-phosphorylatable mutant, Tyr570Phe were created. In an *in vivo* deacetylase assay using acetylation of α-tubulin on Ly40 as readout, phospho-mimicking abolished enzymatic activity dramatically whereas the corresponding non-phosphorylatable mutant maintained comparable activity to wild type HDAC6 (Fig. 22A). The serine residues that were identified to be phosphorylated, i.e. Ser563, 564 and 568 were also mutated to Glu and Ala to mimic and abolish phosphorylation respectively. Testing the mutants in *in vivo* deacetylase assay revealed that Ser568Glu is enzymatically dead whereas Ser568Ala remained active (Fig. 22B). This shows that Ser568 is the serine that is phosphorylated in the peptide and similar to Tyr570 has an important regulatory role on deacetylase activity. To further corroborate these findings, an *in vitro* deacetylase assay was done. Immunopurified HDAC6 was incubated with purified brain-derived microtubules in the presence and absence of calf intestinal phosphatase (CIP). CIP induced dephosphorylation of HDAC6 resulted in a more potent activity than wild-type HDAC6 (Fig. 22C). Taken together, phosphorylation of HDAC6 on Tyr570 by EGFR inhibits its deacetylase activity and is at least one of the reasons for the increased acetylation of   -tubulin following EGF stimulation.

3.7 Effects of HDAC6 on EGFR mediated cellular responses

3.7.1 Downregulation of HDAC6 alters Akt and ERK signalling pathways

PI3K/Akt and ERK pathways constitute two of the most important downstream effecter pathways activated by EGFR. Could the changes in kinetics of EGFR induced by HDAC6 have any effect on these signalling pathways? To address this, control or HDAC6 knockdown A549 cells were stimulated with EGF and cell lysates were probed for pERK 42/44, pSer473Akt, pSer9 GSK3β, pSer380 PTEN. HDAC6 depleted cells have slightly reduced ERK2 phosphorylation in response to EGF. In

contrast, Akt and its downstream target GSK3β have markedly increased phosphorylation (Fig 23). This apparent differential effect on the activation of the two signalling pathways might relate to their distinct mode of activation.

3.7.2 HDAC6 knockdown cells have stunted response to EGF stimulation

EGF stimulation can lead to either cell spreading or contraction very rapidly. On the other hand, prolonged stimulation can induce or inhibit cellular proliferation in a cell line dependent fashion[212-214]. In order to study the possible effects of HDAC6 on these processes, a real time cell analyzer (xCelligence®) was used.
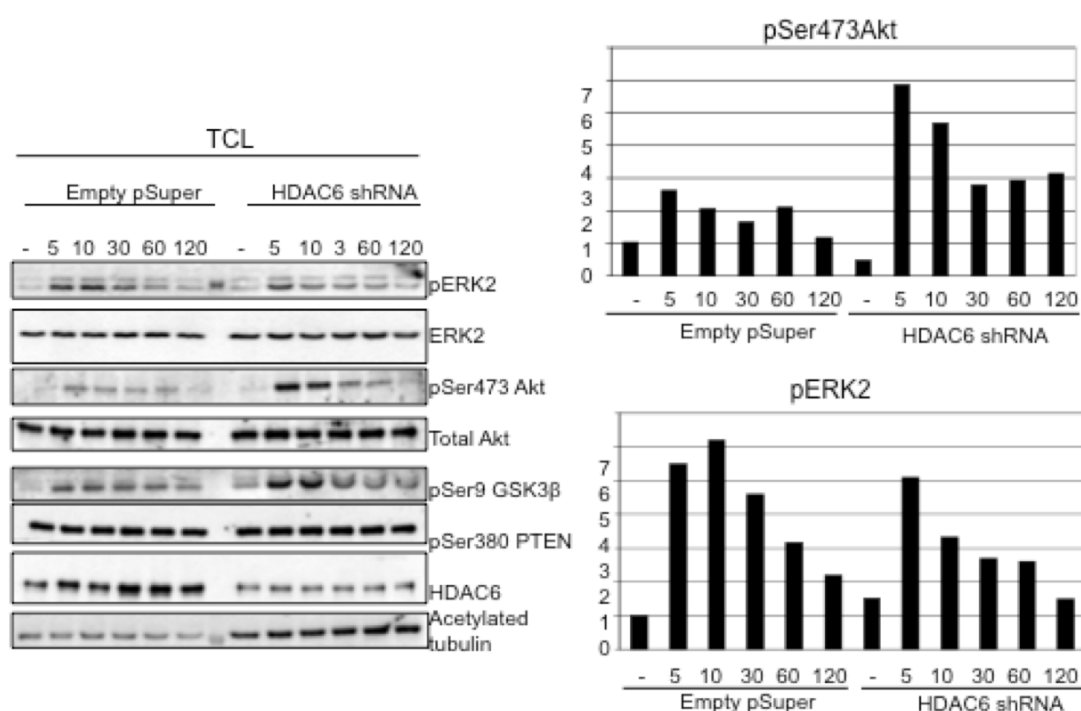
Figure 23. EGFR downstream signaling in HDAC6 knockdown cells. A549 control and HDAC6 knockdown cells were serum starved and stimulated with EGF for up to two hours. Cell lysates from these cells were immunoblotted with pERK2, pSer473Akt, pSer9 GSK3, pSer380 PTEN and acetylated tubulin antibodies. Stripped blots were later probed with ERk2 and Akt to confirm comparable loading of samples (left panel). pSer473 and pERK2 bands were quantified and plotted on the right.

In this system, the bottom of the cell culture dish is covered with a microelectrode array that senses local ionic perturbations caused by attachment of cells. More cells, or more tightly attached cells, mean more impedance to the flow of electric current. This impedance is quantified by the device and plotted as "cell index". The primary advantage of this system is that measurement of cell spreading and cell proliferation is done continuously in real time without any chemical or antibody labelling. A549 control or HDAC6 knockdown cells grown in such dishes were serum starved and

stimulated with EGF. Impedance measurements were done for up to 72 hours post-EGF stimulation. Within a few minutes of applying EGF (peak 20 minutes), control cells contracted by almost 50% of total cell surface. This is in accordance with a previous report where cells were visualized by scanning electron microscopy[212]. Interestingly, this EGF induced cell rounding is very much reduced and slowed in HDAC6 knockdown cells (Fig 24A). Monitoring of the cells for the next few days revealed that EGF stimulation had the expected effect of inducing growth arrest on control cells. Importantly, HDAC6 knockdown cells continued to grow with minimal response to EGF (Fig. 24B). In summary, HDAC6 knockdown cells have markedly attenuated responses to EGF, which could be at least partially explained by their lower receptor level, both at steady state and following ligand stimulation.
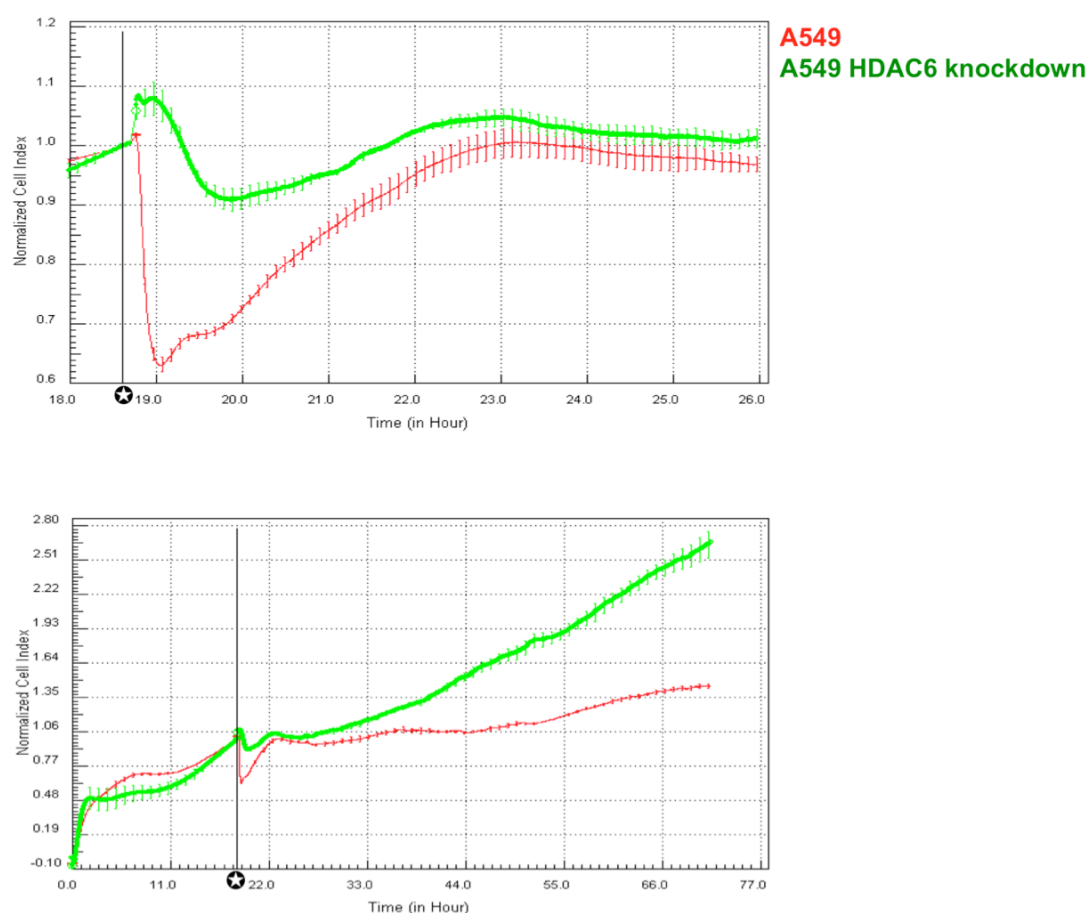
Figure 24. The response of HDAC6 knockdown cells to EGF is markedly attenuated. Serum starved A549 control and knockdown cells were stimulated with EGF and continuously monitored using xCelligence® cell analyzer. Upper panel shows the rapid drop in reading of cell index (the measurement of cell surface adhering to the surface of cell culture dish) in control cells, compared to less pronounced and delayed response in knockdown cells. Longer follow-up shows continued proliferation of knockdown cells whereas control cells are barely growing (lower panel). ✪ shows addition of EGF to growth medium.

4. DISCUSSION

4.1 MYTH screen

This study describes the utilization of split ubiquitin based membrane yeast two-hybrid screen for the identification of novel interacting partners of ligand unoccupied and inactive EGF receptor. Since its initial discovery, EGFR has received a lot of attention by the cell signalling community. This is due to the fact that it is a founding member of RTKs, the ready availability of tools for its study, its dramatic influences on downstream signalling pathways, remarkable growth promoting effects and its association with cancer development. To top this, the recent development of successful blockbuster therapeutics targeting EGFR in the treatment of a variety of cancers has added fuel to this interest. Various biochemical, cell biological and genetic tools have been used to study EGFR. The first proteomic approaches used to investigate EGFR include the application of the conventional yeast two-hybrid system to seek interacting partners of its cytoplasmic domains. Interaction studies have led to the identification of a number of key downstream effectors of EGFR[197, 215]. Due to technical limitations, these studies addressed only fragments of the protein (cytoplasmic domains) and not the full-length membrane localized receptor. Mass spectrometry based studies, spearheaded by the lab of Mathias Mann, coupled with the use of stable isotope labelling by amino acids in cell culture (SILAC) have identified more proteins in complex with the activated receptor[195]. Another impressive work was done by Jones et al who purified all the SH2 and PTP domains in the human genome and constructed a protein microarray which was used to study interactions to multiple peptides from EGFR and other ErbB family members[196]. While the above-mentioned methods have contributed immensely to our understanding of the set of proteins that bind to EGFR, they have major limitations. These are due to the fact that the studies focused either on the proteome recruited to EGFR upon ligand binding or used only the cytoplasmic part of the receptor. To the best of our knowledge, no comprehensive study of proteins that bind to the ligand-unoccupied and membrane-inserted full-length receptor has been reported.

Hence, an important question is how one can search for interactors of receptors while they are still in the membrane environment. Technology drives science and the recent availability of the membrane based yeast-two hybrid system with its ability to detect interacting partners of cell surface receptors proved to be useful in addressing this question[188]. Since its inception, MYTH has been used to search for binding partners of several receptors with promising results. Further modification of bait expressing vectors and availability of high-quality prey libraries have been instrumental in this success[189, 190].

However, a well-validated screen of a single transmembrane protein like a receptor tyrosine kinase is so far not reported. The major hindrance has been the instability and auto-activation of the bait-transcription factor fusion protein. The degradation might be due to misfolding of the heterologous protein and improper insertion into the yeast membrane. In the present work, degradation was avoided by replacing the signal peptide of EGFR (amino acids 1-24) with the membrane targeting N-terminus of the *S.cerevisae* mating factor α protein. Extensive characterization of the bait fusion protein revealed that it was indeed properly inserted into the yeast membrane. The large-scale transformation of human fetal brain library and analyses identified close to three hundred positive clones, corresponding to 87 proteins.

Comparison of the MYTH result with two of the most extensive proteomic studies on EGFR showed a strikingly minimal overlap. Both Jones et al and Blagoev et al reported primarily phosphotyrosine binding proteins that are recruited upon ligand association. Hence, the absence of SH2 and PTB domain containing proteins in the MYTH did not come as a big surprise. About 10% of MYTH clones were previously shown to bind to EGFR experimentally. These were annotated to various protein function classes like metabolic enzymes (GAPDH) and cytoskeletal components such as gelsolin or cofilin. Of utmost interest was the discovery of 16 transmembrane proteins in the screen. This is important in that it validates the ability of the screen to fish out transmembrane proteins as binding partners to other membrane proteins, furthermore it gave us a list of cell surface proteins that directly interact with EGFR.

Bioinformatic analyses were particularly helpful in addressing the specificity of many of the putative interactors. The results of such computations should be taken with certain scepticism unless supported by experimental evidences. Nevertheless one such analysis, computation of the domain-domain co-occurrence between interacting

proteins, points towards an interesting observation that the domains that occurred in at least half of the MYTH clones also occur in other EGFR binding proteins. The statistical significance of this analysis show that this is not due to mere chance but can have real functional importance.

The overall success of this MYTH screen has prompted our collaborators and us to perform additional screens with other RTKs including the other members of ErbB family. As these studies will be presented in other reports, no detailed description is given here. It suffices to say that the results from these studies are also very encouraging.

4.2 HDAC6 is a novel EGFR interactor

One of the interesting proteins identified in the MYTH screen was HDAC6. At first glance, it might be puzzling that a "histone deacetylase" is bound to a cell surface receptor. However, HDAC6 is known to be localized primarily to the cytoplasm, with minimal nuclear staining on immunofluoresence studies[156]. Intriguingly, Zhang et al have reported that HDAC6 can partially translocate to the cell periphery, bind and deacetylate cortactin following EGF stimulation of 3T3 cells[147]. All the evidence accumulated so far convincingly show that HDAC6 is not a histone deacetylase but rather is a cytoplasmic lysine deacetylase.

This study has shown that HDAC6 interacts with endogenous EGFR, irrespective of ligand stimulation. The additional finding that HDAC6 can bind to a kinase dead mutant of EGFR, K721A, expressed in cells that have minimal amount of endogenous EGFR provide additional evidence for the fact that the interaction between the two proteins is not dependent on the activation status of the receptor. The constitutive interaction between the two proteins is also evident in imaging studies where HDAC6 is seen to traffic with the receptor from the cell surface to intracellular endosomes. This is an intriguing result, however its importance is still not fully clear. Most proteins that bind to EGFR are recruited upon phosphorylation of tyrosine residues via SH2 or PTP domains[5, 17]. The exceptions include the zinc finger containing protein, ZPR1 and chaperones that bind to the immature receptor. ZPR1 binds to EGFR in the absence of ligand stimulation but dissociates rapidly upon receptor activation and translocates to the nucleus to be involved in yet unclear processes[197].

Deletion analyses indicate that HDAC6 binds EGFR through its HEBD domain (for what I call the HDAC6 EGFR binding domain). This is a stretch of about 40 amino acids between the second deacetylase domain and the ubiquitin binding zinc finger at the C-terminus. So far, no other protein is known to bind to this region of HDAC6. The surface of EGFR that binds to HDAC6 is mapped to the juxtamembrane region (JM). The JM region of EGFR is known to be important in proper receptor sorting[216]. Additionally, the JM region of ErbB family members activates the kinase domain. This is distinct from other receptor tyrosine kinases where the JM region is inhibitory[217]. Interestingly, a recent structural study indicates that the JM region of EGFR is vital in creating an asymmetric dimer and kinase activation[13]. Unfortunately, we do not have structural data of the EGFR-HDAC6 complex and hence is difficult to imagine how it is organized. The constitutive interaction of HDAC6 and EGFR raises a number of questions regarding the role of HDAC6 in the regulation of EGFR.

4.3 HDAC6 stabilizes ligand-induced degradation of EGFR

Overexpression and RNAi mediated downregulation of HDAC6 coupled to pharmacologic intervention has clearly identified HDAC6 as an important negative regulator of EGFR degradation. It is important to note that the effect of overexpression of HDAC6 is much lower than the knockdown of endogenous HDAC6. This is very likely due to the high endogenous expression of HDAC6. In this case, subtraction would have a more pronounced effect compared to addition as the other protein complexes needed for HDAC6 activity would be saturated. The stabilization of EGFR by HDAC6 also depends on the deacetylase activity and the binding through HEBD domain. Again, the effects of these mutations of HDAC6 are subtler than downregulation of the endogenous protein.

As abolishing of deacetylase activity or binding ability separately leads to partial effects, it is tempting to assume that HDAC6 acts by two independent mechanisms. One may be by deacetylating a certain "target" and the other by acting as an adaptor protein linking EGFR to an unknown third protein. Hence, removing only one activity (catalytic site mutation, binding site deletion or inhibitor treatment) can partially compromise its function, whereas shRNA mediated knockdown of the protein can totally abrogate all the functions of the protein. Many of EGFR signalling principles

have been found to be applicable to other RTKs as well. Therefore, an interesting question is whether HDAC6 affects other RTKs similarly. In this regard, recent reports provide some evidence this might indeed be the case. Kamemura et al showed that stable knockdown of HDAC6 leads to decreased steady-state expression of not only EGFR but also platelet-derived growth factor α (PDGFα)[218]. Additionally, drug inhibition of HDAC6 reduced expression of vascular endothelial growth factor receptors 1 and 2 (VEGFR1 and 2)[219]. Therefore, it seems likely that HDAC6 acts as a regulator of a broad group of RTKs.

4.4 HDAC6 plays a pivotal role in the post-endocytic trafficking of EGFR

What accounts for the profoundly accelerated degradation of EGFR in HDAC6 knockdown cells? Interestingly, HDAC6 does not influence ligand-induced internalization of EGFR to any marked extent suggesting rather the post-endocytic trafficking is affected. The major HDAC6-dependent effect we have observed so far is on the kinetics of EGFR degradation. The challenge was to devise experiments where reliable quantitative measurements could be achieved to dissect the temporal and spatial effects of HDAC6.

These investigations were made possible by a combination of confocal immunofluorescene microscopy to follow the fate of labelled EGF along the endocytic pathway coupled to identification and computational characterization of intracellular vesicles. The algorithm used for identifying and tracking these vesicles, MotionTracker®, was developed primarily by Yannis Kalaidzidis (from the Max-Planck-Institute for Molecular Cell Biology and Genetics in Dresden). Computer based tracking of objects has its origin in the aerospace and military industries where satellites and airplanes are tracked based on data from sources like radar. Recent investigational street surveillance tools that follow individuals have expanded the reach of tracking programs. Algorithms developed for one area of application are difficult to modify for utilization in another setup because of fundamental differences in the propensity to change shape (e.g. compare an aircraft with an endosome), known physical limitations in movement and in the case of intracellular imaging the high level of background noise. This has prompted development of several intracellular tracking programs[220]. Currently, the convergence of improved microscopy,

fluorescent tagging of intracellular "entities" and development of tracking algorithms is having a profound effect on our understanding of the highly dynamic events in cells[61]. Intracellular trafficking of endocytosed receptors is a highly dynamic process that requires a suitable tracking program for reliable analysis. The major problem in automatic identification of vesicles staining positive for EGF or any of endocytic markers (in this case EEA1 and LAMP1) is establishing an appropriate cut-off point for "true" vesicles. This is due to the low signal-to-noise ratio in these samples generated mostly as a result of free fluorescence in non-vesicular structures and auto-fluorescence of biological samples.

Therefore, prior validation of the overall experimental setup by comparing results to previously well-established phenomena was essential. The entry of ligand-loaded EGFR into clathrin-coated vesicles and then into Rab5 or EEA1 positive early endosomes is a rapid process that peaks within minutes. Additionally, as endosomes undergo homo- and hetero-typic fusion and mature to late endosomes, they increase in size concomitant with accumulation of more cargo and organizing proteins[61]. Importantly, we can see all these changes happening in early endosomes carrying EGF in the results presented here.

 The key finding of the present study, however, is the rapid trafficking of EGF to peri-nuclear late endosomes in HDAC6 knockdown cells compared to control cells. Additionally, changes in intensity of the marker EEA1 show accumulation of more content, possibly representing increased fusion of vesicles in knockdown cells. These observations are central to explaining the role of HDAC6 in this process. The absence of HDAC6 is somehow accelerating the motility of these endosomes. Early endosomes are known to travel along microtubules towards the cell centre while undergoing maturation to late endosomes. Late endosomes eventually fuse with lysosomes to degrade their cargo in the peri-nuclear area of the cell where the microtubule-organizing center (MTOC) is located[173-175]. The accelerated transport of EGF is thus consistent with the faster degradation of EGFR seen in lysates of HDAC6 knockdown cells.

These events are highly reminiscent of the effects of another protein, KIF16B, a member of the kinesin family of motor proteins. This kinesin is a plus-end directed motor protein that binds to PtdIns(3)P and drives the motility of early endosomes. Overexpression of KIF16B caused an imbalance in plus- and minus-end (dynein-

dependent) movements that finally resulted in translocation of early endosomes to the cell cortex. Importantly, this inhibited ligand induced degradation of EGFR. In contrast, depletion of KIF16B by siRNAs led to faster translocation of early endosomes to the peri-nuclear degradative region and accelerated degradation of EGFR[221]. Another cytoskeleton-associated protein regulating endocytic transport is the Huntingtin associated protein 40 (HAP40). HAP40 is an effector of the small GTPase, Rab5, which is a vital endocytic regulator. Overexpression of HAP40 disrupts endosomal motility by displacing early endosomes from microtubules and relocating them to actin filaments. Furthermore, HAP40 is upregulated in brain tissue of patients suffering from Huntington's disease where defective trafficking of brain-derived neurotrophic factor is implicated in the pathogenesis[222].

Another example of perturbation in trafficking of EGFR containing vesicles is seen when PI3K activity is disrupted. Class I PI3K gets activated upon growth factors stimulation and phosphorylates PtdIns (4,5) to generate PtdIns (3,4,5) that acts as a docking platform for various PH and FYVE domain containing proteins. Many endocytic regulators (e.g. EEA1, Rabex-5, Rabenosyn) are recruited jointly through interaction with PtdIns (3,4,5) and Rab5. Due to its intricate involvement in generation of competent endosomes, the inhibition of PI3K by the fungal metabolite wortmannin or the synthetic inhibitor LY294002 leads to inhibition of homotypic fusion and slows EGFR trafficking and degradation[223, 224].

In contrast, a constitutively active mutant of Rab5, Q79L, acts in an opposite fashion. Rab5 Q79L lacks GTPase activity and is locked in active mode. It enhances homotypic fusion of early endosomes leading to massively enlarged "giant endosomes" depending on its expression level[204]. Upon EGF stimulation of cells expressing endogenous EGFR and Rab5 Q79L, the receptor is internalized normally but is accumulated in the large endosomes[225]. In summary, there are several proteins that slow degradation of EGFR acting on distinct post-endocytic trafficking stages without influencing the internalization event and HDAC6 appears to be the newest member of this group of modulators.

4.5 EGF induces acetylation of α-tubulin

After analysis of the influence of HDAC6 on EGFR trafficking, the mechanism behind it was addressed. The initial working hypothesis was that there is/are some target/s of HDAC6 acting on the trafficking of the receptor. Acetylation as a post-translational modification is commonly associated with nuclear gene expression regulation. This is not surprising, as the vast majority of known acetylated residues are found in histones, transcription factors and other proteins involved in gene expression. However, there is an increasing amount of evidence showing it is by no means a nuclear-only phenomenon.

With such background, we have tried to seek for acetylated proteins in the endocytic apparatus. The approach used, i.e., inhibition of deacetylase activity by TSA, followed by immunoprecipitating and probing with acetyllysine antibodies is shown to be sensitive for detecting acetylation in the so-far reported target proteins like histones, transcription factors, tubulin, HSP90 and cortactin. However, it is likely that it has limitations as an initial screening strategy.

The only lysine-acetylated proteins that came out of this study were clathrin heavy chain (CHC) and the already known α-tubulin. The major criteria set were that the acetylation should be dependent on HDAC6 (hence up regulated upon TSA treatment) and potentially responsive to growth factor treatment. Acetylation of CHC fulfilled neither criteria in that there was no change upon TSA or EGF addition. On the other hand the acetylation of α-tubulin on K40 was quite dynamic, increasing markedly either upon downmodulation of HDAC6 or activation of EGFR. This was clearly demonstrated by mass spectrometry based analysis and by immunoblotting.

At this juncture, it is worthwhile to mention a recently published report from the group of Mathias Mann. The authors applied SILAC to differentially labelled control cells and cells treated with two different HDAC inhibitors, suberoylanilide hydroxamic acid and MS-275[226]. Proteins were digested with trypsin and the resulting peptides were immunoprecipitated using acetyllysine specific antibody. This was coupled to a high resolution Orbi-trap mass spectrometer that delivered the most comprehensive list of acetylated peptides so far. A total of 3600 lysine acetylation sites on 1750 proteins were identified. Of particular interest to us was the acetylation pattern of endocytic proteins. Proteins like c-Cbl, vps4b and several actin-binding

proteins were found to be acetylated. However, acetylation of these proteins was not at all modified by treatment with the HDAC inhibitors used. These findings are in line with our results, showing even this comprehensive approach did not reveal additional proteins that could be targets of HDAC6 in the endocytic apparatus. It is possible that acetylation of these proteins does not have a regulatory role (hence not dynamic) or there are yet unknown deacetylases that are not inhibited with the above HDAC inhibitors.

Taken together, the evidence provided here shows that acetylation of α-tubulin undergoes dynamic changes upon activation of EGFR. While our study did not identify other acetylated proteins that behave similarly and are targets of HDAC6, their existence cannot be conclusively ruled out.

4.6 Acetylation of α-tubulin modulates motility of endosomes

Two reports have shed light on the possible roles of acetylation of microtubules (MT) in intracellular MT dependent transport. Dompierre et al demonstrated that hyperacetylated MTs recruit and bind the motor proteins dynein and kinesin-1 more efficiently than MTs with normal acetylation in vitro. Importantly, inhibition of HDAC6 activity in neurons accelerated exocytic secretion of brain derived neurotrophic factor (BDNF) in a strictly MT acetylation dependent fashion. Furthermore, postmortem examination of brains of Huntington disease patients revealed a striking reduction in acetylation of MTs[171]. All this is of paramount importance as one of the hypotheses for the origin of Huntington's disease is defective intracellular trafficking and associated neurotoxicity[227, 228].

In another report, Reed et al showed that kinesin-1 preferentially recognizes MTs with acetylated K40. This recognition is important for the delivery of its cargo protein JNK-interacting protein 1 (JIP1) to select neurites in neurons. Furthermore, forced upregulation of MT acetylation by treatment of cells with the inhibitor TSA resulted in increased and non-selective transport of the cargo into all neurites[170]. In summary, acetylation of α-tubulin is an emerging regulatory mechanism for controlling the kinetics of intracellular trafficking.

So, does K40 acetylation of tubulin play any role in trafficking by early endosomes? In order to confirm the involvement of K40 tubulin acetylation in EGF trafficking,

live cell imaging of fluorescent-tagged early endosomes were conducted. The endosomes used for the study (in A431 cells expressing GFP-Rab5) were not enlarged and showed no changes in kinetics of transferrin trafficking and are thus assumed to faithfully represent endogenous endosomes. The two important parameters measured by MotionTracker® were the speed of movement and the processivity of these motilities.

Endosomes are generally found in three states of motion, a short-range non-linear, a long-range linear (processive) movement and a transient immobile state. Additionally, early endosomes have a net directional flow towards the center of the cell (centripetal motion) even though single endosomes move bidirectionally. It is thought that true displacement of endosome is caused by processive movement[229, 230]. Both the speed and processive movement of endosomes in cells expressing a mutant of α-tubulin (K40A) that acts in a dominant negative fashion on acetylation of MTs were significantly lower than control cells. These results are in harmony with the studies discussed above, whereby reduced acetylation of MTs leads to a general slowness in endosomal motility. Unfortunately, a crucial experiment i.e. dynamic measurement after EGF stimulation and direct follow up of EGF/EGFR complex by live cell imaging was not successful. This was primarily due to the unacceptably high photobleaching of the small vesicles that carry EGF/EGFR immediately after internalization. Further optimization of experimental conditions is needed to make such direct measurements possible.

4.7 Phosphorylation of HDAC6 by EGFR modulates its deacetylase activity

Following EGF stimulation, acetylation of α-tubulin is progressively increased. Based on the present work, this is primarily due to the inactivation of HDAC6 by EGFR mediated phosphorylation of a key tyrosine residue. This regulation, by phosphorylation, of HDAC6 is conceivable when compared to the regulation of other HDACs.

The best-known means of regulating nuclear HDACs is by controlling the formation of multi-protein complexes, as most of these HDACs are inactive when alone. In vitro reconstitution assays showed that individual HDACs of the NuRD complex have severely depressed activity compared to the holo-complex[231]. SIR2 group of HDAC

are regulated by availability of metabolic cofactors like NAD^+ and by proteolytic cleavage of the inactive precursor as in the case of the human SIRT3 [232]. Sumoylation also plays a role by regulating intracellular localization. However, phosphorylation is the most prevalent regulatory modification with diverse effects. HDAC1 is phosphorylated on two serine residues and mutation of these to alanine abrogated enzymatic activity[209]. On the other hand inhibition of phosphatases by okadaic acid and hyperphosphorylation of HDAC1 and HDAC2 disrupted association of the complex they normally function in[233]. Phosphorylation of HDAC8 on Ser39 by protein kinase A (PKA) abolished its enzymatic activity almost completely in vivo and in vitro[234]. On the contrary HDAC4 is associated with ERK1/2 and phosphorylation does not influence catalytic activity per se but changes its sub-cellular localization[235].

Here, based on initial mass spectrometry, HDAC6 is shown to be phosphorylated on serine and tyrosine residues. The effect of Y570 was studied intensively in vitro as well as in vivo. The lack of good phosphoserine antibodies hampered the effort to study the phosphorylation of S568 further. Based on mutagenesis assays, phospho-mimicry of Y570 and S568 abolished enzymatic activity. HDAC6 is involved in a variety of cellular processes at different localizations; hence it would not be surprising if it were regulated by different kinases. At the plasma membrane it can be phosphorylated by EGFR and probably also by other RTKs. At other subcellular sites, HDAC6 can be phosphorylated by serine kinases. It is highly likely that phosphorylation at these residues leads to conformational changes that is propagated to the active site. However, elucidation of the exact mechanism will have to await the determination of the high-resolution structure of the protein.

In summary, a simplified model of the interplay between EGFR and HDAC6 is presented (Figure 25). HDAC6 is enzymatically active prior to and some time after EGFR activation. During this time, HDAC6 slows the transport of the receptor by favoring a state of deacetylated MTs. However, once a critical amount of HDAC6 is phosphorylated and inactivated by EGFR, the acetylation of MTs increases. This suppression of a negative regulator facilitates trafficking of EGFR-carrying endosomes towards signal termination and degradation.
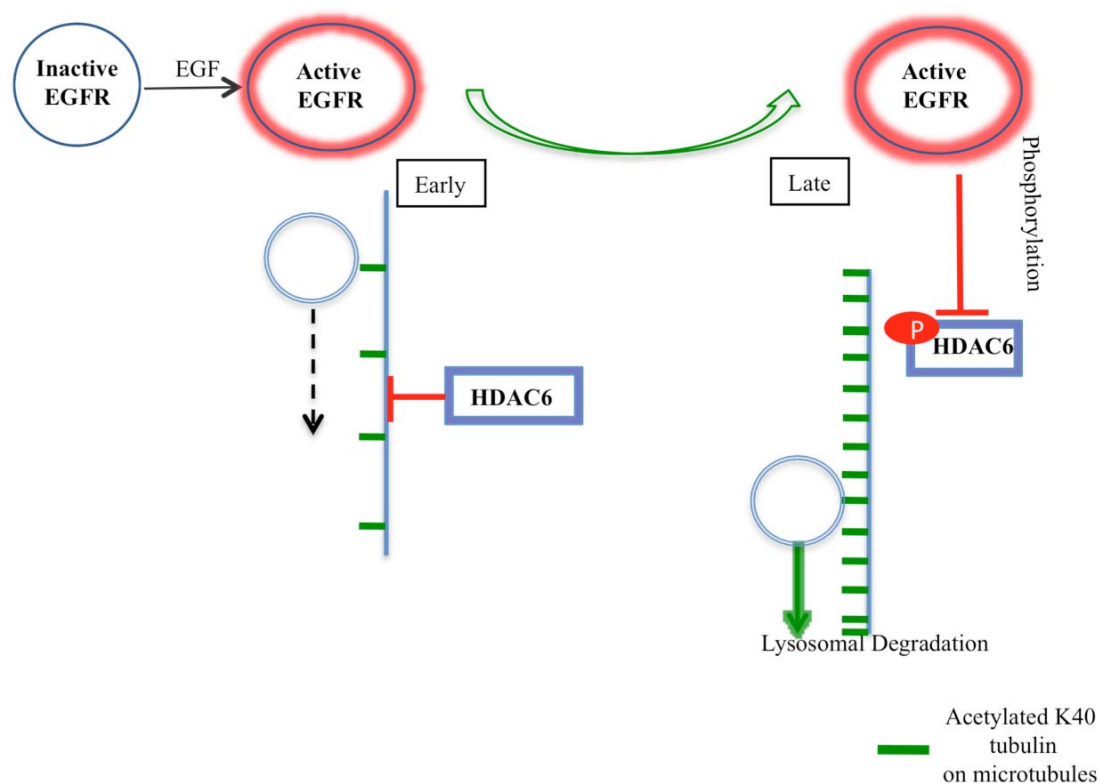
Figure 25. Regulation of EGFR trafficking by HDAC6.
HDAC6 has high basal deacetylase activity that keeps acetylation of microtubules (MT) relatively low. This results in slower trafficking of EGFR along MTs in the initial minutes of ligand binding and activation. However, later on, HDAC6 gets progressively phosphorylated by EGFR and looses its deacetylase activity. The resulting build up of acetylated MTs enhance trafficking of EGFR for degradation in lysosomes.

4.8 HDAC6 depletion results in perturbations in cellular physiology

EGF stimulation of A549 cells result in activation of certain downstream pathways like the PI3K/Akt and MAP kinase cascades. The depletion of HDAC6 in these cells resulted in marginally reduced ERK2 activation but markedly accentuated activation of Akt and its substrate GSK3β. This apparently conflicting observation can be explained by the different mode of activation of ERk1/2 and Akt.

ERK1/2 phosphorylation and activation is known to require, at least partially, localization in early endosomes[236, 237]. In HDAC6 knockdown cells, there is a rapid transit of the receptor complex into late endosomes with relatively less time spent in early endosomes (Fig. 18A and B). These late endosomes are not competent for ERK1/2 signalling and thus led to the moderately lowered phosphorylation observed.

On the other hand, activation of Akt is primarily driven by its recruitment to the plasma membrane through its lipid binding PH domain and internalization is not at all required for its signalling[237, 238]. Additionally, the transport of cytosolic Akt to the plasma membrane has been reported to be microtubule dependent[239, 240]. Hence, it is tempting to speculate that the increased acetylation induced by HDAC6 knockdown also facilitates Akt transport to the plasma membrane and its subsequent activation. However, this needs to be addressed further by detailed analyses, for instance, by studying localization of Akt in response to microtubule acetylation.

The other important observation seen was the lack of EGF induced cell rounding and growth arrest in HDAC6 depleted A549 cells compared to parental cells. In A431 and A549 cells, which express relatively high amount of EGFR, EGF stimulation results in massive contraction of the plasma membrane from the edges of cells facilitated by cortical actin polymerization[212, 241]. These cells also respond to EGF by arresting cellular growth and proliferation when grown in serum-lacking media that is supplemented with EGF. This is postulated to occur by the induction of cell cycle inhibitors like p21[213]. HDAC6 knockdown cells express reduced amount of EGFR at the cell surface. Hence, it is likely that their stunted response to EGF is due to this "downregulated receptor level" much like the lack of response of cells to hormones when subjected to sustained exposure (desensitization). This is a phenomenon widely seen in biological systems that reduce their responses to persistent stimuli in order to adequately respond to new stimuli[242].

The complex regulatory mechanisms put in place to modulate signalling is astounding and the sheer amount of recent publications addressing these issues is not surprising. These regulatory mechanisms are not only numerous in number but also appear to be organized in different levels. In EGFR signalling for example, these levels can be envisioned as receptor level such as dephosphorylation by phosphatases (first level), internalization (second level), trafficking (third level) and degradation (fourth level). This is a rather simplistic categorization but nonetheless provide a framework of thought. Each of these levels is regulated by many players that are able to communicate with other levels. The resulting redundancy would be expected to impart robustness to the system.

It is thus helpful to think of HDAC6 in this context, a fine-tuner among many. Recently, mice lacking HDAC6 have been created by targeted gene disruption. The

mice are viable, fertile and lack gross defects. In all the tissues examined, the level of acetylation of α-tubulin is profoundly increased proving HDAC6 as the bona-fide tubulin deacetylase. The only defects observed in these mice were reduced antibody generation in response to stimuli and slightly increased cancellous bone mineral density[165]. It is unclear how much detailed analyses were done on different organ systems. As a regulator of EGFR signalling, which plays essential roles in development; the lack of HDAC6 might be expected to have severe consequences. However, the redundant nature of regulation of EGFR signalling can result in activation of compensatory mechanisms that lead to acceptable level of signal output and normal development of the organism.

5. SUMMARY and FUTURE OUTLOOKS

The present study has demonstrated the power of the membrane-based yeast two-hybrid screening technique to identify novel interacting partners of a receptor tyrosine kinase. Several detailed investigations have provided compelling evidences for the specificity of the interactions identified. Functional analysis of one of the novel interactors, HDAC6, has identified it as a novel regulator of EGFR trafficking. HDAC6 interacts with EGFR in a constitutive fashion and traffics with EGFR after internalization. Gain-of-function and loss-of-function studies indicated that HDAC6 stabilizes the receptor from ligand-induced degradation. Imaging studies show that HDAC6 primarily affects the post-endocytic trafficking of the receptor. HDAC6 is able to achieve this feat by deacetylating α-tubulin. Acetylation of α-tubulin is demonstrated to be important for proper kinetics of early endosome motility. Hence, deacetylation of α-tubulin results in slower transport of cargo proteins carried by these endosomes. In a remarkable turn of events, a negative feedback loop was also discovered. Activation of EGFR leads to a progressively increasing phosphorylation of HDAC6 on Y570, which inactivates the deacetylase activity. Thus, the inhibition of an inhibitor results in activation of the pathway, which in this case leads to increase in acetylation of α-tubulin that facilitates transport of EGFR to its final degradative destination.

While these findings are interesting, they also raise a number of questions that need to be addressed to get a clearer picture of the whole process. One of the most important issues is a better understanding of the molecular mechanisms behind acetylation of microtubule dependent regulation of trafficking in vivo. The increase in acetylation of α-tubulin following EGF stimulation is clearly demonstrated, however its in vivo significance is still not understood. A complementation experiment where endogenous tubulin is depleted and replaced with wt or relevant mutants (a non-acetylable K40A, charge-retaining K40R and an acetylation mimicking K40Q) would yield crucial information on the relevance of acetylation of α-tubulin in vivo. The presence of many genes and gene products for α-tubulin in mammalian cells made the use of RNAi mediated knockdown impractical. An ideal model organism for this study is the ciliate *Tetrahymena thermophila* that encodes α-tubulin as a single gene.

Replacement of wt α-tubulin with mutants has already been successfully accomplished in this organism and can be replicated to study the role of acetylation in vesicular trafficking[243].

Acetylation of α-tubulin occurs progressively after EGFR activation. Hence, investigation of the temporal and spatial organization of this acetylation in mammalian cells would be an important part of future studies. This acetylation can occur as a selective "wave of acetylation" along microtubules that carry EGFR-containing endosomes or as a global change in all microtubules. To distinguish between these two scenarios, an acetylation sensing "biosensor" can be constructed. This is based on the principle of FRET (fluorescent resonance energy transfer) where non-radiative energy is transferred from a photo-excited donor to an acceptor fluorescent protein found in close proximity (<10nm)[244]. In biosensors, FRET is induced/abolished by a biological event that results in conformational change of the biosensor. It has been used for study of dynamic signal transduction events such as activation of kinases, proteases and GTPases[245, 246].

A microtubule acetylation sensor can hypothetically be constructed by fusing FRET pairs (e.g. CFP and YFP-cyan and yellow fluorescent proteins) at opposite ends of a chimeric protein that responds to acetylation. This chimera would consist of α-tubulin (for localization to microtubules), a peptide containing K40 (to be acetylated) and a bromodomain (that interacts with acetylated lysines) connected by flexible linker sequences. In the absence of acetylation, K40 is not bound to the bromodomain, the FRET pairs are not brought close together and hence no FRET signal is generated (Fig. 26 upper panel). Once acetylation occurs on K40, the bromodomain recognizes and interacts with it. This results in internal conformational changes of the sensor that will generate a measurable FRET signal (Fig. 26 lower panel). This, of course, is only one of many designs that can be deployed and need to be empirically tested. Potential problems that could arise include lack of localization of the biosensor to microtubules, absence of bromodomain and acetylated K40 interaction or a conformational change that is incompatible with generation of FRET signal.

Another major question to answer is whether the effect of HDAC6 on EGFR is an isolated event or part of a generalized mechanism whereby HDAC6 and acetylation of α-tubulin regulate other RTKs. As expression levels of VEGFR and PDGFR have

been observed to be affected by HDAC6 depletion, it would be worthwhile to study

the interaction of HDAC6 with different RTKs. It is also important to investigate
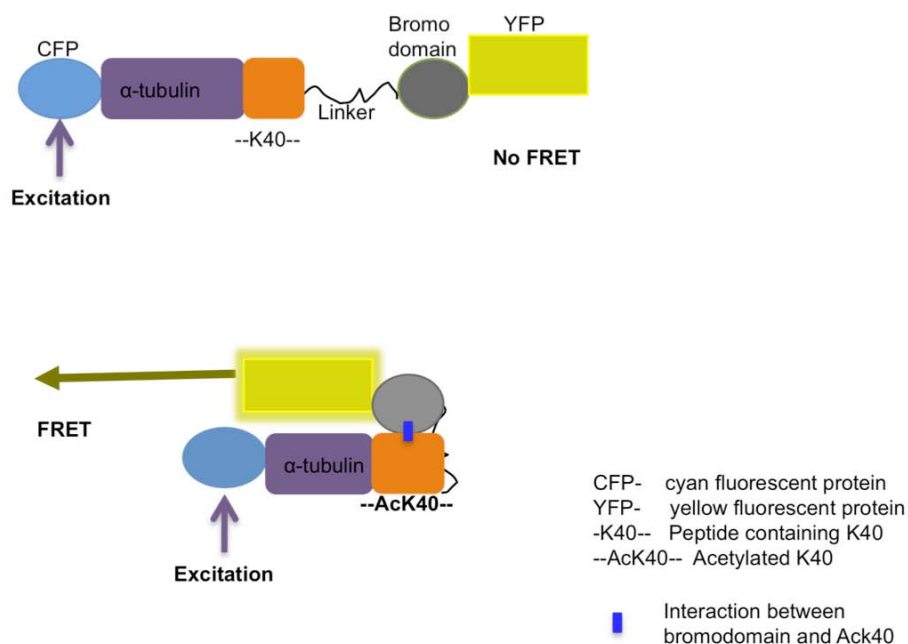
Figure 26. Proposed design of a microtubule acetylation biosensor.
This hypothetical sensor utilizes the principle of FRET (fluorescent resonance energy transfer) between CFP and YFP fused to a chimera that responds to acetylation. The chimera is composed of -tubulin, K40 containing peptide and acetylated lysine binding bromodomain. In the absence of acetylation of K40, bromodomain and the associated YFP are not interacting with K40 and no FRET is produced **(upper panel).** Once acetylation of K40 occured on -tubulin and K40 peptide, bromodomain binds to Ack40 leading to conformational changes that generate FRET signal **(lower panel)**.

whether other RTKs can phosphorylate and inactivate the deacetylase activity of

HDAC6. Another tantalizing question, with far reaching implications, is whether

acetylation of α-tubulin also influences other intracellular vesicular trafficking

pathways. To answer this, the dynamics of vesicular trafficking between the ER and

Golgi complex, other organelles' movements and their correlation with the acetylation

status of microtubules should be studied.

6. REFERENCES

1.   Cohen, S. Origins of growth factors: NGF and EGF. *J Biol Chem* 283, 33793-33797 (2008).
2.   Cohen, S., Carpenter, G. & King, L., Jr. Epidermal growth factor-receptor-protein kinase interactions. Co-purification of receptor and epidermal growth factor-enhanced phosphorylation activity. *J Biol Chem* 255, 4834-4842 (1980).
3.   Hunter, T. The Croonian Lecture 1997. The phosphorylation of proteins on tyrosine: its role in cell growth and disease. *Philos Trans R Soc Lond B Biol Sci* 353, 583-605 (1998).
4.   Ullrich, A. & Schlessinger, J. Signal transduction by receptors with tyrosine kinase activity. *Cell* 61, 203-212 (1990).
5.   Schlessinger, J. Cell signaling by receptor tyrosine kinases. *Cell* 103, 211-225 (2000).
6.   Yarden, Y. & Sliwkowski, M.X. Untangling the ErbB signalling network. *Nat Rev Mol Cell Biol* 2, 127-137 (2001).
7.   Citri, A. & Yarden, Y. EGF-ERBB signalling: towards the systems level. *Nat Rev Mol Cell Biol* 7, 505-516 (2006).
8.   Jones, J.T., Akita, R.W. & Sliwkowski, M.X. Binding specificities and affinities of egf domains for ErbB receptors. *FEBS Lett* 447, 227-231 (1999).
9.   Schneider, M.R. & Wolf, E. The epidermal growth factor receptor ligands at a glance. *J Cell Physiol* 218, 460-466 (2009).
10.   Ferguson, K.M. *et al.* EGF activates its receptor by removing interactions that autoinhibit ectodomain dimerization. *Mol Cell* 11, 507-517 (2003).
11.   Burgess, A.W. *et al.* An open-and-shut case? Recent insights into the activation of EGF/ErbB receptors. *Mol Cell* 12, 541-552 (2003).
12.   Zhang, X., Gureasko, J., Shen, K., Cole, P.A. & Kuriyan, J. An allosteric mechanism for activation of the kinase domain of epidermal growth factor receptor. *Cell* 125, 1137-1149 (2006).
13.   Jura, N. *et al.* Mechanism for activation of the EGF receptor catalytic domain by the juxtamembrane segment. *Cell* 137, 1293-1307 (2009).
14.   Red Brewer, M. *et al.* The juxtamembrane region of the EGF receptor functions as an activation domain. *Mol Cell* 34, 641-651 (2009).
15.   Levinson, A.D., Oppermann, H., Levintow, L., Varmus, H.E. & Bishop, J.M. Evidence that the transforming gene of avian sarcoma virus encodes a protein kinase associated with a phosphoprotein. *Cell* 15, 561-572 (1978).
16.   Hunter, T. & Cooper, J.A. Protein-tyrosine kinases. *Annu Rev Biochem* 54, 897-930 (1985).
17.   Pawson, T. Specificity in signal transduction: from phosphotyrosine-SH2 domain interactions to complex cellular systems. *Cell* 116, 191-203 (2004).
18.   Sadowski, I., Stone, J.C. & Pawson, T. A noncatalytic domain conserved among cytoplasmic protein-tyrosine kinases modifies the kinase function and transforming activity of Fujinami sarcoma virus P130gag-fps. *Mol Cell Biol* 6, 4396-4408 (1986).

19. van der Geer, P. & Pawson, T. The PTB domain: a new protein module implicated in signal transduction. *Trends Biochem Sci* 20, 277-280 (1995).

20. Kuriyan, J. & Cowburn, D. Modular peptide recognition domains in eukaryotic signaling. *Annu Rev Biophys Biomol Struct* 26, 259-288 (1997).

21. Ferguson, K.M., Lemmon, M.A., Schlessinger, J. & Sigler, P.B. Structure of the high affinity complex of inositol trisphosphate with a phospholipase C pleckstrin homology domain. *Cell* 83, 1037-1046 (1995).

22. Marshall, M.S. Ras target proteins in eukaryotic cells. *FASEB J* 9, 1311-1318 (1995).

23. Kolch, W. Coordinating ERK/MAPK signalling through scaffolds and inhibitors. *Nat Rev Mol Cell Biol* 6, 827-837 (2005).

24. Marshall, C.J. Specificity of receptor tyrosine kinase signaling: transient versus sustained extracellular signal-regulated kinase activation. *Cell* 80, 179-185 (1995).

25. Czech, M.P. PIP2 and PIP3: complex roles at the cell surface. *Cell* 100, 603-606 (2000).

26. Engelman, J.A., Luo, J. & Cantley, L.C. The evolution of phosphatidylinositol 3-kinases as regulators of growth and metabolism. *Nat Rev Genet* 7, 606-619 (2006).

27. Cantley, L.C. The phosphoinositide 3-kinase pathway. *Science* 296, 1655-1657 (2002).

28. Ridley, A.J., Paterson, H.F., Johnston, C.L., Diekmann, D. & Hall, A. The small GTP-binding protein rac regulates growth factor-induced membrane ruffling. *Cell* 70, 401-410 (1992).

29. Ridley, A.J. & Hall, A. The small GTP-binding protein rho regulates the assembly of focal adhesions and actin stress fibers in response to growth factors. *Cell* 70, 389-399 (1992).

30. Narumiya, S. The small GTPase Rho: cellular functions and signal transduction. *J Biochem* 120, 215-228 (1996).

31. Quesnelle, K.M., Boehm, A.L. & Grandis, J.R. STAT-mediated EGFR signaling in cancer. *J Cell Biochem* 102, 311-319 (2007).

32. Athale, C., Mansury, Y. & Deisboeck, T.S. Simulating the impact of a molecular 'decision-process' on cellular phenotype and multicellular patterns in brain tumors. *J Theor Biol* 233, 469-481 (2005).

33. Aroian, R.V. & Sternberg, P.W. Multiple functions of let-23, a Caenorhabditis elegans receptor tyrosine kinase gene required for vulval induction. *Genetics* 128, 251-267 (1991).

34. Schweitzer, R., Shaharabany, M., Seger, R. & Shilo, B.Z. Secreted Spitz triggers the DER signaling pathway and is a limiting component in embryonic ventral ectoderm determination. *Genes Dev* 9, 1518-1529 (1995).

35. Schweitzer, R., Howes, R., Smith, R., Shilo, B.Z. & Freeman, M. Inhibition of Drosophila EGF receptor activation by the secreted protein Argos. *Nature* 376, 699-702 (1995).

36.   Shilo, B.Z. Signaling by the Drosophila epidermal growth factor receptor pathway during development. *Exp Cell Res* 284, 140-149 (2003).

37.   Threadgill, D.W. *et al.* Targeted disruption of mouse EGF receptor: effect of genetic background on mutant phenotype. *Science* 269, 230-234 (1995).

38.   Hynes, N.E. & Lane, H.A. ERBB receptors and cancer: the complexity of targeted inhibitors. *Nat Rev Cancer* 5, 341-354 (2005).

39.   Pao, W. *et al.* Acquired resistance of lung adenocarcinomas to gefitinib or erlotinib is associated with a second mutation in the EGFR kinase domain. *PLoS Med* 2, e73 (2005).

40.   Baselga, J. & Swain, S.M. Novel anticancer targets: revisiting ERBB2 and discovering ERBB3. *Nat Rev Cancer* 9, 463-475 (2009).

41.   Giovannini, M. *et al.* Clinical Significance of Skin Toxicity due to EGFR-Targeted Therapies. *J Oncol* 2009, 849051 (2009).

42.   Shilo, B.Z. Regulating the dynamics of EGF receptor signaling in space and time. *Development* 132, 4017-4027 (2005).

43.   Chen, P., Xie, H. & Wells, A. Mitogenic signaling from the egf receptor is attenuated by a phospholipase C-gamma/protein kinase C feedback mechanism. *Mol Biol Cell* 7, 871-881 (1996).

44.   Xu, Y., Tan, L.J., Grachtchouk, V., Voorhees, J.J. & Fisher, G.J. Receptor-type protein-tyrosine phosphatase-kappa regulates epidermal growth factor receptor function. *J Biol Chem* 280, 42694-42700 (2005).

45.   Sorkin, A. & Goh, L.K. Endocytosis and intracellular trafficking of ErbBs. *Exp Cell Res* 314, 3093-3106 (2008).

46.   Carpenter, G. & Cohen, S. 125I-labeled human epidermal growth factor. Binding, internalization, and degradation in human fibroblasts. *J Cell Biol* 71, 159-171 (1976).

47.   Stoscheck, C.M. & Carpenter, G. Down regulation of epidermal growth factor receptors: direct demonstration of receptor degradation in human fibroblasts. *J Cell Biol* 98, 1048-1053 (1984).

48.   Doherty, G.J. & McMahon, H.T. Mechanisms of endocytosis. *Annu Rev Biochem* 78, 857-902 (2009).

49.   Mellman, I. & Warren, G. The road taken: past and future foundations of membrane traffic. *Cell* 100, 99-112 (2000).

50.   Kirchhausen, T. Clathrin. *Annu Rev Biochem* 69, 699-727 (2000).

51.   Peter, B.J. *et al.* BAR domains as sensors of membrane curvature: the amphiphysin BAR structure. *Science* 303, 495-499 (2004).

52.   Kirchhausen, T., Bonifacino, J.S. & Riezman, H. Linking cargo to vesicle formation: receptor tail interactions with coat proteins. *Curr Opin Cell Biol* 9, 488-495 (1997).

53.   Bonifacino, J.S. & Traub, L.M. Signals for sorting of transmembrane proteins to endosomes and lysosomes. *Annu Rev Biochem* 72, 395-447 (2003).

54.   Le Roy, C. & Wrana, J.L. Clathrin- and non-clathrin-mediated endocytic regulation of cell signalling. *Nat Rev Mol Cell Biol* 6, 112-126 (2005).

55. Gruenberg, J. & Stenmark, H. The biogenesis of multivesicular endosomes. *Nat Rev Mol Cell Biol* 5, 317-323 (2004).

56. Griffiths, G. & Gruenberg, J. The arguments for pre-existing early and late endosomes. *Trends Cell Biol* 1, 5-9 (1991).

57. Murphy, R.F. Maturation models for endosome and lysosome biogenesis. *Trends Cell Biol* 1, 77-82 (1991).

58. Schekman, R. & Orci, L. Coat proteins and vesicle budding. *Science* 271, 1526-1533 (1996).

59. Henry, R.M., Hoppe, A.D., Joshi, N. & Swanson, J.A. The uniformity of phagosome maturation in macrophages. *J Cell Biol* 164, 185-194 (2004).

60. Woodman, P.G. & Futter, C.E. Multivesicular bodies: co-ordinated progression to maturity. *Curr Opin Cell Biol* 20, 408-414 (2008).

61. Rink, J., Ghigo, E., Kalaidzidis, Y. & Zerial, M. Rab conversion as a mechanism of progression from early to late endosomes. *Cell* 122, 735-749 (2005).

62. Seaman, M.N. Endosome protein sorting: motifs and machinery. *Cell Mol Life Sci* 65, 2842-2858 (2008).

63. Hicke, L. & Dunn, R. Regulation of membrane protein transport by ubiquitin and ubiquitin-binding proteins. *Annu Rev Cell Dev Biol* 19, 141-172 (2003).

64. Katzmann, D.J., Babst, M. & Emr, S.D. Ubiquitin-dependent sorting into the multivesicular body pathway requires the function of a conserved endosomal protein sorting complex, ESCRT-I. *Cell* 106, 145-155 (2001).

65. Raiborg, C. & Stenmark, H. The ESCRT machinery in endosomal sorting of ubiquitylated membrane proteins. *Nature* 458, 445-452 (2009).

66. Hurley, J.H. ESCRT complexes and the biogenesis of multivesicular bodies. *Curr Opin Cell Biol* 20, 4-11 (2008).

67. Raiborg, C., Bache, K.G., Mehlum, A., Stang, E. & Stenmark, H. Hrs recruits clathrin to early endosomes. *EMBO J* 20, 5008-5021 (2001).

68. Raiborg, C. *et al.* Hrs sorts ubiquitinated proteins into clathrin-coated microdomains of early endosomes. *Nat Cell Biol* 4, 394-398 (2002).

69. Haglund, K. *et al.* Multiple monoubiquitination of RTKs is sufficient for their endocytosis and degradation. *Nat Cell Biol* 5, 461-466 (2003).

70. Huang, F., Kirkpatrick, D., Jiang, X., Gygi, S. & Sorkin, A. Differential regulation of EGF receptor internalization and degradation by multiubiquitination within the kinase domain. *Mol Cell* 21, 737-748 (2006).

71. Katzmann, D.J., Odorizzi, G. & Emr, S.D. Receptor downregulation and multivesicular-body sorting. *Nat Rev Mol Cell Biol* 3, 893-905 (2002).

72. Futter, C.E., Pearse, A., Hewlett, L.J. & Hopkins, C.R. Multivesicular endosomes containing internalized EGF-EGF receptor complexes mature and then fuse directly with lysosomes. *J Cell Biol* 132, 1011-1023 (1996).

References

73.   Luzio, J.P., Pryor, P.R. & Bright, N.A. Lysosomes: fusion and function. *Nat Rev Mol Cell Biol* 8, 622-632 (2007).

74.   Mayor, S. & Pagano, R.E. Pathways of clathrin-independent endocytosis. *Nat Rev Mol Cell Biol* 8, 603-612 (2007).

75.   Kirkham, M. & Parton, R.G. Clathrin-independent endocytosis: new insights into caveolae and non-caveolar lipid raft carriers. *Biochim Biophys Acta* 1746, 349-363 (2005).

76.   Simons, K. & Toomre, D. Lipid rafts and signal transduction. *Nat Rev Mol Cell Biol* 1, 31-39 (2000).

77.   Anderson, R.G. & Jacobson, K. A role for lipid shells in targeting proteins to caveolae, rafts, and other lipid domains. *Science* 296, 1821-1825 (2002).

78.   Parton, R.G. & Hancock, J.F. Lipid rafts and plasma membrane microorganization: insights from Ras. *Trends Cell Biol* 14, 141-147 (2004).

79.   Nabi, I.R. & Le, P.U. Caveolae/raft-dependent endocytosis. *J Cell Biol* 161, 673-677 (2003).

80.   Parton, R.G. & Simons, K. The multiple faces of caveolae. *Nat Rev Mol Cell Biol* 8, 185-194 (2007).

81.   Parton, R.G., Hanzal-Bayer, M. & Hancock, J.F. Biogenesis of caveolae: a structural model for caveolin-induced domain formation. *J Cell Sci* 119, 787-796 (2006).

82.   Pelkmans, L., Burli, T., Zerial, M. & Helenius, A. Caveolin-stabilized membrane domains as multifunctional transport and sorting devices in endocytic membrane traffic. *Cell* 118, 767-780 (2004).

83.   Pelkmans, L., Kartenbeck, J. & Helenius, A. Caveolar endocytosis of simian virus 40 reveals a new two-step vesicular-transport pathway to the ER. *Nat Cell Biol* 3, 473-483 (2001).

84.   Nichols, B.J. *et al.* Rapid cycling of lipid raft markers between the cell surface and Golgi complex. *J Cell Biol* 153, 529-541 (2001).

85.   Heltianu, C., Dobrila, L., Antohe, F. & Simionescu, M. Evidence for thyroxine transport by the lung and heart capillary endothelium. *Microvasc Res* 37, 188-203 (1989).

86.   Drab, M. *et al.* Loss of caveolae, vascular dysfunction, and pulmonary defects in caveolin-1 gene-disrupted mice. *Science* 293, 2449-2452 (2001).

87.   Lamaze, C. *et al.* Interleukin 2 receptors and detergent-resistant membrane domains define a clathrin-independent endocytic pathway. *Mol Cell* 7, 661-671 (2001).

88.   Sabharanjak, S., Sharma, P., Parton, R.G. & Mayor, S. GPI-anchored proteins are delivered to recycling endosomes via a distinct cdc42-regulated, clathrin-independent pinocytic pathway. *Dev Cell* 2, 411-423 (2002).

89.   Kirkham, M. *et al.* Ultrastructural identification of uncoated caveolin-independent early endocytic vehicles. *J Cell Biol* 168, 465-476 (2005).

90.   Sharma, P. *et al.* Nanoscale organization of multiple GPI-anchored proteins in living cell membranes. *Cell* 116, 577-589 (2004).

91. Goswami, D. *et al.* Nanoclusters of GPI-anchored proteins are formed by cortical actin-driven activity. *Cell* 135, 1085-1097 (2008).

92. Lundmark, R. *et al.* The GTPase-activating protein GRAF1 regulates the CLIC/GEEC endocytic pathway. *Curr Biol* 18, 1802-1808 (2008).

93. Amyere, M. *et al.* Constitutive macropinocytosis in oncogene-transformed fibroblasts depends on sequential permanent activation of phosphoinositide 3-kinase and phospholipase C. *Mol Biol Cell* 11, 3453-3467 (2000).

94. Mercer, J. & Helenius, A. Virus entry by macropinocytosis. *Nat Cell Biol* 11, 510-520 (2009).

95. Dharmawardhane, S. *et al.* Regulation of macropinocytosis by p21-activated kinase-1. *Mol Biol Cell* 11, 3341-3352 (2000).

96. Chhabra, E.S. & Higgs, H.N. The many faces of actin: matching assembly factors with cellular structures. *Nat Cell Biol* 9, 1110-1121 (2007).

97. Grimmer, S., van Deurs, B. & Sandvig, K. Membrane ruffling and macropinocytosis in A431 cells require cholesterol. *J Cell Sci* 115, 2953-2962 (2002).

98. Jutras, I. & Desjardins, M. Phagocytosis: at the crossroads of innate and adaptive immunity. *Annu Rev Cell Dev Biol* 21, 511-527 (2005).

99. Botelho, R.J., Scott, C.C. & Grinstein, S. Phosphoinositide involvement in phagocytosis and phagosome maturation. *Curr Top Microbiol Immunol* 282, 1-30 (2004).

100. Akira, S., Uematsu, S. & Takeuchi, O. Pathogen recognition and innate immunity. *Cell* 124, 783-801 (2006).

101. Trombetta, E.S. & Mellman, I. Cell biology of antigen processing in vitro and in vivo. *Annu Rev Immunol* 23, 975-1028 (2005).

102. Abrami, L., Lindsay, M., Parton, R.G., Leppla, S.H. & van der Goot, F.G. Membrane insertion of anthrax protective antigen and cytoplasmic delivery of lethal factor occur at different stages of the endocytic pathway. *J Cell Biol* 166, 645-651 (2004).

103. Le Blanc, I. *et al.* Endosome-to-cytosol transport of viral nucleocapsids. *Nat Cell Biol* 7, 653-664 (2005).

104. Pizarro-Cerda, J. & Cossart, P. Bacterial adhesion and entry into host cells. *Cell* 124, 715-727 (2006).

105. Beauregard, K.E., Lee, K.D., Collier, R.J. & Swanson, J.A. pH-dependent perforation of macrophage phagosomes by listeriolysin O from Listeria monocytogenes. *J Exp Med* 186, 1159-1163 (1997).

106. Malik, Z.A., Iyer, S.S. & Kusner, D.J. Mycobacterium tuberculosis phagosomes exhibit altered calmodulin-dependent signal transduction: contribution to inhibition of phagosome-lysosome fusion and intracellular survival in human macrophages. *J Immunol* 166, 3392-3401 (2001).

107. Vergne, I. *et al.* Mechanism of phagolysosome biogenesis block by viable Mycobacterium tuberculosis. *Proc Natl Acad Sci U S A* 102, 4033-4038 (2005).

108. Kusner, D.J. Mechanisms of mycobacterial persistence in tuberculosis. *Clin Immunol* 114, 239-247 (2005).

109.	Wiley, H.S. *et al.* The role of tyrosine kinase activity in endocytosis, compartmentation, and down-regulation of the epidermal growth factor receptor. *J Biol Chem* 266, 11083-11094 (1991).

110.	Wiley, H.S. Trafficking of the ErbB receptors and its influence on signaling. *Exp Cell Res* 284, 78-88 (2003).

111.	Resat, H., Ewald, J.A., Dixon, D.A. & Wiley, H.S. An integrated model of epidermal growth factor receptor trafficking and signal transduction. *Biophys J* 85, 730-743 (2003).

112.	Lund, K.A., Opresko, L.K., Starbuck, C., Walsh, B.J. & Wiley, H.S. Quantitative analysis of the endocytic system involved in hormone-induced receptor internalization. *J Biol Chem* 265, 15713-15723 (1990).

113.	Hanover, J.A., Willingham, M.C. & Pastan, I. Kinetics of transit of transferrin and epidermal growth factor through clathrin-coated membranes. *Cell* 39, 283-293 (1984).

114.	Carpentier, J.L. *et al.* Co-localization of 125I-epidermal growth factor and ferritin-low density lipoprotein in coated pits: a quantitative electron microscopic study in normal and mutant human fibroblasts. *J Cell Biol* 95, 73-77 (1982).

115.	Damke, H., Gossen, M., Freundlieb, S., Bujard, H. & Schmid, S.L. Tightly regulated and inducible expression of dominant interfering dynamin mutant in stably transformed HeLa cells. *Methods Enzymol* 257, 209-220 (1995).

116.	Huang, F., Khvorova, A., Marshall, W. & Sorkin, A. Analysis of clathrin-mediated endocytosis of epidermal growth factor receptor by RNA interference. *J Biol Chem* 279, 16657-16661 (2004).

117.	Kazazic, M. *et al.* EGF-induced activation of the EGF receptor does not trigger mobilization of caveolae. *Traffic* 7, 1518-1527 (2006).

118.	Haigler, H.T., McKanna, J.A. & Cohen, S. Direct visualization of the binding and internalization of a ferritin conjugate of epidermal growth factor in human carcinoma cells A-431. *J Cell Biol* 81, 382-395 (1979).

119.	Lamaze, C. & Schmid, S.L. Recruitment of epidermal growth factor receptors into coated pits requires their activated tyrosine kinase. *J Cell Biol* 129, 47-54 (1995).

120.	Sorkin, A., Waters, C., Overholser, K.A. & Carpenter, G. Multiple autophosphorylation site mutations of the epidermal growth factor receptor. Analysis of kinase activity and endocytosis. *J Biol Chem* 266, 8355-8362 (1991).

121.	Sorkina, T., Huang, F., Beguinot, L. & Sorkin, A. Effect of tyrosine kinase inhibitors on clathrin-coated pit recruitment and internalization of epidermal growth factor receptor. *J Biol Chem* 277, 27433-27441 (2002).

122.	Jiang, X., Huang, F., Marusyk, A. & Sorkin, A. Grb2 regulates internalization of EGF receptors through clathrin-coated pits. *Mol Biol Cell* 14, 858-870 (2003).

123.	Johannessen, L.E., Pedersen, N.M., Pedersen, K.W., Madshus, I.H. & Stang, E. Activation of the epidermal growth factor (EGF) receptor

induces formation of EGF receptor- and Grb2-containing clathrin-coated pits. *Mol Cell Biol* 26, 389-401 (2006).

124. Schmidt, M.H. & Dikic, I. The Cbl interactome and its functions. *Nat Rev Mol Cell Biol* 6, 907-918 (2005).

125. Waterman, H., Levkowitz, G., Alroy, I. & Yarden, Y. The RING finger of c-Cbl mediates desensitization of the epidermal growth factor receptor. *J Biol Chem* 274, 22151-22154 (1999).

126. Levkowitz, G. *et al.* Ubiquitin ligase activity and tyrosine phosphorylation underlie suppression of growth factor signaling by c-Cbl/Sli-1. *Mol Cell* 4, 1029-1040 (1999).

127. Hime, G.R., Dhungat, M.P., Ng, A. & Bowtell, D.D. D-Cbl, the Drosophila homologue of the c-Cbl proto-oncogene, interacts with the Drosophila EGF receptor in vivo, despite lacking C-terminal adaptor binding sites. *Oncogene* 14, 2709-2719 (1997).

128. Yoon, C.H., Lee, J., Jongeward, G.D. & Sternberg, P.W. Similarity of sli-1, a regulator of vulval development in C. elegans, to the mammalian proto-oncogene c-cbl. *Science* 269, 1102-1105 (1995).

129. Sorkin, A.D., Teslenko, L.V. & Nikolsky, N.N. The endocytosis of epidermal growth factor in A431 cells: a pH of microenvironment and the dynamics of receptor complex dissociation. *Exp Cell Res* 175, 192-205 (1988).

130. Sorkin, A. & Von Zastrow, M. Signal transduction and endocytosis: close encounters of many kinds. *Nat Rev Mol Cell Biol* 3, 600-614 (2002).

131. Longva, K.E. *et al.* Ubiquitination and proteasomal activity is required for transport of the EGF receptor to inner membranes of multivesicular bodies. *J Cell Biol* 156, 843-854 (2002).

132. Piper, R.C. & Katzmann, D.J. Biogenesis and function of multivesicular bodies. *Annu Rev Cell Dev Biol* 23, 519-547 (2007).

133. Raiborg, C., Malerod, L., Pedersen, N.M. & Stenmark, H. Differential functions of Hrs and ESCRT proteins in endocytic membrane trafficking. *Exp Cell Res* 314, 801-813 (2008).

134. Shih, S.C. *et al.* Epsins and Vps27p/Hrs contain ubiquitin-binding domains that function in receptor endocytosis. *Nat Cell Biol* 4, 389-393 (2002).

135. Wong, E.S. *et al.* Sprouty2 attenuates epidermal growth factor receptor ubiquitylation and endocytosis, and consequently enhances Ras/ERK signalling. *EMBO J* 21, 4796-4808 (2002).

136. Dikic, I. CIN85/CMS family of adaptor molecules. *FEBS Lett* 529, 110-115 (2002).

137. Jozic, D. *et al.* Cbl promotes clustering of endocytic adaptor proteins. *Nat Struct Mol Biol* 12, 972-979 (2005).

138. Allfrey, V.G., Faulkner, R. & Mirsky, A.E. Acetylation and Methylation of Histones and Their Possible Role in the Regulation of Rna Synthesis. *Proc Natl Acad Sci U S A* 51, 786-794 (1964).

139. Polevoda, B. & Sherman, F. The diversity of acetylated proteins. *Genome Biol* 3, reviews0006 (2002).

140. Kouzarides, T. Acetylation: a regulatory modification to rival phosphorylation? *EMBO J* 19, 1176-1179 (2000).

141. Grunstein, M. Histone acetylation in chromatin structure and transcription. *Nature* 389, 349-352 (1997).
142. Roth, S.Y., Denu, J.M. & Allis, C.D. Histone acetyltransferases. *Annu Rev Biochem* 70, 81-120 (2001).
143. Drummond, D.C. *et al.* Clinical development of histone deacetylase inhibitors as anticancer agents. *Annu Rev Pharmacol Toxicol* 45, 495-528 (2005).
144. L'Hernault, S.W. & Rosenbaum, J.L. Chlamydomonas alpha-tubulin is posttranslationally modified by acetylation on the epsilon-amino group of a lysine. *Biochemistry* 24, 473-478 (1985).
145. Westermann, S. & Weber, K. Post-translational modifications regulate microtubule function. *Nat Rev Mol Cell Biol* 4, 938-947 (2003).
146. Kovacs, J.J. *et al.* HDAC6 regulates Hsp90 acetylation and chaperone-dependent activation of glucocorticoid receptor. *Mol Cell* 18, 601-607 (2005).
147. Zhang, X. *et al.* HDAC6 modulates cell motility by altering the acetylation level of cortactin. *Mol Cell* 27, 197-213 (2007).
148. Yuan, Z.L., Guan, Y.J., Chatterjee, D. & Chin, Y.E. Stat3 dimerization regulated by reversible acetylation of a single lysine residue. *Science* 307, 269-273 (2005).
149. Yang, X.J. Lysine acetylation and the bromodomain: a new partnership for signaling. *Bioessays* 26, 1076-1087 (2004).
150. Ianari, A., Gallo, R., Palma, M., Alesse, E. & Gulino, A. Specific role for p300/CREB-binding protein-associated factor activity in E2F1 stabilization in response to DNA damage. *J Biol Chem* 279, 30830-30835 (2004).
151. Simonsson, M., Heldin, C.H., Ericsson, J. & Gronroos, E. The balance between acetylation and deacetylation controls Smad7 stability. *J Biol Chem* 280, 21797-21803 (2005).
152. Taunton, J., Hassig, C.A. & Schreiber, S.L. A mammalian histone deacetylase related to the yeast transcriptional regulator Rpd3p. *Science* 272, 408-411 (1996).
153. Grozinger, C.M., Hassig, C.A. & Schreiber, S.L. Three proteins define a class of human histone deacetylases related to yeast Hda1p. *Proc Natl Acad Sci U S A* 96, 4868-4873 (1999).
154. Blander, G. & Guarente, L. The Sir2 family of protein deacetylases. *Annu Rev Biochem* 73, 417-435 (2004).
155. de Ruijter, A.J., van Gennip, A.H., Caron, H.N., Kemp, S. & van Kuilenburg, A.B. Histone deacetylases (HDACs): characterization of the classical HDAC family. *Biochem J* 370, 737-749 (2003).
156. Hubbert, C. *et al.* HDAC6 is a microtubule-associated deacetylase. *Nature* 417, 455-458 (2002).
157. Bertos, N.R., Wang, A.H. & Yang, X.J. Class II histone deacetylases: structure, function, and regulation. *Biochem Cell Biol* 79, 243-252 (2001).
158. Finnin, M.S. *et al.* Structures of a histone deacetylase homologue bound to the TSA and SAHA inhibitors. *Nature* 401, 188-193 (1999).

159. Sauve, A.A., Wolberger, C., Schramm, V.L. & Boeke, J.D. The biochemistry of sirtuins. *Annu Rev Biochem* 75, 435-465 (2006).
160. Tissenbaum, H.A. & Guarente, L. Increased dosage of a sir-2 gene extends lifespan in Caenorhabditis elegans. *Nature* 410, 227-230 (2001).
161. Guarente, L. & Picard, F. Calorie restriction--the SIR2 connection. *Cell* 120, 473-482 (2005).
162. Hook, S.S., Orian, A., Cowley, S.M. & Eisenman, R.N. Histone deacetylase 6 binds polyubiquitin through its zinc finger (PAZ domain) and copurifies with deubiquitinating enzymes. *Proc Natl Acad Sci U S A* 99, 13425-13430 (2002).
163. Verdel, A. *et al.* Active maintenance of mHDA2/mHDAC6 histone-deacetylase in the cytoplasm. *Curr Biol* 10, 747-749 (2000).
164. Zhang, Y. *et al.* HDAC-6 interacts with and deacetylates tubulin and microtubules in vivo. *EMBO J* 22, 1168-1179 (2003).
165. Zhang, Y. *et al.* Mice lacking histone deacetylase 6 have hyperacetylated tubulin but are viable and develop normally. *Mol Cell Biol* 28, 1688-1701 (2008).
166. Scroggins, B.T. *et al.* An acetylation site in the middle domain of Hsp90 regulates chaperone function. *Mol Cell* 25, 151-159 (2007).
167. Murphy, P.J., Morishima, Y., Kovacs, J.J., Yao, T.P. & Pratt, W.B. Regulation of the dynamics of hsp90 action on the glucocorticoid receptor by acetylation/deacetylation of the chaperone. *J Biol Chem* 280, 33792-33799 (2005).
168. Kawaguchi, Y. *et al.* The deacetylase HDAC6 regulates aggresome formation and cell viability in response to misfolded protein stress. *Cell* 115, 727-738 (2003).
169. Pandey, U.B. *et al.* HDAC6 rescues neurodegeneration and provides an essential link between autophagy and the UPS. *Nature* 447, 859-863 (2007).
170. Reed, N.A. *et al.* Microtubule acetylation promotes kinesin-1 binding and transport. *Curr Biol* 16, 2166-2172 (2006).
171. Dompierre, J.P. *et al.* Histone deacetylase 6 inhibition compensates for the transport deficit in Huntington's disease by increasing tubulin acetylation. *J Neurosci* 27, 3571-3583 (2007).
172. Szebenyi, G. *et al.* Neuropathogenic forms of huntingtin and androgen receptor inhibit fast axonal transport. *Neuron* 40, 41-52 (2003).
173. Gruenberg, J., Griffiths, G. & Howell, K.E. Characterization of the early endosome and putative endocytic carrier vesicles in vivo and with an assay of vesicle fusion in vitro. *J Cell Biol* 108, 1301-1316 (1989).
174. Aniento, F., Emans, N., Griffiths, G. & Gruenberg, J. Cytoplasmic dynein-dependent vesicular transport from early to late endosomes. *J Cell Biol* 123, 1373-1387 (1993).
175. Bomsel, M., Parton, R., Kuznetsov, S.A., Schroer, T.A. & Gruenberg, J. Microtubule- and motor-dependent fusion in vitro between apical and basolateral endocytic vesicles from MDCK cells. *Cell* 62, 719-731 (1990).

176. Merrifield, C.J. *et al.* Endocytic vesicles move at the tips of actin tails in cultured mast cells. *Nat Cell Biol* 1, 72-74 (1999).

177. Lamaze, C., Fujimoto, L.M., Yin, H.L. & Schmid, S.L. The actin cytoskeleton is required for receptor-mediated endocytosis in mammalian cells. *J Biol Chem* 272, 20332-20335 (1997).

178. Schliwa, M. & Woehlke, G. Molecular motors. *Nature* 422, 759-765 (2003).

179. Bananis, E. *et al.* Microtubule-dependent movement of late endocytic vesicles in vitro: requirements for Dynein and Kinesin. *Mol Biol Cell* 15, 3688-3697 (2004).

180. Soldati, T. & Schliwa, M. Powering membrane traffic in endocytosis and recycling. *Nat Rev Mol Cell Biol* 7, 897-908 (2006).

181. de Hoog, C.L. & Mann, M. Proteomics. *Annu Rev Genomics Hum Genet* 5, 267-293 (2004).

182. Hanash, S.M., Pitteri, S.J. & Faca, V.M. Mining the plasma proteome for cancer biomarkers. *Nature* 452, 571-579 (2008).

183. Phizicky, E., Bastiaens, P.I., Zhu, H., Snyder, M. & Fields, S. Protein analysis on a proteomic scale. *Nature* 422, 208-215 (2003).

184. Aebersold, R. & Mann, M. Mass spectrometry-based proteomics. *Nature* 422, 198-207 (2003).

185. Fields, S. & Song, O. A novel genetic system to detect protein-protein interactions. *Nature* 340, 245-246 (1989).

186. Johnsson, N. & Varshavsky, A. Split ubiquitin as a sensor of protein interactions in vivo. *Proc Natl Acad Sci U S A* 91, 10340-10344 (1994).

187. Stagljar, I., Korostensky, C., Johnsson, N. & te Heesen, S. A genetic system based on split-ubiquitin for the analysis of interactions between membrane proteins in vivo. *Proc Natl Acad Sci U S A* 95, 5187-5192 (1998).

188. Iyer, K. *et al.* Utilizing the split-ubiquitin membrane yeast two-hybrid system to identify protein-protein interactions of integral membrane proteins. *Sci STKE* 2005, pl3 (2005).

189. Paumi, C.M. *et al.* Mapping protein-protein interactions for the yeast ABC transporter Ycf1p by integrated split-ubiquitin membrane yeast two-hybrid analysis. *Mol Cell* 26, 15-25 (2007).

190. Gisler, S.M. *et al.* Monitoring protein-protein interactions between the mammalian integral membrane transporters and PDZ-interacting partners using a modified split-ubiquitin membrane yeast two-hybrid system. *Mol Cell Proteomics* 7, 1362-1377 (2008).

191. Dirnberger, D., Messerschmid, M. & Baumeister, R. An optimized split-ubiquitin cDNA-library screening system to identify novel interactors of the human Frizzled 1 receptor. *Nucleic Acids Res* 36, e37 (2008).

192. Soubeyran, P., Kowanetz, K., Szymkiewicz, I., Langdon, W.Y. & Dikic, I. Cbl-CIN85-endophilin complex mediates ligand-induced downregulation of EGF receptors. *Nature* 416, 183-187 (2002).

193. Gallop, J.L. *et al.* Mechanism of endophilin N-BAR domain-mediated membrane curvature. *EMBO J* 25, 2898-2910 (2006).

194. Moncalian, G. *et al.* Atypical polyproline recognition by the CMS N-terminal Src homology 3 domain. *J Biol Chem* 281, 38845-38853 (2006).

195. Blagoev, B. *et al.* A proteomics strategy to elucidate functional protein-protein interactions applied to EGF signaling. *Nat Biotechnol* 21, 315-318 (2003).

196. Jones, R.B., Gordus, A., Krall, J.A. & MacBeath, G. A quantitative protein interaction network for the ErbB receptors using protein microarrays. *Nature* 439, 168-174 (2006).

197. Galcheva-Gargova, Z. *et al.* Binding of zinc finger protein ZPR1 to the epidermal growth factor receptor. *Science* 272, 1797-1802 (1996).

198. Brown, K.R. & Jurisica, I. Online predicted human interaction database. *Bioinformatics* 21, 2076-2082 (2005).

199. Brown, K.R. & Jurisica, I. Unequal evolutionary conservation of human protein interactions in interologous networks. *Genome Biol* 8, R95 (2007).

200. Su, A.I. *et al.* A gene atlas of the mouse and human protein-encoding transcriptomes. *Proc Natl Acad Sci USA* 101, 6062-6067 (2004).

201. Ashburner, M. *et al.* Gene ontology: tool for the unification of biology. The Gene Ontology Consortium. *Nat Genet* 25, 25-29 (2000).

202. Lord, P.W., Stevens, R.D., Brass, A. & Goble, C.A. Semantic similarity measures as tools for exploring the gene ontology. *Pacific Symposium on Biocomputing*, 601-612 (2003).

203. Hunter, T. & Cooper, J.A. Epidermal growth factor induces rapid tyrosine phosphorylation of proteins in A431 human tumor cells. *Cell* 24, 741-752 (1981).

204. Stenmark, H. *et al.* Inhibition of rab5 GTPase activity stimulates membrane fusion in endocytosis. *Embo J* 13, 1287-1296 (1994).

205. Xu, W. *et al.* Sensitivity of mature Erbb2 to geldanamycin is conferred by its kinase domain and is mediated by the chaperone protein Hsp90. *J Biol Chem* 276, 3702-3708 (2001).

206. Sawai, A. *et al.* Inhibition of Hsp90 down-regulates mutant epidermal growth factor receptor (EGFR) expression and sensitizes EGFR mutant tumors to paclitaxel. *Cancer Res* 68, 589-596 (2008).

207. Shimamura, T., Lowell, A.M., Engelman, J.A. & Shapiro, G.I. Epidermal growth factor receptors harboring kinase domain mutations associate with the heat shock protein 90 chaperone and are destabilized following exposure to geldanamycins. *Cancer Res* 65, 6401-6408 (2005).

208. Creppe, C. *et al.* Elongator controls the migration and differentiation of cortical neurons through acetylation of alpha-tubulin. *Cell* 136, 551-564 (2009).

209. Pflum, M.K., Tong, J.K., Lane, W.S. & Schreiber, S.L. Histone deacetylase 1 phosphorylation promotes enzymatic activity and complex formation. *J Biol Chem* 276, 47733-47741 (2001).

210. Pugacheva, E.N., Jablonski, S.A., Hartman, T.R., Henske, E.P. & Golemis, E.A. HEF1-dependent Aurora A activation induces disassembly of the primary cilium. *Cell* 129, 1351-1363 (2007).

211. Berdeaux, R. *et al.* SIK1 is a class II HDAC kinase that promotes survival of skeletal myocytes. *Nat Med* 13, 597-603 (2007).
212. Chinkers, M., McKanna, J.A. & Cohen, S. Rapid rounding of human epidermoid carcinoma cells A-431 induced by epidermal growth factor. *J Cell Biol* 88, 422-429 (1981).
213. Fan, Z. *et al.* Prolonged induction of p21Cip1/WAF1/CDK2/PCNA complex by epidermal growth factor receptor activation mediates ligand-induced A431 cell growth inhibition. *J Cell Biol* 131, 235-242 (1995).
214. Gross, M.E. *et al.* Cellular growth response to epidermal growth factor in colon carcinoma cells with an amplified epidermal growth factor receptor derived from a familial adenomatous polyposis patient. *Cancer Res* 51, 1452-1459 (1991).
215. Hackel, P.O., Gishizky, M. & Ullrich, A. Mig-6 is a negative regulator of the epidermal growth factor receptor signal. *Biol Chem* 382, 1649-1662 (2001).
216. Herbst, J.J., Opresko, L.K., Walsh, B.J., Lauffenburger, D.A. & Wiley, H.S. Regulation of postendocytic trafficking of the epidermal growth factor receptor through endosomal retention. *J Biol Chem* 269, 12865-12873 (1994).
217. Thiel, K.W. & Carpenter, G. Epidermal growth factor receptor juxtamembrane region regulates allosteric tyrosine kinase activation. *Proc Natl Acad Sci U S A* 104, 19238-19243 (2007).
218. Kamemura, K. *et al.* Effects of downregulated HDAC6 expression on the proliferation of lung cancer cells. *Biochem Biophys Res Commun* 374, 84-89 (2008).
219. Park, J.H. *et al.* Class II histone deacetylases play pivotal roles in heat shock protein 90-mediated proteasomal degradation of vascular endothelial growth factor receptors. *Biochem Biophys Res Commun* 368, 318-322 (2008).
220. Kalaidzidis, Y. Intracellular objects tracking. *Eur J Cell Biol* 86, 569-578 (2007).
221. Hoepfner, S. *et al.* Modulation of receptor recycling and degradation by the endosomal kinesin KIF16B. *Cell* 121, 437-450 (2005).
222. Pal, A., Severin, F., Lommer, B., Shevchenko, A. & Zerial, M. Huntingtin-HAP40 complex is a novel Rab5 effector that regulates early endosome motility and is up-regulated in Huntington's disease. *J Cell Biol* 172, 605-618 (2006).
223. Jones, A.T. & Clague, M.J. Phosphatidylinositol 3-kinase activity is required for early endosome fusion. *Biochem J* 311 (Pt 1), 31-34 (1995).
224. van Dam, E.M., Ten Broeke, T., Jansen, K., Spijkers, P. & Stoorvogel, W. Endocytosed transferrin receptors recycle via distinct dynamin and phosphatidylinositol 3-kinase-dependent pathways. *J Biol Chem* 277, 48876-48883 (2002).
225. Dinneen, J.L. & Ceresa, B.P. Expression of dominant negative rab5 in HeLa cells regulates endocytic trafficking distal from the plasma membrane. *Exp Cell Res* 294, 509-522 (2004).

References

226. Choudhary, C. *et al.* Lysine acetylation targets protein complexes and co-regulates major cellular functions. *Science* 325, 834-840 (2009).

227. Gil, J.M. & Rego, A.C. Mechanisms of neurodegeneration in Huntington's disease. *Eur J Neurosci* 27, 2803-2820 (2008).

228. Caviston, J.P. & Holzbaur, E.L. Huntingtin as an essential integrator of intracellular vesicular trafficking. *Trends Cell Biol* 19, 147-155 (2009).

229. Nielsen, E., Severin, F., Backer, J.M., Hyman, A.A. & Zerial, M. Rab5 regulates motility of early endosomes on microtubules. *Nat Cell Biol* 1, 376-382 (1999).

230. Ichikawa, T. *et al.* Digital fluorescence imaging of trafficking of endosomes containing low-density lipoprotein in brain astroglial cells. *Biochem Biophys Res Commun* 269, 25-30 (2000).

231. Zhang, Y. *et al.* Analysis of the NuRD subunits reveals a histone deacetylase core complex and a connection with DNA methylation. *Genes Dev* 13, 1924-1935 (1999).

232. Sengupta, N. & Seto, E. Regulation of histone deacetylase activities. *J Cell Biochem* 93, 57-67 (2004).

233. Galasinski, S.C., Resing, K.A., Goodrich, J.A. & Ahn, N.G. Phosphatase inhibition leads to histone deacetylases 1 and 2 phosphorylation and disruption of corepressor interactions. *J Biol Chem* 277, 19618-19626 (2002).

234. Lee, H., Rezai-Zadeh, N. & Seto, E. Negative regulation of histone deacetylase 8 activity by cyclic AMP-dependent protein kinase A. *Mol Cell Biol* 24, 765-773 (2004).

235. Zhou, X. *et al.* Histone deacetylase 4 associates with extracellular signal-regulated kinases 1 and 2, and its cellular localization is regulated by oncogenic Ras. *Proc Natl Acad Sci U S A* 97, 14329-14333 (2000).

236. Sadowski, L., Pilecka, I. & Miaczynska, M. Signaling from endosomes: location makes a difference. *Exp Cell Res* 315, 1601-1609 (2009).

237. Ceresa, B.P., Kao, A.W., Santeler, S.R. & Pessin, J.E. Inhibition of clathrin-mediated endocytosis selectively attenuates specific insulin receptor signal transduction pathways. *Mol Cell Biol* 18, 3862-3870 (1998).

238. Scheid, M.P. & Woodgett, J.R. PKB/AKT: functional insights from genetic models. *Nat Rev Mol Cell Biol* 2, 760-768 (2001).

239. Eyster, C.A., Duggins, Q.S., Gorbsky, G.J. & Olson, A.L. Microtubule network is required for insulin signaling through activation of Akt/protein kinase B: evidence that insulin stimulates vesicle docking/fusion but not intracellular mobility. *J Biol Chem* 281, 39719-39727 (2006).

240. Flusberg, D.A., Numaguchi, Y. & Ingber, D.E. Cooperative control of Akt phosphorylation, bcl-2 expression, and apoptosis by cytoskeletal microfilaments and microtubules in capillary endothelial cells. *Mol Biol Cell* 12, 3087-3094 (2001).

241. Malliri, A. *et al.* The transcription factor AP-1 is required for EGF-induced activation of rho-like GTPases, cytoskeletal

rearrangements, motility, and in vitro invasion of A431 cells. *J Cell Biol* 143, 1087-1099 (1998).

242. Pitcher, J.A., Freedman, N.J. & Lefkowitz, R.J. G protein-coupled receptor kinases. *Annu Rev Biochem* 67, 653-692 (1998).

243. Gaertig, J. *et al.* Acetylation of lysine 40 in alpha-tubulin is not essential in Tetrahymena thermophila. *J Cell Biol* 129, 1301-1310 (1995).

244. Giepmans, B.N., Adams, S.R., Ellisman, M.H. & Tsien, R.Y. The fluorescent toolbox for assessing protein location and function. *Science* 312, 217-224 (2006).

245. Li, I.T., Pham, E. & Truong, K. Protein biosensors based on the principle of fluorescence resonance energy transfer for monitoring cellular dynamics. *Biotechnol Lett* 28, 1971-1982 (2006).

246. Johnson, S.A., You, Z. & Hunter, T. Monitoring ATM kinase activity in living cells. *DNA Repair (Amst)* 6, 1277-1284 (2007).

Abbreviations

ATP	Adenosine 5`-triphosphate
BDNF	Brain derived neurotrophic factor
C-terminus	Carboxy terminal end
CCP	Clathrin coated pits
CCV	Clathrin coated vesicles
CIE	Clathrin independent endocytosis
CIP	Calf intestinal phosphatase
CLIC	Clathrin and dynamin independent vesicles
CME	Clathrin mediated endocytosis
Cub	Carboxy terminal end of ubiquitin (amino acids 35-76)
DABCO	1,4 diazabicyclo (2,2,2)dextran
DAG	Diacylglycerol
DAPI	4,6-diamidino-2-phenylindole dihydrochloride
DER	Drosophila melangogaster EGF-like ligand receptor
EDTA	Ethylenediamine tetracetic acid
EE	Early endosome
EEA1	Early endosomal antigen 1
EGF	Epidermal growth factor
EGFR	Epidermal growth factor receptor
EPOR	Erythropoietin receptor
ErbB	Erythroblastosis oncogene B
ERK	Extracellular signal regulated kinase
ESCRT	Endosomal sorting complex required for transport
GAPDH	Glyceraldehyde-3- dehydrogenase
GDP	Guanine 5`-diphosphosphate
GEEC	glycosyl-phosphatidylinositol–anchored protein enriched early endosomal compartments
GEF	Guanine nucleotide exchange factor
GFP	Green fluorescent protein
GHR	Growth hormone receptor
GPI	Glycosylphosphatidyl inositol
GPI-AP	Glycosylphosphatidyl inositol-anchored protein
GST	Glutathione-s-transferase
GTP	Guanosine 5`-triphosphosphate
HDAC	Histone deacetylase
HRS	Hepatocyte growth factor regulated tyrosine kinase substrate
HSP90	Heat shock protein 90
ILV	Intraluminal vesicles
IP	Immunoprecipitation
KDa	Kilodalton
LAMP1	Lysosome associated membrane protein 1
LDLR	Low density lipoprotein receptor
LBPA	Lysophosphatidic acid
MAPK	Mitogen activated protein kinase
MFα	Mating factor α
MHC	Major histocompatibility complex

MS	Mass spectrometry
MT	Microtubules
MTOC	Microtubule organizing center
MVB	Multivesicular body
MYTH	Membrane based yeast two-hybrid
N-terminus	Amino terminal end
NGF	Nerve growth factor
NSCLC	Non-small cell lung cancer
Nub	Amino terminal end of ubiquitin (amino acids 1-34)
PDGFR	Platelet derived growth factor receptor
PFA	Paraformaldehyde
PH	Plekstrin homology
PI3K	Phosphoinositide-3 kinase
PKC	Protein kinase C
PLC	Phospholipase C
PTB	Phosphotyrosine binding
PtdIns	Phosphatidyl inositol
PTP	Protein tyrosine phosphatase
RIPA	Radioimmunoprecipitation assay
RTK	Receptor tyrosine kinase
SDS-PAGE	Sodium dodecyl sulfate-polyacrylamide gel electrophoresis
SH2	Src-homology 2
shRNA	Short hair pin ribonucleic acid
STAT	Signal transduction and activators of transcription
TCL	Total cell lysates
TF	Transcription factor
TGF	Transforming growth factor
TSA	Trichostatin A
UIM	Ubiquitin interacting motif
VEGFR	Vascular endothelial growth factor receptor
WB	Western blot
YTH	Yeast two-hybrid

List of original publications

Cbl promotes clustering of endocytic adaptor proteins
Jozic D**, Cardenes N**, **Deribe YL**, Moncalian G, Hoeller D, Groemping Y, Dikic I, Rittinger K, Bravo J.
Nature Structural and Molecular Biology 2005 Nov;12(11):972-9

Atypical polyproline recognition by the CMS N-terminal Src homology 3 domain
Moncalián G, Cárdenes N, **Deribe YL**, Spínola-Amilibia M, Dikic I, Bravo J.
J Biol Chem. 2006 Dec 15;281(50):38845-53

Caspase-8 is involved in neovascularization-promoting progenitor cell functions
Scharner D, Rössig L, Carmona G, Chavakis E, Urbich C, Fischer A, Kang TB, Wallach D, Chiang YJ, **Deribe YL**, Dikic I, Zeiher AM, Dimmeler S.
Arterioscler Thromb Vasc Biol. 2009 Apr;29(4):571-8

EGFR trafficking is regulated by the lysine deacetylase HDAC6
Yonathan Lissanu Deribe, Philipp Wild, Akhila Chandrashaker, Jasna Curak Mirko H.H. Schmidt, Yannis Kalaidzidis, Natasa Milutinovic, Irina Kratchmarova, Lukas Buerkle, Michael J.Fetchko, Philipp Schmidt, Saranya Kittanakom, Kevin R. Brown, Igor Jurisica, Blagoy Blagoev, Marino Zerial, Igor Stagljar and Ivan Dikic
Science Signaling, in press, scheduled for publication on 22nd December, 2009

** Equally contributing first authors

Acknowledgments

I would like to extend my heartfelt gratitude to members of the institute of biochemistry II, of the Goethe University medical school for creating a wonderful atmosphere to work in. I give my thanks to Prof. Ivan Dikic who gave me the opportunity to work in his laboratory, for providing guidance and encouragement to work independently. His unwavering support and encouragement has helped me through difficult times when the fate of my project was unclear.

I thank Philipp Wild, who recently joined the project, for a great collaborative work.

Special thanks go to Kaisa Haglund and Grzegorz Zapart who introduced me to the intricate workings of the lab and techniques used. I thank Magda Bienko, Fumiyo Ikeda, Christina Hecker, Nicola Crosseto, David McEwan, Koraljka Husniak and Mirko Schmidt for valuable suggestions and discussions. My appreciations to Ingrid Konrad and Masuda Sader for countless technical help, and Birgit Lipke who assisted me in all the official procedures. I express my thanks to all we collaborated with in the last few years; the lab of Igor Stagljar (Zurich and Toronto), Marino Zerial (Dresden) and the ever good-spirited Blagoy Blagoev in Denmark.

The many hours of extra-lab activities and intense discussions, scientific and otherwise, with Igor Kovacevic, Fumiyo Ikeda, Magda Galovic, and Julio Granados has left warm feelings and memories in me. "Messob" with Sami and Kefe provided me with the tropical setting and have been home away from home. To top it all, I have been luck to meet my dearest friend Nicoline Schaap during an endocytosis conference! Her love, support and patience have been my constant companions for the last years. Final thanks for my family far, far away in Addis. Thank you father, thank you mother for providing me with the education that you loved above all but was not lucky enough to get. I dedicate this work to Dereje, my brother in every sense of the word.

Curriculum Vitae

PERSONAL DATA

Yonathan Lissanu Deribe
Date of Birth	August 9, 1978
Place of Birth	Addis Ababa, Ethiopia
Nationality	Ethiopian

EDUCATION

High school study

1991-1994	Medhane Alem High school, Addis Ababa, Ethiopia
	Ethiopian School Leaving Certificate (ESLC)

Higher Education

09/1995 - 08/2001	Gondar College of Medical Sciences, Gondar Ethiopia,
	Doctor of Medicine (MD) degree
09/2002- 08/2004	International Masters Program in Molecular and Cellular Biology, University of Heidelberg, Heidelberg, Germany,
	Master of Science (MSc) degree
	Thesis under Prof. Dr. Klaus Unsicker

WORK EXPERIENCE

09/2000-09/2001	Internship at the teaching hospital of Gondar College Of Medical Sciences, Gondar, Ethiopia
11/2001-08/2002	Assistant lecturer, Department of Biochemistry, Gondar College of Medical Sciences
09/2004- present	Scientific employee of the Institute of Biochemistry II, Frankfurt Medical School, Frankfurt, Germany, under supervision of Prof.Dr Ivan Dikic

AWARDS AND PRIZES

08/2001	"Gold Medal" for overall outstanding academic excellence, Gondar College of Medical Sciences
08/2001	"Best Medical Student 2000" by Ethiopian Medical Association, Addis Ababa, Ethiopia

Erklärung

Hiermit erkläre ich an Eides Statt, dass ich die vorliegende Dissertation selbständig und nur mit den angegebenen Hilfsmitteln angefertigt und dass ich noch keinen Promotionsversuch unternommen habe.

Frankfurt am Main, den   8 December 2009

Yonathan Lissanu Deribe